NON-VIRAL GENE DELIVERY WITH pH-SENSITIVE GEMINI NANOPARTICLES: SYNTHESIS OF GEMINI SURFACTANT BUILDING BLOCKS, CHARACTERIZATION AND *IN VITRO* SCREENING OF TRANSFECTION EFFICIENCY AND TOXICITY

A Thesis Submitted to the College of Graduate Studies and Research

in Partial Fulfillment of the Requirements for the

Degree of Master of Science

in the College of Pharmacy and Nutrition, University of Saskatchewan

Saskatoon, Saskatchewan, Canada

By

McDonald Donkuru

PERMISSION TO USE

In presenting this thesis in partial fulfillment of the requirements for a postgraduate degree from the University of Saskatchewan, I agree that the Libraries of this University may make it freely available for inspection. I further agree that permission for copying this thesis in any manner, in whole or in part, for scholarly purposes may be granted by the professor(s) who supervised my thesis work or, in their absence, by the Head of the Department or the Dean of the College in which my thesis work was done. It is understood that any copying, publication or use of this thesis or parts thereof for financial gain shall not be allowed without my written permission. It is also understood that due recognition shall be given to me and to the University of Saskatchewan in any scholarly use which may be made of any material in my thesis.

Requests for permission to copy or make any other use of material in this thesis in whole or in part should be addressed to:

Dean of the College of Pharmacy & Nutrition

University of Saskatchewan

Saskatoon, Saskatchewan, S7N 5C9

ABSTRACT

Research on self-assembling gemini surfactants and other amphiphiles for potential gene delivery applications in research as well as in clinical practice, and as alternatives to viral gene delivery vectors, is beginning to focus more on 'structure–activity relationships' to address the current low gene delivery efficiencies of amphiphiles. Some underlying structure–activity relations are beginning to emerge. But, as a better understanding of the factors that govern the transfection abilities of amphiphile molecules emerges, development of improved non-viral vectors with clinical potential may also emerge.

The research conducted for this thesis was aimed at the design, synthesis and *in vitro* investigation of gemini surfactants as one of a family of novel amphiphiles being investigated for gene therapeutic applications. The properties of these compounds can be controlled as well as allowed to vary naturally. Gemini surfactant-based gene delivery systems were prepared and characterized for transfer of Luciferase plasmid (pMASIA.Luc) to both COS-7 and PAM 212 cells. Characterization was accomplished using microscopy, dynamic light scattering (DLS) and zeta (ζ) potential analysis. *In vitro* gene expression and toxicities were evaluated in COS-7 cell and PAM 212 keratinocyte cultures.

The level of *in vitro* transfection in general was found to correlate strongly with the structure of the gemini surfactants. Among the 12-spacer-12 surfactants, incorporation of a pH-sensitive aza (N-CH_3) group, which is also steric hindrance-imposing, in the spacer chain yielded increased transfection, particularly for the 12-7N-12 surfactant. In

comparison, the incorporation of the more pH-sensitive imino (N-H) group in the 12-7NH-12 surfactant yielded the highest increase in transfection among the 12-spacer-12 surfactants. The deleterious effect of steric hindrance due to the aza group is more evident when comparing the transfection efficiency of 12-5N-12 (1 × aza, higher) vs. 12-8N-12 (2 × aza, lower transfection). Another highlighted structural feature is provided by the fact that both the 12-7NH-12 and 12-7N-12 surfactants had higher transfection efficiencies than 12-5N-12 and 12-8N-12 surfactants; the first pair has trimethylene spacing, which constitutes an optimal separation between nitrogen centres, while the second pair has shorter dimethylene spacings.

After expanding the structure of surfactants, transfection efficiencies were found to increase in response to increase in hydrocarbon tail length, but were much lower for surfactants with no amino functional groups, those that lacked the optimal trimethylene spacing, or those having both of these limitations in the gemini surfactant spacer. The 18-7NH-18 surfactant had the highest overall transfection in both COS-7 and PAM 212 cells. Gemini surfactant-based gene delivery systems capable of adopting both polymorphic structural phases and which could undergo pH-induced structural transition demonstrated high transfection efficiencies. Gemini surfactants with both characteristics (e.g., 12-7NH-12-based complexes are both polymorphic and pH-sensitive) had higher transfection than gemini surfactants with only one (e.g., 12-3-12-based complexes are only polymorphic).

Overall, the m-7NH-m surfactants, the most efficient surfactants studied, had transfection efficiencies similar to that of the commercial Lipofectamine Plus™ reagent and imposed no higher toxicity on cells relative to the less efficient surfactants. Thus, the design of the m-7NH-m surfactants to enhance their transfection abilities also

ensured that their toxicity to cells were kept minimal. Overall, the design, synthesis and *in vitro* transfection screening of gemini surfactant candidates has revealed that the m-7NH-m surfactants have the highest transfection efficiencies; they have emerged as suitable candidates for non-viral gene delivery *in vivo* or at higher levels. Gene delivery investigations for six of the gemini surfactant candidates are being reported for the first time.

ACKNOWLEDGEMENTS

My appreciation is first to my supervisor, Dr. Marianna Foldvari, for her professional and moral support and guidance. By the same measure I also thank the members of my advisory committee, Drs. Ronald Verrall, Adil Nazarali and Jane Alcorn, for their guidance. Dr. Gordon McKay travelled to voluntarily chair my first two committee meetings, and I owe him much thanks.

I thank Dr. Shawn Wettig from whose expertise I learnt the design and synthesis of gemini surfactants. He also provided other technical assistance, and was closely associated with my advisory committee, offering solid guidance. Colleagues of our research group, including Dr. Ildiko Badea (who currently conducts and manages her own research as a professor) and Mukasa Bagonluri, are also very much appreciated for their technical assistance. Martin Abu facilitated my settling in Saskatoon for these studies and I am highly appreciative of his support.

The following institutions are duly recognized: Saskatchewan Structural Science Centre (Saskatoon, SK), Transmission Electron Microscopy Laboratory (College of Veterinary Medicine, Saskatoon, SK) and the National Synchrotron Light Source (Brookhaven National Laboratory, NY) for the use of instruments/equipment. The research was funded with grants from the Canadian Institutes of Health Research and the Natural Sciences and Engineering Research Council of Canada. The workspace and other facilities were also provided by the College of Pharmacy and Nutrition (University of Saskatchewan, Saskatoon, SK).

DEDICATION

To my wife and crony, Beata Kaatori, and my parents, who are my roots.

TABLE OF CONTENTS

LIST OF TABLES

LIST OF FIGURES

LIST OF ABBREVIATIONS

12-3-12	1,3-propanediyl-bis(dimethyldodecylammonium) dibromide
12-7-12	1,7-heptanediyl-bis(dimethyldodecylammonium) dibromide
12-5N-12	1,5-bis(dodecyl)-1,1,3,5,5-pentamethyl-3-aza-1,5-pentanediammonium dibromide
12-7N-12	1,9-bis(dodecyl)-1,1,5,9,9-pentamethyl-5-aza-1,9-nonanediammonium dibromide
12-8N-12	1,10-bis(dodecyl)-1,1,4,7,10,10-hexamethyl-4,7-diaza-1,10-dodecane-diammonium dibromide
12-7NH-12	1,9-bis(dodecyl)-1,1,9,9-tetramethyl-5-imino-1,9-nonanediammonium dibromide
16-3-16	1,3-propanediyl-bis(dimethylhexadecylammonium) dibromide
16-7-16	1,7-heptanediyl-bis(dimethylhexadecylammonium) dibromide
16-7NH-16	1,9-bis(hexadecyl)-1,1,9,9-tetramethyl-5-imino-1,9-nonanediammonium dibromide
18-3-18	1,3-propanediyl-bis(dimethyl-octadecylammonium) dibromide
18:1-3-18:1	1,3-propanediyl-bis(dimethyl-*cis*-oleylammonium) dibromide
18-7-18	1,7-heptanediyl-bis(dimethyl-octadecylammonium) dibromide
18-7NH-18	1,9-bis(octadecyl)-1,1,9,9-tetramethyl-5-imino-1,9-nonanediammonium dibromide
18:1-7NH-18:1	1,9-bis(*cis*-oleyl)-1,1,9,9-tetramethyl-5-imino-1,9-nonanediammonium dibromide
Ab	antibiotic-antimycotic
AMP	adenosine monophosphate
ATP	adenosine triphosphate
bp	base-pair, in reference to DNA
CH&N	carbon, hydrogen and nitrogen
CMC	critical micelle concentration
CMV	cytomegalovirus
CO_2	carbon dioxide
Dc-chol	3ß-[N-(N',N'-dimethylaminoethane)-carbamoyl]cholesterol hydrochloride
^oC	degrees Celcius
DLS	dynamic light scattering
DMEM	Dulbecco's Modified Eagle's Medium
DOGS	dioctadecyl amino glycyl spermine
DOPE	1,2-Dioleyl-*sn*-glycerophosphatidylethanolamine
DOSPA	2,3-dioleyloxy-N-[2(sperminecarboxyamido)ethyl]-N,N-dimethyl-1-propaniminium bromide
DOTMA	N-[1-(2,3-dioleyloxy)propyl]-N,N,N-trimethylammonium chloride
ESI-MS	electrospray ionization mass spectrometry
GFP	green fluorescent protein
FBS	fetal bovine serum
HCl	hydrogen chloride
IFN	interferon

keV	kilo electronvolts
log C	logarithm of concentration, to base ten
MEM	Minimum Essential Medium
mL	millilitre
mM	millimolar concentration
µL	microlitre
m-s-m	N,N'-bis(alkyldodecyl)-α,ω-alkanediammonium dirbromide surfactant, with alkyl tail length = m and alkyl spacer length = s
NaOH	sodium hydroxide
nm	nanometre
PEI	polyethylenimine
%	percent
PG	plasmid–gemini complex
PGL	plasmid–gemini–DOPE system
pK_a	negative logarithm of the equilibrium constant (Ka) for an acidic species
pMASIA.Luc	plasmid containing the luciferase gene from firefly
PP_i	pyrophosphate
R_H	hydronamic radius, denoting particle size
SAXS	small-angle X-ray scattering
TEM	transmission electron microscopy
UV	ultraviolet
w/v	weight per volume
XP	xeroderma pigmentosum

1. INTRODUCTION

1.1. Human Genes to Combat Diseases: an Overview

Since the first proof of principle of gene therapy, that is, a disease caused by a known genetic defect can be treated or cured by delivering the correct copy of a defective gene via a specially designed vector to directly correct the gene-related pathological condition [1], decades of research have focused on realizing the clinical treatment of genetic diseases [2]. Along with the treatment of genetic defects, the treatment of acquired diseases can be effected by provoking a disruptive effect on the disease pathophysiology by delivering a genetic material [3]. In another type of application, gene therapy or modification could also involve instituting the function of a required alien gene in a biological host regardless of whether or not the host is diseased. For instance, genetic immunization is based on the delivery of DNA encoding for a protein-antigen from a pathogen to healthy cells to induce both cell-mediated and humoral immune responses. The vectors for carrying genes to target cells might be used to deliver not only genes but also other nucleic acid agents (‘drugs’), such as antisense oligonucleotides or mRNA to diseased cells for therapeutic purpose [4]. The focus of research has mainly been (1) developing the drugs (nucleic acids), and (2) transferring developed drugs to diseased cells or tissues in patients via vectors. Available technologies for design and engineering of nucleic acids have made it possible for plasmids containing various transgenes [5] to be constructed and produced on a large

scale [6]. This has put to rest the question of availability of nucleic acid drugs. However, the latter question of delivery or transfer of therapeutic genes via vectors is still a technological hurdle [7]. Neither of the two early classes of vectors, viral (natural) and non-viral (synthetic) [2], can be considered as representing a perfect choice for nucleic acid delivery [8]. Various groups have within the past decade tested the ability of bacteria to transfer genes to mammalian cells (*in vitro* and *in vivo*) [9-14], and the recent report by Loessner *et al* [15] demonstrates the somewhat effective transfer of genes by bacterial vectors. Thus, a third category of vectors, bacterial gene delivery vectors (the latest) [16], has been named.

1.2. Current Gene Therapy

Following the success of the first clinical trial of human gene therapy in 1990 (at NIH, USA) in which a 4-year-old girl was treated for fetal severe combined immunodeficiency (SCID) caused by adenosine deaminase (ADA) deficiency, the way was opened for other potential genetic-level treatments. Treatment at the genetic level, which by implication eliminates the cause of the disease [17; 18], was earlier examined for such diseases as cystic fibrosis [19-21], haemophelia [22] and hypercholesterolemia [23]. But as the base of potential therapy widened other inclusions have been made, such as sickle cell anemia, hepatitis [24; 25], cardiovascular disorders, neurological disorders such as Parkinson's disease and Alzheimer's disease, cancer and AIDS [5; 26; 27]. The recently approved first ever adenoviral gene therapy treatment, *Gendicine* (by SioBiono GeneTech, 2003, China), for the treatment of head and neck squamous cell carcinoma (HNSCC) is considered a ground-breaking success that could allow for the treatment of a wide-spectrum of cancers [5; 28; 29]. In September 2005, the State Food and Drug

Administration of China approved a second drug based on gene therapy, *Endostar*, for treatment of cancerous tumours in the lungs and other organs [30]. In addition to application to diseases, some gene therapy protocols have diversified into genetic immunization or DNA vaccines, heralded as the third vaccine revolution [31; 32].

Despite the promise of gene therapy, current difficulties in regards to safe and effective transfer of available nucleic acid drugs to mammalian cells, whether cytosolic delivery or the introduction of DNA into the cell nucleus (transfection) [33], has not allowed gene therapy to fully evolve as a new treatment or disease-prevention [34]. Among all the technologies generalized as non-viral (artificial) approaches, molecular carrier systems (synthetic) capable of self-assembling [35; 36] and DNA condensation [37], such as gemini surfactant-based systems, show promise as prime candidates for gene delivery [33]. They represent safer alternatives to viral vectors [33], which have sparked safety concerns and provoked an urgent search for safe, non-viral vectors for nucleic acid delivery [38; 39].

1.3. Gene Delivery and Transfection

The susceptibility of DNA and other nucleic acids to nuclease degradation and the rather unmatched abundance of nucleases usually in the pathway of *in vitro*- or *in vivo*-administered genes generally call for a delivery vector/system that will provide an initial packaging. The packaging vectors not only protect the genes through the delivery process [17], but also preserve the activity of the nucleic acid drugs [5]. In particular, when a transgene is proposed to arrive at the nucleus (transfection), the requirement of a delivery system for packaging is emphasized by the fact that the transport processes involved in transfection can be deleterious to naked or unpacked genes. The processes

leading to eventual nuclear entry are migration from entry port to target cells, internalization or entry of 'drug' into cells (through endocytosis [40], fusion or other possible means), endosomal escape of free or vector-associated genes, and, finally, migration from cytosol to the nucleus [5]. In cases where transgene progression can be realized for DNA released into the cytosol, its migration from the cytosol to the nucleus is not needed. A combination of such transport phases gives rise to a complex pharmacokinetic profile [41; 42] to which a significant amount of research is dedicated. Even in cases of successful migration to the nucleus, a large amount of the genetic 'drug' is usually intercepted and degraded by cytoplasmic nucleases during migration to the nucleus [17].

Delivery systems also facilitate/mediate both cellular uptake and nuclear entry of therapeutic DNA, marking an improvement over naked DNA which, due to its large size, negative charge, and membrane barriers imposed by cells, shows weak cell entry [37]. In the absence of delivery systems naked DNA may show some amount of cellular internalization only after local administration, as seen after intramuscular, intratumoral or intradermal injections [43-45]. It is hoped that the ultimate development of gene delivery vectors that combine safety with high delivery efficiency will see the realization of full-scale clinical treatment and prevention of diseases [46; 47]. Non-viral vectors are attracting significant research interest [33; 48] mainly because they have better safety profiles than viruses [3; 18; 37; 49-51], which nonetheless, are the most encountered vectors in clinical trials because of their higher delivery efficiencies. Both viral and synthetic (non-viral) types of vectors currently suffer from disadvantages [3], as do the relatively new bacterial types [16], driving continued research on all these vector types.

1.3.1. Viral Gene Delivery Systems

Until 1987, when a report of studies involving the use of amphiphile molecular carriers (cationic lipids in the specific case) to transfer genes into cells was first published by Felgner *et al.* [37], research into DNA transfection focused mainly on the use of viral vectors (engineered viruses). Viral vectors have been demonstrated to be the most effective vectors currently used for DNA transfection [33; 52-55], with adenoviruses giving better results as compared with retroviruses, poxviruses or herpes simplex viruses [26; 56-59]. Viruses possess a natural capability of infecting cells, with their specific biological "keys" (e.g., glycoproteins in a viral envelope [58]) allowing passage initially across the cell membrane, and then across the nuclear membrane (into the nucleus) via a speedy cytosolic passage along dynein-based active linear translocation microtubules. This achieves high gene expression in most of a transfected population of cells *in vitro* and opens a wide range of cell targets for viral delivery. However, several concerns with viral vectors have arisen. These include strong immune response in host cells due to viral proteins (preventing virus reuse), endogenous viral recombination, oncogenic effects, possible large-scale contamination of the engineered viruses and high cost of production [17; 34; 37; 43; 52; 60].

Since the tragic death of an 18-year-old viral gene therapy research subject (in Sept 1999, USA), who was being treated for partial ornithine transcarbamylase (OTC) deficiency [61], and the therapy-turned-setback situation in which two out of eleven children developed a blood disorder similar to leukemia following an adenoviral treatment against SCID by a French gene therapy team [39], viral gene therapy has come

under severe scrutiny, provoking a sense of urgency to search for safer alternatives to viral vectors [62].

1.3.2. Bacterial Gene Delivery Vectors

Loessner *et al.*'s report of bacteria-mediated DNA transfer (for gene therapy and vaccination) [15] is one of the latest on the subject. Gene transfer from bacteria to mammalian cells [9-14], and even yeast [63] and plants [64], have been reported. Therapeutic benefits, such as vaccinations against infectious diseases, immunotherapy against cancer and topical delivery of immunomodulatory cytokines in inflammatory bowel disease, have been achieved via bacteria-mediated DNA transfer. Of the types of bacteria tested (human clinical trial) such as *Salmonella* [9; 12], *Shigella* [10] and *Listeria* [11], attenuated strain of the first affords tumour-targeted gene delivery, but also highlights potential problems including toxicity. For large-scale production, the observed limited colonization properties could imply the potential to cause low yields. In addition, questions about the mechanism of DNA transfer from bacteria to mammalian cells are yet to be settled: the first limiting step can occur at cell entry [16] or earlier.

1.3.3. Non-viral Gene Delivery Vectors

The unpredictable immune response and inherent safety issues with the use of viral vectors have mainly necessitated non-viral vector development [65]. A number of physical techniques for introducing naked DNA into cells, including DNA co-precipitation with calcium phosphate [66; 67], bioballistics (using gene gun) [68; 69], microinjection [70] and electroporation [71], have evolved in the search for non-viral means of gene delivery. Electroporation gene delivery is an approach in which DNA is driven across cell membranes by the application of controlled electric current. The above approaches have managed to show effectiveness in a few cases (*in vitro*), but the clinical application of, especially the last two, have been questioned [3]. Particularly for electroporation, which results in cell motility, there could be aggravated consequences due to voltage shoot up resulting from current control failure.

The latest trend of non-viral vector development includes the use of supramolecular and macromolecular systems with positive charges. These include gemini surfactants [72-74], lipids [17; 37; 51; 75; 76], polyelectrolytes such as DEAE-dextran [77; 78], polyamine (or polyamidoamine) dendrimers [79; 80], polynorborane [81], and polyethyleneimine (PEI) [82]. Supramolecular systems of lipids or gemini surfactants (amphiphiles) are of particular interest because of their ability to self-assemble into vesicular structures, commonly described as liposomes [3]. Gemini surfactants in particular demonstrate advanced ability to self-assemble (form liposomes), a feature which is of primary importance for their application in gene therapy (packaging of DNA for cellular uptake). Molecular delivery systems (generally termed ‘lipofection agents’) have seen an increasing application in gene therapy clinical trials recently, accounting

for 18% of all trials in 2000 [83]. The number of individual trials involving lipofection agents has since more than doubled, even though this has not translated into a proportionate rise in the percentage of these trials relative to the total number of trials (compare refs [33; 83], [39], [84]).

In principle, gemini surfactant-based gene delivery vectors are developed to circumvent the problems faced by viral vectors, which also includes low DNA carriage-capacity. The vector design is targeted at forming particles that mimic virus-like infection behaviour, including cellular attachment and rapid internalization, followed by endosomal escape and nuclear localization, ultimately achieving high gene expression [85]. Impressive transfection efficiencies for a few tested gemini surfactants, with low toxicity in host cells (*in vitro*, transgene expressed in most transfected cells) have received major highlights in recent reviews [86]. Unlike viruses, amphiphile aggregates have virtually no limitation on the quantity of plasmid they can carry. While viral capsids have been able to contain 40,000 DNA base pairs at maximum [87], it has been possible for amphiphile aggregates to package multiple genes and regulatory sequences, ranging from hundreds of thousands of DNA base-pairs to one million base-pairs for cellular uptake [88; 89].

Gemini surfactants allow a broad range of modification of their structures, allowing for structural optimization of gemini surfactant candidates for gene delivery. This structural optimization is important in the formation of effective gemini surfactant-based gene delivery systems for transfer of DNA to cells. There is also the ease of large-scale manufacture of gemini surfactants or other non-viral molecular delivery agents, and the low cost compared with the propagative production of viral systems [90]. Emerging design of gemini based-gene delivery vectors demonstrates that the incorporation of

selected functional groups can be used to augment vector efficacy and provide targeted gene delivery to cells and tissues [33; 65]. Because of the need for safer alternatives to viral and bacterial vectors, and also because amphiphile molecules such as gemini surfactants form inherently safe vectors, a growing number of studies, including this research, are aimed at developing molecular vectors for gene delivery.

1.3.4. Cellular Gene Delivery using Non-viral Vectors

The mechanism of cellular gene delivery continues to be probed in an attempt to gain improved insight into the design of more efficient non-viral–DNA systems, (including those referred to as lipoplexes and polyplexes), which can interface with cellular processes to yield better transfection. For *in vitro* transfection, an established concentration of lipoplexes is added to cell cultures, followed by a duration of incubation of the cell–lipoplex mixture. The added lipoplexes can diffuse freely through the supernatant medium and become attached to cells and can be internalized by cells [40; 91]; *in vitro* transfection as a result is simpler. This is relative to *in vivo* delivery in which the broad range of interactions between lipoplexes and multiple cells types or molecules within a host organism can present several challenges [17]. In terms of *in vitro* transfection, preparation of cationic lipoplexes with positive surface charge is a significant practice that ensures electrostatic interaction with cells. The overall positive charge allows lipoplexes to bind to the negative sulfated proteoglycans on cell surfaces, with such attachments leading to internalization of lipoplexes [92], either by cell-lipoplex fusion [93; 94] or endocytosis (engulfment) [17; 40]. Cellular internalization of lipoplexes by endocytosis places the endocytosed lipoplexes in endosomes (Figure

1.3.4-1) [95; 96]. Endocytosis is believed to account for the majority of DNA that enters cells [91; 97-99].

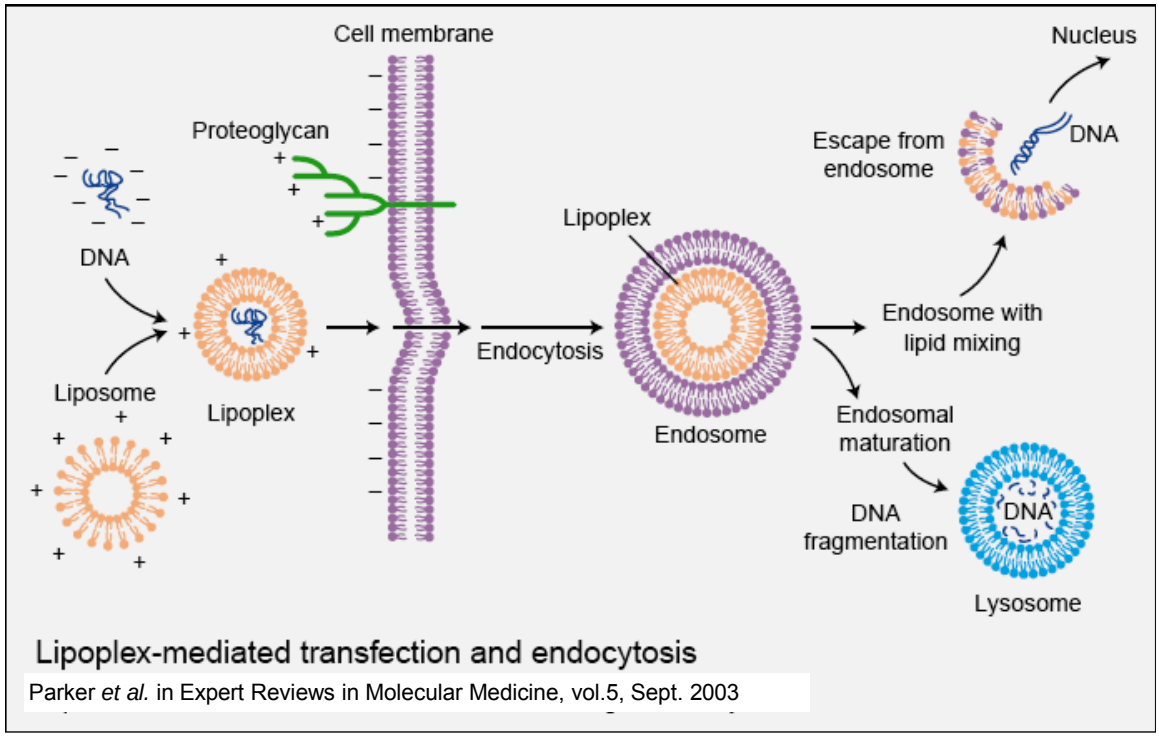

Figure 1.3.4-1. Model summary of cellular delivery of DNA with surfactant vectors. Cellular internalization is an important step in gene delivery. As shown, internalization is achieved here through endocytosis [100].

Endocytosis resulting from proteoglycan interactions [101; 102] can be effective *in vitro*. However, internalization can be increased several fold through ligand-receptor interactions, which can be elicited by attaching ligands to lipoplexes via polymeric tether. Fusion (cell-lipoplex fusion) makes a minimal contribution to internalization [37; 103] (Figure 1.3.4-1), and permits the entry of only the contents of lipoplexes [104; 105]. Fusion, also described as lipid-mediated poration, results from mixing or rearrangement of constituent amphiphile molecules (gemini surfactants, lipids) [17] from vesicle bilayer membrane of lipoplexes and the phospholipid bilayer membrane of cells. The result is a change in membrane conformation that leads to creation of an open channel or pore between a previously attached lipoplex and a cell [92].

Endosomal escape of endocytosed lipoplexes must occur before endosomes advance into a powerful hydrolytic state (low pH) or ultimately fuse with lysosomes. Though DNA is protected in lipoplexes, its degradation is inevitable unless there is endosomal escape (Figure 1.3.4-1) [40]. In reality, only a fraction of lipoplexes make it to the cytoplasm, the rest being destroyed in the destructive, hydrolytic phase involving endosomes and lysosomes [3]. As such, assisted endosomal escape by the use of gemini surfactant-based or other molecular delivery systems capable of bilayer-to-micelle or lamellar-to-inverted hexagonal (H_{II}) transition is helpful [106-108]. After endosomal escape, dissociation of lipoplexes should allow nuclear entry of DNA. This entry of unbound, decondensed DNA competes with its rapid degradation by cytoplasmic nucleases. The timeliness of this step is key to getting increased transfection [17; 33]. In many cases, the amount of DNA making successful entry into the nucleus (through nuclear pores) is further reduced.

Though gene expression is achieved from the delivery of target-free DNA [109], the possibility of better gene expression from the use of targeted DNA exists. Cytoplasmic receptors (importins) responsible for the transport of oligopeptides (and other proteins) to and from the nucleus (nuclear localization) are constantly shuttling across the nuclear membrane [65]. This offers an opportunity to tag recognition molecules (such as oligopeptide moieties) to DNA. The tagged DNA can then be picked and expressly transported to the nucleus, allowing DNA to escape degradation by cytoplasmic nucleases. Enhanced gene expression via nuclear localization signals has been reported [110; 111]. Nuclear entry can also be increased in dividing cells, as there is transient opening of their nuclei. This, however, may not be easily employed for routine delivery of DNA.

1.4. Clinical Opportunities for Gene Therapy

Of the many areas into which gene therapy research has diversified, such as gene (therapy) delivery to the lungs [112-114], kidney [115], heart [5], muscles [116], and to cell categories such as macrophages [11; 117], and the haematopoietic system [118; 119], the opportunity provided by topical delivery in particular holds the key to many prospects. Topical gene delivery, a mode of transfer of DNA to skin cells and hair follicles, is gaining increasing popularity for a variety of applications ranging from alopecia treatment to DNA vaccination [120]. Also for the skin, dermal delivery systems provide a means of transferring DNA, which can be taken up and expressed by follicular and dermal stem cells to obtain local or systemic effects [121; 122].

1.4.1. Gene Delivery via the Topical Route

Opportunities for treatment of pathological conditions (localized or systemic) via transfer of genes to and across the skin are many [123; 124]. The skin is the largest tissue in the body [125], which makes it the most accessible, exploitable port of entry for therapeutic agents, including therapeutic genes and DNA vaccines [126]. Topical delivery to the skin is pain-free, eliminates the need for invasive procedures (such as microinjection, which typically causes pain), and minimizes cost related to the use of expensive, invasive technology or equipment (such as microinjection and gene gun). It provides a proximal route of delivery for localized skin conditions, which could potentially increase bioavailability compared with systemic administration in which non-specific reactions and particle removal by the reticuloendothelial system can significantly reduce bioavailability [127].

Given the opportunities of genetic treatment and genetic immunization (Sections 1.4.2, 1.4.3, ahead) that can be elicited in the skin, delivery systems are being sought that will allow improved permeation by way of effective penetration through the outermost stratum corneum into and beyond the inner layers of skin. Use of penetration enhancers is sometimes resorted to because the skin naturally presents a tight chemical-assisted physical barrier against invading pathogens and particles [126]. The stratum corneum is a major barrier against percutaneous adsorption, and yet is also the main pathway for penetration after topical administration [128]. Permeation through the skin is enhanced by gemini surfactants (and lipids), which primarily function as delivery systems. These compounds are able to loosen or fluidize the lipid matrix of the stratum corneum which are made of double-layered lipid membranes [129]. The hair follicle,

which is appendaged to the skin, can be selectively targeted for delivery as has been shown by Hoffmann and Li. The authors observed that liposome-follicle-targeting delivery allowed delivery of exogenous melanin to hair follicles in hair-producing histocultured skin [122]. The same authors previously showed that phosphatidylcholine-containing liposomes can deliver DNA directly into the hair follicles of histocultured skin [130].

1.4.2. Keratinocyte Gene Delivery and Dermal Gene Therapy

PAM 212 keratinocytes, a cell line developed from BALB/C mice, were used in this research as model skin cells for which gene delivery applications could be targeted. The introduction and expression of exogenous genetic material in cultured keratinocytes, which undergo terminal differentiation and mimic many of the biochemical and genetic properties of the intact epidermis, have enabled researchers to culture epithelial autografts used for treating burn patients. The expression of appropriate transgenes in keratinocytes can also enable transduction-mediated correction of mutant keratinocytes from patients with lamellar ichthyosis. Such corrected keratinocytes when transplanted to nude mice results in the formation of normal epidermal tissue [131]. Transduction-mediated gene expression in keratinocytes also provides the opportunity to deal with various abnormal skin conditions.

A variety of genetic or acquired conditions occur in humans in which the normal function of skin is altered, calling for gene-mediated correction of such conditions. Gene transfer to the skin has been employed to assess genetic treatment of skin cell carcinoma (cancer or tumour in skin) [124], scleroderma [132], acute and chronic skin wounds [133], and xeroderma pigmentosum (XP) [134]. Malignant melanoma and squamous

cell carcinoma are two cancer types that affect the skin. Most skin cancers have been traced to mutant genes, and UV radiation is considered the commonest risk factor [134], with its damaging effect on DNA. However, providing the functional copies of relevant genes [135] to especially XP individuals, who are hypersensitive to sunlight and are predisposed to skin cancer [136] (~1,000-fold increased risk), prevents the development of cancer at sun-exposed areas, primarily the skin (e.g., squamous cell carcinoma) [137-139]. In XP patients, who typically have inactivating mutations in one of seven genes designated as *XPA* – *XPG*, nucleotide excision repair of sunlight-damaged DNA is impaired [140]. The functional copy of *XPA* gene when transferred to the skin (basal keratinocytes) expresses the XPA protein, which plays a role in initial damage recognition needed for nucleotide excision repair, and stabilizes the multiprotein repair complex assembled at the site of DNA damage [140]. Successful repair and stabilization ultimately stops the initiation of squamous cell carcinoma. In the absence of genetic treatment, the surest way for XPA patients to be safe is to stringently avoid all ultra-violet B radiation from their very early childhood [141-144].

Similarly for scleroderma, a skin condition which arises from overproduction and deposition of collagen by fibroblasts [145], transfer of T-cell-derived interferon-γ (IFN-γ) gene to fibroblasts and the consequent reduction of fibroblast collagen synthesis as well as repression of fibroblast proliferation (observed *in vitro*) indicates the possibility to genetically treat scleroderma via expression of IFN-γ protein [132]. Indeed, Jimenez *et al.* [146] reported an improvement in the skin from an early treatment of scleroderma via transfection-assisted expression of exogenous IFN-γ gene. Badea *et al*. [132] have recently shown similar enhancement in skin condition using gemini surfactant-based dermal delivery for the interferon gene. Acute and chronic skin wounds are yet other

types of skin defects for which potential treatment lies in gene therapy. A group of proteins including platelet-derived growth factors [133] and vascular endothelial growth factors [133] promote and accelerate wound healing. But the commonly noted drastic reduction of the physiological half-life of purified or recombinant peptides after application to affected skin limits protein-mediated treatment of these defects [147]. The transient cutaneous transgene expression of these proteins marks an improvement over the use of synthetically derived proteins. Transgene expression relies on the cellular machinery of the host to locally manufacture the needed proteins, eliminating problems associated with shortened half-life of topically applied proteins [120]. Transgene delivery to the skin thus holds a viable alternative for the treatment of skin wounds and ulcers.

Advances in gene therapy have gone beyond the skin to include hair follicles, which are a complex appendage of the skin. Hair serves important functions for humans, both cosmetically and by scalp protection, and the hair follicles produce sweat gland products that help to balance body temperature and release pheromones [148]. However, loss of hair pigment and hair itself (e.g., during aging), and conditions including albinism and severe hair loss either caused by alopecia areata or chemotherapy, can be of concern to those affected. There have been few treatments for the underlying causes of hair changes during aging or as a result of the aforementioned disorders, and gene therapy is expected to settle all such problems [120]. Following Li and Hoffman's [122] earlier demonstration of selective gene therapy of hair follicle in mice via topical application of liposomes-entrapped *lacZ* reporter gene, Alexeev *et al*. [149] advanced the approach by using an RNA-DNA (chimeric) oligonucleotide to correct albino mutation of the mouse tyrosinase gene. Chimeric oligonucleotides when placed in hair follicle melanocytes are

able to correct albino point mutations by using the cellular machinery for homologous recombination and mismatch DNA repair [150]. The correction restores tyrosinase activity and activates concomitant melanin synthesis, resulting in the production of pigmented hair shafts in albino mice. The effect lasted for three months. The same chimeric oligonucleotide was previously shown by Alexeev *et al*. to correct the albino mutation in cultured melanocytes, rendering clonal, heritable melanin production, as exhibited in the *in vivo* study mentioned above [151].

Genetic corrections of not only unpigmented hair (albinism) but also conditions of loss of hair such as alopecia universalis or baldness have been researched. Sato *et al*. [150; 152] showed that antigen development leading to production of hair shaft could be stimulated in C57BL/6 mice via transfer of the sonic hedgehog (*shh*) gene. With the cloning of the human hairless gene [153], which is responsible for alopecia universalis, a stage has been set for the genetic correction of hairlessness in humans [120].

1.4.3. DNA Vaccines for Genetic Immunization

The skin is a site at which important cellular and molecular-level immunologic responses to foreign species and tissue-specific antigens originate [125; 154]. This provides the basis for development of DNA vaccines, targeting the skin or for administration via the skin in order to mitigate disease states prophylactically. DNA-mediated immunization involves delivery of plasmid DNA (i.e., DNA vaccine) encoding for a protein-antigen (from a pathogen) into cells of the skin (such as keratinocytes). Genetic immunization takes advantage of the fact that host cells produce appropriate antigens *in situ* which, when presented to the immune system including T lymphocytes (by antigen-presenting cells), induce specific cytotoxic T lymphocyte response via MHC

class I-restricted pathway. As well, antigens released extracellularly are linked to the induction of humoral response and helper T lymphocytes (Th) via MHC class-II restricted antigen presentation. Keratinocytes can be transfected to produce antigens of interest, which can be presented to CD4+ T or CD8+ T cells, also directly [155; 156]. Langerhans cells are capable of migration and are able to present antigens to lymphoid tissues to induce immune response from T lymphocytes. Antigen-specific immune responses induced by DNA vaccines give protection against infectious diseases caused by viruses, bacteria, and parasites. Other diseases such as cancer, allergy and autoimmunity are also targeted for DNA vaccination [157; 158]. DNA vaccines encoding antigens as well as cytokines can express the two types of molecules concomitantly for enhancement of immune response. IFN-γ (a cytokine), for example plays an active role in cellular immunogenicity, is observed to arrest progress of mice lymphoma and destroy existing tumours [159]. Fan *et al* [160] have shown that topical application of DNA encoding the hepatitis B surface antigen (HBsAg) elicits an antigen-specific immune response. This depends on the presence of normal hair follicles, suggesting that follicular cells could be made targets of DNA vaccination to take advantage of their special protein synthesis.

1.5. Genes and Biomaterials for Gene Therapy

The nature of clinical benefits and applications to basic science research that can emerge from gene delivery is diverse. Added to this, research has focused on the development of DNA-based products (e.g., plasmids) and biomaterials, including gemini surfactants, lipids and polymers for use as gene delivery systems. The molecules of gene delivery systems have functional groups or other structural components that can be

modified to improve the functional effectiveness of the biomaterials they constitute. These biomaterials yield better safety, allow ease of manufacture and structural manipulation, encapsulate and preserve the activity of therapeutic DNA. They thus represent ideal models for realizing ultimate drug delivery in humans. However, current hurdles associated with them include low gene delivery efficiency.

1.5.1. DNA-based Therapeutic Materials

Since the double helix structure of DNA (Figure 1.5.1-1) was elucidated in the 1950s through the combined research of Watson and Crick [161; 162] and others such as Wilkins and R. Franklin [163-165], a large proportion of scientific research has evolved based on DNA. Some of this research has focused on concepts such as gene therapy, which is expected to have a greater impact in the fight against diseases. The two complementary polynucleotide strands of DNA, which run head-to-toe [166; 167], are held on to each other by hydrogen bonds. Each strand is a long polymer of nucleotides (i.e., a polynucleotide chain). The nucleotide units are in turn made of a sugar (deoxyribose), a phosphate and one of five kinds of nucleobases (per nucleotide). Nucleotides on adjacent single strands are held to each other through hydrogen bonding creating the double strand helix. The pairings are predetermined such that only the following possible pairings are allowed: adenine–thymine, thymine–adenine, cytosine–guanine and guanine–cytosine. A fifth base, uracil is rarely found in DNA, except as a result of chemical degradation of cytosine, or in some viruses, notably PBS1 phage DNA, where uracil completely replaces the usual thymine in its DNA [166-168].

DNA, most of which is found in the cell nucleus and the rest in mitochondria (in the case of eukaryotic cells), contains genetic information that is passed down from a parent

to its progeny. The correct (and precise) sequence of base pairs ultimately determines the specific sequences of amino acids in peptides, enzymes and other proteins, and is essential for every gene to function normally [166; 167]. On rare occasions, incorrect pairing does occur, or the full sequence for a particular gene can be missing. Such genetic anomalies lead to deficient gene function or entire loss of gene function, both of which entail serious health consequences. Imperfections in DNA, referred to as mutations, are due not only to incorrect base pairing, for instance during synthesis of a new DNA strand, but can also occur after chemical damage by mutagens or UV damage [166]. Cells may or may not be able to successfully repair mutant genes by themselves.

When mutation leads to conditions such as adenosine deaminase (ADA) deficiency, a correction of the condition to normalcy can be accomplished by introducing normal exogenous DNA or transgenes, referred to as therapeutic DNA, usually into the nucleus of affected cells. For instance, in adenosine deaminase (ADA) deficiency the normal ADA gene (the therapeutic DNA coding for the enzyme adenosine deaminase) can be transferred to white blood cells or bone marrow cells [169] for protein synthesis and thus correction of the deficiency. The structure, size (weight) and charge of DNA constitute important parameters that can either present challenges or be manipulated to advantage in application-based DNA research. Of the three slightly different geometries of DNA, the "B" form described by Watson and Crick is thought to be predominantly native to cells. It is 2 nm wide and extends 3.4 nm per 10 bp of sequence (Figure 1.5.1-1). The actual size ranges from tens of base-pairs to over thousands of base-pairs, and depends on the particular piece of genetic material and the regulatory sequences present [166]. For instance, there are approximately 220 million bp in human chromosome number 1, making it the largest chromosome in humans [170; 171]. Whereas DNA can be in many

cases linear (such as during replication), the ends of a piece of double-helical DNA can be joined so that it forms a circle, as in plasmid DNA. The phosphate groups account for the negative charge of DNA.

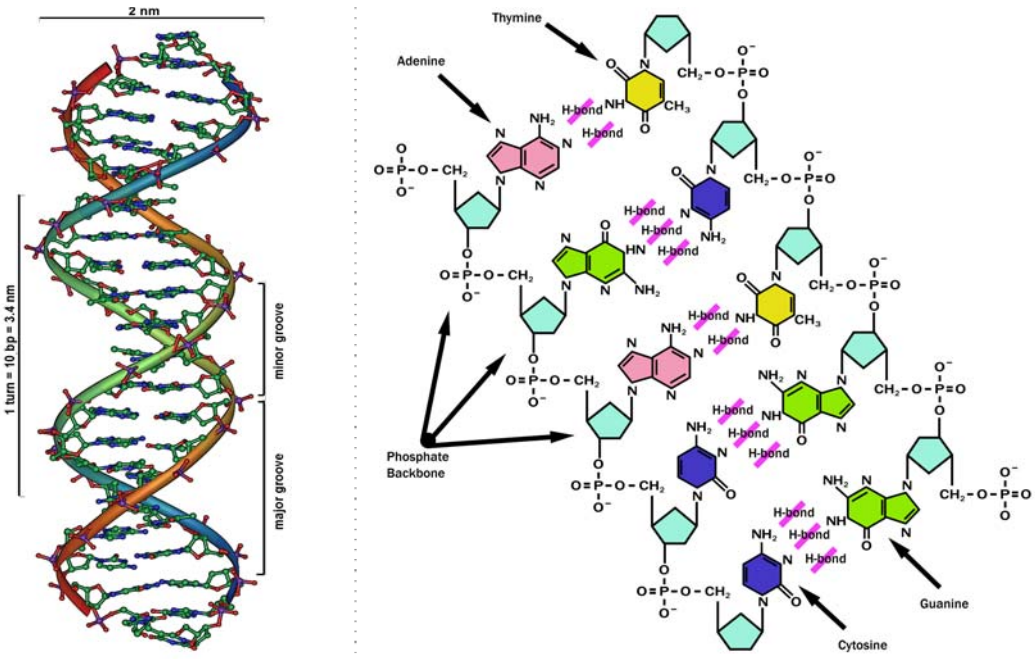

Figure 1.5.1-1. Structure of DNA.
To the left of the figure is shown the double helix of DNA, portraying the major and minor groove. To the right is the chemical structure showing connections between phosphates, deoxyribose sugar groups and various nucleobases. Hydrogen-bonded base-pairs are also shown. Adopted from www.wikipedia.com in accordance with GNU General Public License policy [166].

1.5.2. Advantages of DNA-based Therapeutics

Because of the specificity that underlines the action of a gene, therapeutic agents modelled on the structure of DNA offer rare advantages over currently used low molecular weight pharmaceuticals [5]. For instance, whereas the later typically show less specificity, their DNA-based counterparts have high specificity and selectivity for recognition of their molecular targets, which means reduced incidence of drug toxicity, fewer negative side-effects, and safer drugs [157]. In addition, a therapeutic transgene after insertion into the genome of a cell can express a protein persistently, meaning long therapeutic half-life relative to synthetic, therapeutic proteins, which typically have shortened half-lives. Proteins synthesized *in situ* from therapeutic DNA are without the toxicities associated with high levels of intravenously administered proteins, and mammalian post-translational modifications of *in situ* produced proteins eliminate other challenges (such as incompatibility) associated with making recombinant proteins in non-mammalian hosts [157].

For instance, although live attenuated virus vaccines have existed before DNA vaccines and have been extremely effective against a variety of diseases in both the past and present (including the elimination of small pox), the risk of their reversion to the wild-type, though probably a remote possibility, cannot be dismissed. In the special case of HIV, viral vaccine development must occur with great caution because of the threat that the virus-based vaccine could revert to the wild type responsible for the disease. Against this backdrop, DNA vaccines are emerging as an ideal class of vaccines. Their manufacture can be fairly less resource-demanding relative to traditional live viruses that require significant effort for proper pathogen attenuation and design of cellular

production systems [157]. For diseases with multiple virus strains such as HIV or influenza, their viral vaccines have to be reformulated to antigens for evolving strains. Not only is this resource demanding or poses a problem for the yearly supply of vaccines, but such vaccines also give no protection against epidemic strains that may arise in the very near future. Most notable is the novel pandemic strain of influenza in the infamous 1919 Spanish Influenza that killed millions of people worldwide. In contrast, it has been demonstrated that a DNA vaccine made from the genetic sequence of one influenza virus strain can protect against a subtype, and this is a relieving indication that DNA offers the opportunity to make vaccines for diseases with multiple strains [157].

1.5.3. Gemini Surfactants for Gene Delivery

Gemini surfactants, or simply bis-surfactant molecules, are attracting increasing interest in research as non-viral gene delivery systems. The term "gemini," meaning "twin," has been traced to Menger who originally coined the term in 1991 to describe bis-surfactants [35] (Figure 1.4.3-1). Bis-surfactants were generally not new around that time; some studies on bis-surfactants occurred well in advance of Menger's work [172-176]. But there was a renaissance, triggered by Menger's work, in the synthesis and material property studies of these types of surfactants due to new potential applications including gene therapy. The specific gemini surfactant molecules, synthesized and studied by Menger, were made by coupling two individual surfactant molecules by a rigid spacer. The individual surfactants used for making gemini surfactants, whether now or then, usually have a polar/ionic headgroup and a nonpolar hydrocarbon moiety or tail [35; 90; 177; 178]. Over time, non-rigid spacers [90; 177; 179-182], many of

which are symmetrical [33] (but may be asymmetrical), were also used for gemini surfactant synthesis. Using the effective tool of synthesis, gemini surfactants exhibiting special and enhanced properties (including vesicle formation) relative to the early ones have been synthesized and reported in the literature.

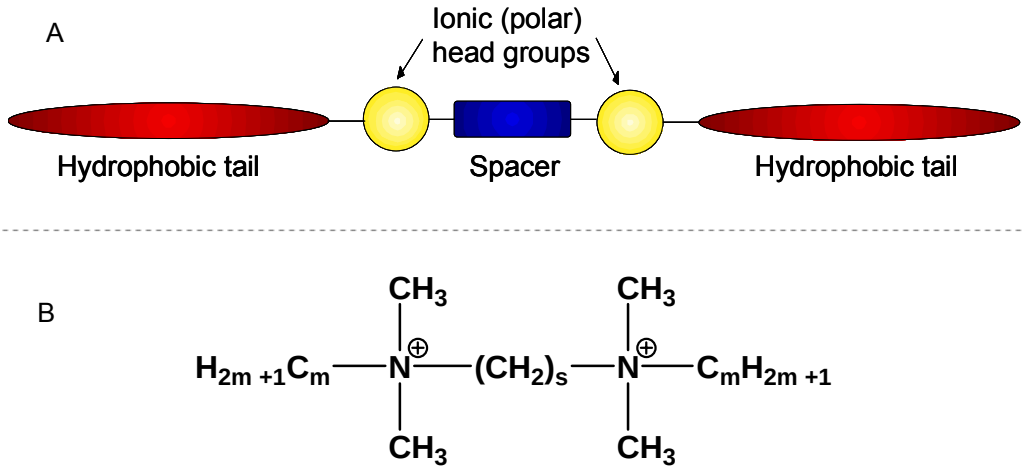

Figure 1.5.3-1. General structural schemes of gemini surfactants.
(A) General structure, showing how any two monomer surfactants can be connected using a spacer group. (B) Structure of the m-s-m gemini surfactants. Two traditional monomeric surfactants with C_m alkyl tails are connected at their quaternary ammonium heads via a polymethylene chain containing **s** methylene units. That is, m = number of carbons in the hydrocarbon or alkyl tail, s = number of methylene units in the spacer chain.

Of the properties of gemini surfactants (dimers), their greatly enhanced ability to spontaneously aggregate [35; 36; 183] (~1000-fold superiority over monomer surfactants [33]) into complex structures including micelles, bilayers and vesicles put them at the front line of drug delivery. Their extremely low critical micelle concentration (CMC) [33; 35; 36] allow these surfactants to effectively package or encapsulate DNA, and this is an important first in gene delivery. Low CMC values are also essential for minimizing the amount of gemini surfactant used to achieve gene delivery, which is in turn essential for ensuring an optimal safety profile of any foreign compound used in a biological host, as well as ensuring reduced cost [33].

The gemini surfactants encountered in gene delivery are generally symmetric, with their headgroup being made of quaternary ammonium, or primary, secondary or tertiary amines groups. Such kinds of headgroups (cationic or protonable) present the necessary features for binding to the negative phosphate groups in DNA, so as to neutralize and condense DNA [33]. The simplest gemini surfactants (according to the general structure in Figure 1.5.3-1) which can be used for gene delivery have a divalent (dicatonic) head made of two quaternary ammonium groups and two hydrocarbon tails (usually $C_8 - C_{18}$). Such a combination of head and tail ensures the presence of the cationic character necessary for neutralizing and compacting DNA, and the presence of the hydrophobic moiety to initiate co-aggregation with DNA to form vesicle-DNA complexes. Advances in organic synthesis allow for making gemini surfactants [90] with multivalent headgroups [73] for improved DNA compaction, implying that synthetic expertise could be used to modify and tailor properties of gemini surfactants for application in gene delivery.

1.5.4. Condensation of DNA in Gene Delivery

The first important characteristic of an effective molecular gene delivery system is its ability to spontaneously interact with DNA. Cationic delivery systems have evolved with the ability to efficiently neutralize, condense and encapsulate DNA into complexes whose sizes range from less than 100 nm to about 1000 nm, depending on the molecular system and other factors [184; 185]. Such interactions allow the shape and size of macromolecular DNA to be changed into a form (i.e., into complexes) readily taken up by cells, without loss of biological function of the genetic material [186; 187]. The complexes formed between cationic polymers and DNA, and referred to as polyplexes, generally have smaller sizes due to more efficient DNA condensation by the polymers [188; 189]. Complexes formed between DNA and the relatively smaller cationic lipids or surfactant molecules (these complexes are termed lipoplexes), on the other hand, can have fairly large sizes. For both lipoplexes and polyplexes, the size of complexes displays some dependence on the cationic molecular agent-to-DNA charge ratio [105; 190-194]. As noted earlier, the neutralization, condensation and encapsulation of DNA is achieved through a combination of interactive forces. These include electrostatic forces (between phosphate groups of DNA and positive charges from a cationic molecular transfection system) and hydrophobic–hydrophobic as well as van de Waal's interactions, which allow for self-association of the hydrophobic moieties of gene delivery molecules to form micelles or vesicles [33; 195].

The positive charge in cationic lipids or surfactants are usually concentrated on the polar headgroups, more commonly termed cationic headgroups, while the positive charge of cationic polymers are incorporated along with the repeating units of the

polymer chain. Because of the important role of the cationic headgroups, many investigations have focused on the number of positive charges and their chemical structure (which predominantly fall into the following categories: quaternary ammonium, or primary, secondary or tertiary amines). Univalent cationic lipids, such as DOTMA (the first to be used for transfection [37]) and sphingosine [196], contain one quaternary ammonium and one primary amine, respectively, for interaction with DNA. However, such lipopolyamines or multivalent lipids as DOGS and DOSPA contain 4 and 5 amine or ammonium groups, respectively, which give them the ability to interact with and condense DNA more efficiently, and to transfect cells more efficiently [95; 197; 198]. As a result, both DOGS and DOSPA are commercially available. Within the context of efficient interaction with and condensation of DNA, cationic gemini surfactants present cationic headgroups, which at minimum are divalent. This is because gemini surfactants contain two separate monomeric surfactants chemically linked through a spacer (see general structure, Figure 1.4.3-1), a concept that has also been extended into 'gemini lipids' [199; 200]. By virtue of the wide scope of structural variation permitted by the polar or cationic headgroup, a significantly large number of gemini surfactants have been developed and investigated based on the rationale of enhancing interactions with DNA, improving the interaction profile in biological hosts and ultimately increasing transfection efficiency. Wettig *et al*. [86] have recently reviewed and classified gemini surfactants that were investigated for DNA transfection in various reports into four comprehensive categories: (1) m-s-m [132; 201-204], (2) carbohydrate-based [33; 52; 205-209], (3) peptide-substituted [33; 73; 210; 211] and (4) disulfide-containing gemini surfactants [212-216]. Similar to lipids, the improved interaction of DNA with developed gemini surfactants containing multiple amine or

quaternary ammonium groups or both kinds of groups, combined, gives efficient DNA condensation as well as increased transfection.

2. PURPOSE OF RESEARCH

2.1. Current Perspectives on the Hurdle of Non-viral Gene Delivery

The path or assisted path of a gene, transported by molecular delivery systems, from the route of administration to the nuclei of target cells is complex. Whether or not there is eventual nuclear delivery, and the efficiency of delivery is dependent on a rather large number of factors [33; 191; 217]. As a result, the efficiency of gene delivery using molecular delivery systems still ranges from very low to modest, especially relative to viral-mediated gene delivery. As a way to improve the delivery efficiencies of molecular systems, considerable attention is being paid to the factors that come into play as a genetic material is 'cargoed' to the cytoplasm or further into nucleus of a cell via a molecular system. These factors can be grouped into two main categories. The first is the type of target cells (or tissue), and the second relates to the properties of the molecular system. From the view point of synthetic and material science, the properties of molecules can be tailored to allow them to mediate gene delivery at significantly higher efficiencies [33; 65; 195] using carefully conceived molecular design approaches. In fact, non-viral gene delivery has already evolved from an early generation of molecules, which achieved very low transfection efficiency, to the recent generation of molecules, which yield remarkably improved efficiency.

2.2. Rationale for the Focus of this Research

Gemini surfactants, as a focus of this research aimed at developing non-viral vectors for gene therapy, have a general structure that presents an unlimited versatility in their design and synthesis. This gives a significant opportunity in the search for clinically efficient gemini surfactant molecules for routine gene therapy applications. For gemini surfactants to pass a test of optimal utility in gene therapy, the surfactant molecules must meet important requirements; these include the ability to efficiently mediate gene delivery and to exert minimal or no toxic effects on their biological hosts. This calls for the use of rational design schemes for generating and testing gemini surfactants. Through rational design, gemini surfactants are progressively modified with reference to chosen compound templates, making a defined structural modification per step. This allows certain properties to be conferred on the surfactants for subsequent testing in biological hosts. The larger goal of the design process is to improve the particle properties of gemini surfactant-based DNA transfection complexes. This would improve their interaction characteristics with host cells and lead to efficient DNA transfection.

2.3. Hypotheses

The various non-viral gene delivery molecules that are currently studied in research, such as gemini surfactants, must be able to achieve a number of critical functions, above which any molecular gene delivery agent will be able to attract attention to its potential. Thus, among other important things these molecular agents should be able to spontaneously interact with DNA and create effects including:

- compaction of DNA into nanometre-scale particles,

- electrostatic binding of the compact nanoparticles to cells, and
- after passage of nanoparticles into cells, the gene delivery molecules should dissociate from the DNA to allow subsequent protein expression either after nuclear translocation of DNA or after recognition of its presence in the cytoplasm by cellular protein expression machinery.

Hypothesis:

It is therefore hypothesized that for the purpose of improving cellular gene delivery,

- **Imino-substitution in gemini surfactants induce endosomal escape**

This hypothesis relates to the release of DNA encapsulated within the gemini surfactant vesicles. An indicator to signify (or validate) release of DNA during cellular transfection will be a higher level of transfection efficiency imino-substituted gemini surfactants relative to an appropriate 'negative gemini surfactant control'.

2.4. Objective of Research

This research is focused on the overall objective of developing new gemini surfactant-based non-viral gene delivery systems for gene therapy applications. First, a library of gemini surfactants will be created from a process of gemini surfactant design and synthesis. Second, these surfactants, after preparation into transfection systems and characterization, will be applied in transgene delivery experiments and the level of gene expression evaluated. This ultimately allows the transfection abilities of constituent surfactants to be assessed. To ensure that emerging gemini surfactants with high

transfection abilities also have low/acceptable level of toxicity, transfection-related toxicity experiments were run alongside transgene delivery experiments.

2.4.1. Specific Objectives

To achieve the overall goal of this research, the major objective has been restated into specific objectives. These include:

1. Rational design, synthesis and characterization of gemini surfactants,
2. Preparation and characterization of gemini surfactant-DNA nanoparticles, i.e., transfection complexes,
3. Transfection pre-screening in COS-7 cells and quantitative gene expression studies of plasmid DNA delivered to PAM 212 cells, and
4. Toxicology studies of COS-7 and PAM 212 cells involved in transfection pre-screening and quantitative gene expression studies, respectively.

2.5. Outline of Proposed Research

1. Preparation of gemini surfactants for creation of surfactant library
    a. Synthesis
    b. Isolation and purification
    c. Structural confirmation and purity assessment

2. Preparation and characterization of gemini surfactant-DNA nanoparticles

a. Preparation of gemini surfactant-based DNA transfection mixtures (complexes) using gemini surfactants obtained from a rational design scheme (Table 3.1.2-1)
b. Determination of physicochemical properties of gemini surfactant-DNA nanoparticles:
    i. Determination of size and zeta potential
    ii. Determination of particle morphological distribution

3. Transfection of COS-7 cells in a pre-screening phase using 12-spacer-12 surfactants (Table 3.1.2-1)
    a. Quantitation of luciferase gene expression in COS-7 cells after transfection with gemini surfactant-based transfection mixtures containing luciferase plasmid

4. PAM 212 cell ultrastructural studies and stereological examination
    a. Electron microscopic examination of the cells, including size and morphologies adopted by the cells

5. Transfection of PAM 212 cells using three different gemini surfactant series (m-3-m, m-7-m, m-7NH-m) – advanced transfection phase
    a. Quantitation of luciferase gene expression in PAM 212 cells after transfection with gemini surfactant-based transfection mixtures containing luciferase plasmid: various composition of mixtures, time study of gene expression

6. Toxicology studies on COS-7 and PAM 212 cells

    a. Measurement of cell viabilities of transfected cells for assessment of the level of cellular toxicity caused by transfection

3. MATERIALS AND METHODS

3.1. Gemini Surfactants

The gemini surfactants investigated in this study were each enlisted to fit within a rational design scheme that will enable the determination of organic structural units or moieties as well as the architectural arrangement of these units/moieties within a molecule that is necessary for achieving effective DNA transfer to cells. Equally importantly, any features (architectural, structural units/moieties) that derail the ability of a molecule to transfer DNA to cells, if noted, will be indicated. Out of a library of over 30 gemini surfactants designed and synthesized for testing of their transfection abilities, 14 surfactants, each of which falls into at least one of four categories below, were investigated over the course of this study.

	Surfactant series	**Members**
1.	12-spacer-12	12-3-12, 12-5N-12, 12-8N-12, 12-7N-12, 12-7NH-12
2.	m-7NH-m	12-7NH-12, 16-7NH-16, 18-7NH-18, 18:1-7NH-18:1
3.	m-3-m	12-3-12, 16-3-16, 18-3-18, 18:1-3-18:1
4.	m-7-m	12-7-12, 16-7-16, 18-7-18

3.1.1. Synthesis

1. Synthesis of the five 12-spacer-12 surfactants used in this research (namely the 12-3-12 [218], 12-5N-12, 12-8N-12, 12-7N-12 and 12-7NH-12 [219] surfactants) was carried out in work done prior to this research. However, to cater for arising needs, synthesis of the 12-7NH-12 surfactant, which also belongs to the m-7NH-m series, was repeated in this study, making it available in sufficient quantities (synthesis is described below). In both previous work and work under this study, the syntheses of all gemini surfactants followed the general scheme described by Menger and Littau [35; 36]. Figure 3.1.1-1 (below) exemplifies the routine procedure for generating gemini surfactants in this research, with specific reference to the 18-3-18 surfactant.
2. Following previous synthesis of the 12-7NH-12 gemini surfactant [219] belonging to the m-7NH-m series, the 12-7NH-12 surfactant was resynthesized. The higher members (having longer tails, i.e., m = C_{16}, C_{18}, C_{oleyl} representing oleyl chain) were synthesized as follows: the surfactants resulted from the reaction of 1 equivalent of 3,3'-iminobis(N,N-dimethyl-propyl amine) (Aldrich) with 2.1 equivalents of the appropriate tail group in acetonitrile or anhydrous acetonitrile in the case of unsaturated tail species. The species 1-bromohexadecane (C_{16}), 1-bromooctadecane (C_{18}) and 1-bromo-*cis*-9-octadecene (C_{oleyl}) (all from Aldrich) were used as tail groups. Prior to its use, 1-bromo-*cis*-9-octadecene was obtained by conversion of the corresponding *cis*-9-octadecen-1-ol into the bromide compound using a previously described conversion method [220]. The conversion was by addition of solid Ph_3PBr_2 (10.62 g, 24.18 mmol, 96% purity, Aldrich), over the course of 10 min, to a solution of *cis*-9-octadecen-ol (5.74 g, 18.62 mmol, 85% purity, Spectrum) and

pyridine (2.33 g, 29.78 mmol, 99.8% purity, Aldrich) in anhydrous acetonitrile (36 mL) maintained at 0 ^{o}C. The complete mixture was stirred for 1 h (disappearance of alcohol checked by TLC) and was filtered through a short pad of silica gel. The recovered filtrate was rinsed with l:10 ether/pentane (200 mL). A final mass of 4.64 g (14.00 mmol, 75% yield) of pure 1-bromo-*cis*-9-octadecene was obtained upon further work up.

3. Previous synthesis of the m-3-m surfactants carried out prior to this research made available the 12-3-12 [221], 16-3-16 [222] and 18:1-3-18:1 [223] surfactants. These previous syntheses were accomplished via a bis-Menshutkin reaction of 1 equivalent of tetramethyl-1,3-propanediamine with 2.1 equivalents of the appropriate alkyl bromide (saturated or unsaturated). Thus, for the synthesis of 18-3-18 surfactant, which was carried out in this research, 1 equivalent of 1,3-dibromopropane (Aldrich) was reacted with 2.1 equivalents of N,N-dimethyloctadecylamine (Akzo Nobel) using the bis-Menshutkin method.
4. The m-7-m surfactants were synthesized from reaction of 1 equivalent of 1,7-dibromoheptane (Aldrich) with 2.1 equivalents of either N,N-dimethyloctadecylamine (Akzo Nobel) or N,N-dimethyl-n-hexadecylamine (TCI America) or N,N-dimethyldodecyldecylamine (Aldrich).

Synthetic process – exemplified for 18-3-18 surfactant

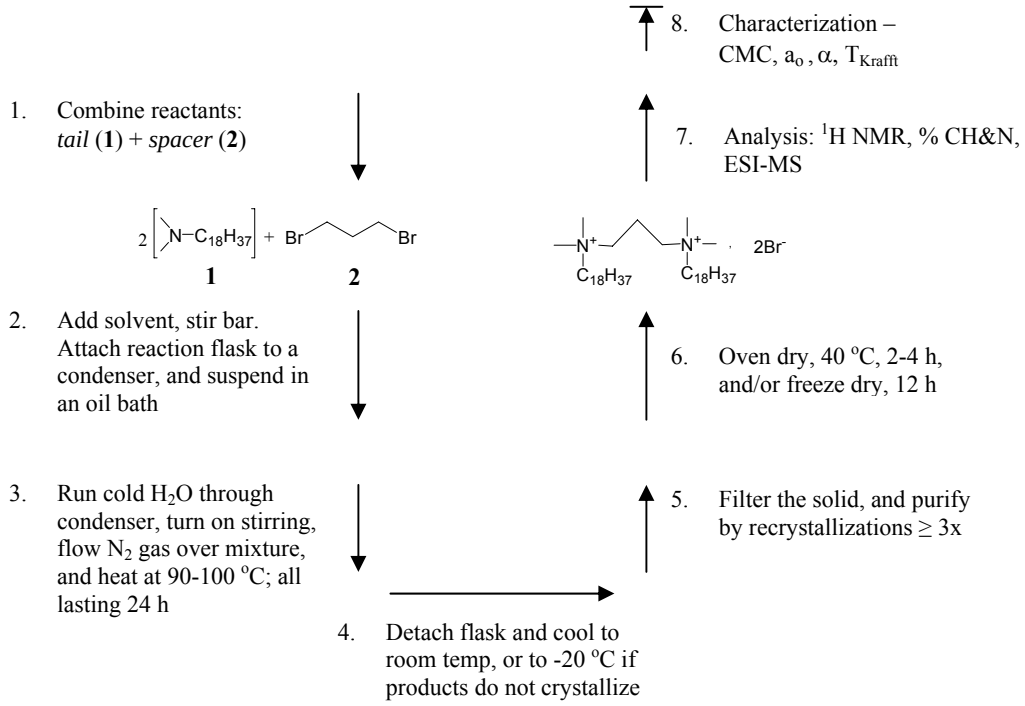

Figure 3.1.1-1. Outline of synthetic process for the target gemini surfactants.
Formation of the 18-3-18 gemini surfactant from the constituent reactants was achieved through quaternization reaction between 2 mol of dimethyloctadecylamine (i.e., the alkyl tails) and 1 mol of dibromo-1,3-propane (i.e., spacer group). The reactants can alternatively be selected such that the alkyl tail is an alkyl bromide while the propyl spacer chain bears the two terminal tertiary amine groups to be quaternized.

3.1.2. Gemini Surfactants Prepared – The Library

The reactions leading to the formation of final surfactants (Table 3.1.2-1, below) were all carried out under reflux for 24 h or more in acetonitrile, but not exceeding 72 h. The product compounds crystallized out as white solids upon cooling of each reaction. The white solids were recovered by filtration, followed by purification by several recrystallizations from acetonitrile or a mixture of acetonitrile/diethyl ether (anhydrous acetonitrile, in the case of unsaturated surfactants). Additional purification for the unsaturated surfactant 18:1-7NH-18:1 was done by soxhlet extraction in anhydrous diethyl ether for 72 h for removal of trace impurities.

Structures of the purified surfactants were confirmed by ^{1}H NMR spectroscopy ($CDCl_3$, 500 MHz Bruker) and electro-spray mass spectrometry, while their purities were verified by aqueous surface tension measurements and elemental analysis. The surface tension (γ) vs. log C plots for all surfactants showed the absence of a minimum, in the plateau region above the CMC, indicating all surfactant products were highly pure. These purity assessments are particularly important regarding the need to use pharmaceutically pure grade materials in biological hosts.

Table 3.1.2-1. Structure of the gemini surfactant candidates

1. 12-spacer-12 series

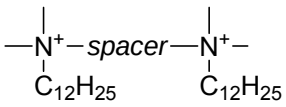

Spacer group	Symbol
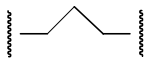	12-3-12
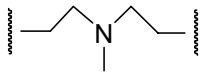	12-5N-12
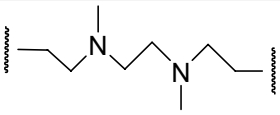	12-8N-12
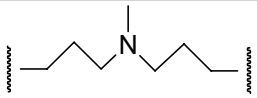	12-7N-12
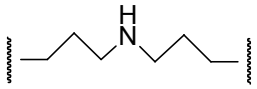	12-7NH-12

2. m-7NH-m series

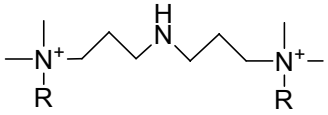

R group	Symbol
n-$C_{12}H_{25}$	12-7NH-12
n-$C_{16}H_{33}$	16-7NH-16
n-$C_{18}H_{37}$	18-7NH-18
n-$C_{18}H_{35}$	18:1-7NH-18:1

3. m-3-m series

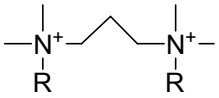

R group	Symbol
n-$C_{12}H_{25}$	12-3-12
n-$C_{16}H_{33}$	16-3-16
n-$C_{18}H_{37}$	18-3-18
n-$C_{18}H_{35}$	18:1-3-18:1

4. m-7-m series

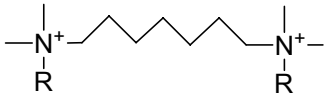

R group	Symbol
n-$C_{12}H_{25}$	12-7-12
n-$C_{16}H_{33}$	16-7-16
n-$C_{18}H_{37}$	18-7-18

The molecular properties were varied from surfactant to surfactant through variation of the nature of both the spacer and alkyl tail groups. The resultant surfactant library was assessed in terms of transfection abilities.

3.1.3. Determination of Krafft Temperatures

To guide the solution preparation process, determination of the Krafft temperatures was carried out as a step prior to the determination of critical micelle properties. Saturated surfactant-in-water solutions (prepared at ≥ 1% w/v, for surfactants with *m* = 16, 18, 18:1) were prepared by adding excess gemini surfactant to water. Conductivities of the saturated solutions were then measured as a function of increasing temperature, using a Weyne-Kerr precision component analyzer (Model 6425), to determine the Krafft temperature. The initial temperature was set to ≤ 10 ^{o}C for each set of conductivity vs temperature measurements to determine the Krafft temperature. Determination of critical micellar properties of the gemini surfactants, including critical micelle concentrations (CMC), was carried out once gemini surfactants solutions were prepared using the Krafft temperatures as dissolution guidelines.

3.1.4. Surface Tension Measurements

Surface tension measurements were performed using a Kruss (Model K10T) tensiometer, applying the du Nouy ring technique. The measured surface tension values (γ) were corrected using the method of Harkins and Jordan [224]. Experimental temperatures were maintained at 25.0 ± 0.1^{o}C (for m = 12) and 45.0 ± 0.1^{o}C (for m = 16, 18, 18:1) using a VWR Scientific (Model 1160A) circulating water bath. The stock gemini surfactant solutions were titrated into 15 mL of water and the surface tension was measured after each addition.

3.1.5. Specific Conductivity Measurements

Specific conductivities were measured using a Weyne-Kerr precision component analyzer (Model 6425) operating at 1.5 kHz in conjunction with a Tacussel electrode as employed in previous analysis [221]. The current operating cell constant of the electrode was found to be 1.52 cm^{-1}. Experimental temperatures (T ^{o}C) were maintained at 25.0 ± 0.1^{o}C (for m = 12) and 45.0 ± 0.1^{o}C (for m = 16, 18, 18:1) using a Haake (Model F3) circulating water bath. The specific conductance was measured after each addition of an aqueous solution of concentrated surfactant to 15 mL water under nitrogen atmosphere, allowing the solution to equilibrate.

Generally, preparation of gemini surfactant stock solutions prior to both surface tension and specific conductivity measurements was done using a combination of appropriate dissolution techniques including one or any combination of stirring, sonication and warming in warm water bath. Samples were then finally kept to equilibrate (overnight) at temperatures not less than the Krafft temperature for each gemini surfactant.

3.2. Characterization: Gemini Surfactant-based Transfection Systems

Solutions for individual gemini surfactants as well as the corresponding gemini surfactant–plasmid–lipid transfection mixture systems (or formulations, used for transfection) were prepared and subjected to physicochemical analyses. These analyses allow the determination of critical properties of these materials that influence or govern the efficiency of non-viral transfections, and so allow correlations to be determined between physiochemical properties and level of transfection.

3.2.1. Gemini Surfactant, Lipid Vesicles and Plasmid Solutions

Aqueous solutions at various concentrations, including notably 1.5 and 2 mM which are well above the CMC values for all gemini surfactants, were prepared and filtered through 0.2 μm Acrodisc® filters (Pall Gelman, Ann Arbor, MI, USA). Lipid vesicles were prepared as follows: 1,2-Dioleyl-*sn*-glycerophosphatidylethanolamine (DOPE) (Avanti Polar Lipids, Alabaster, AL, USA) and α-tocopherol (Spectrum, Gardena, CA, USA) in 1:0.2 weight ratios were dissolved in 100% ethanol (Commercial Alcohols Inc., Brampton, ON, Canada) and deposited as a thin film on a round-bottomed flask. The lipid film was vacuum-dried (12 h) to remove traces of solvent, followed by resuspension in 9.25% w/v isotonic sucrose (Spectrum) solution (pH 9) via sonication to yield a 1 mM solution. The final solution was filtered through 0.45 μm Acrodisc® filters giving DOPE vesicles with average size of 124 ± 5 nm (n = 3).

Two plasmids were used in this research. Luciferase plasmid (pMASIA.Luc), commonly employed to take advantage of bioluminescence analysis for the assessment of transfection levels, was propagated and purified in our laboratory prior to this research using established methods [225]. Similarly, the plasmid pGTmCMV.IFN-GFP was previously constructed in our laboratory [132], with optimized utility for analyses relating to cell transfection. Both plasmids were routinely used as 0.1 μg/μL solutions.

3.2.2. Determination of pK_a Values

pK_a values for nitrogen centres in the gemini surfactants having aza- or imino-substituents in their spacers were measured using a Beckman pH meter (Model 350) with a glass calomel electrode (Beckman Model 511083). Solutions (2 mM) of the

gemini surfactants were prepared in 1 mM NaOH to ensure complete deprotonation of the nitrogen, initially, and then titrated with 0.5 mM HCl at room temperature.

3.2.3. Measurement of Particle Sizes

Particle sizes (hydrodynamic radius, R_H) for gemini surfactant aggregates (in solution) as well as gemini surfactant-based transfection mixtures were determined as a function of pH using a ZetaSizer NanoZs working in conjunction with an MPT-2 auto-titrator (Malvern Instruments, Worcestershire, UK). The samples, each in a volume of 10 mL and having the required concentration, were placed in the titration cell of the auto-titrator and titrated (in 0.2–0.5 pH unit increments) with 0.1 M NaOH and 0.1 M HCl over the desired pH range – basic to acidic pH. The surfactant-only samples were made at pre-titration concentration of 2 mM, which is above the critical micelle concentration in all cases. Titrations for the transfection mixtures (prepared as described in Section 3.3.3.) were performed for those mixtures with a DNA:surfactant charge ratio of 1:10. The solvent medium for the surfactant-only samples was either double-distilled/deionized water (used for the 12-spacer-12 surfactants) or aqueous 9.25% w/v sucrose solution (for only the remaining surfactants) whilst the solvent medium for all transfection mixtures was aqueous 9.25% w/v sucrose solution.

3.2.4. Measurement of Zeta Potential

Determination of zeta potentials used the same instrumental set up, sample volumes and concentrations as for size determinations (Section 3.2.3). However, the analysis was performed for fresh samples, with the instrument switched to a zeta potential standard

operation procedure mode. The titrations were performed by varying pH and measuring the corresponding values of zeta potential.

3.2.5. Physical State of Transfection Systems by TEM

The physical state of both the gemini surfactant solutions and the equilibrated transfection complexes, formed from aqueous mixtures of plasmid and gemini surfactants, was studied using transmission electron microscopy (TEM). Each sample to be visualized was prepared by placing a small drop of about 10 μL of pre-made surfactant solutions or transfection mixtures on a carbon coated and glow discharged 200 mesh copper grid. After blotting off excess liquid, a thin layer of the sample was allowed to dry and absorb onto the grids. Negative staining of absorbed sample was performed using 1% w/v phosphotungstic acid. Images of surfactant aggregates and the transfection nanocomplexes were obtained using a Philips Model 410LS transmission electron microscope operating at 60 keV.

3.3. Cell Preparation and Transfection

3.3.1. Cell Preparation

The incubation conditions, i.e., 5% CO_2/95% air atmosphere, 37 ^{o}C, were kept constant through the entire cell culture period, while sterility principles were followed over the entire duration. PAM 212 cells used for the experiments were routinely cultured in Minimal Eagle's Medium (MEM) supplemented with 10% fetal bovine serum (FBS) and antibiotic-antimycotic (Ab) at 1 unit/mL. COS-7 African Green monkey kidney fibroblast cells, also used herein, were cultured in Dulbecco's Modified Eagle's Medium

(DMEM) supplemented with FBS and Ab in the same manner as done for MEM. In each case, cells were harvested from substrate after 85% confluence to initiate a transfection experiment or a cellular ultrastructural study.

3.3.2. PAM 212 Cell Ultrastructural Study by TEM

The confluent cells were detached from the growth substrate and washed with serum-free medium. Pellets of the cells, obtained from centrifugation of cells during washing process, were processed for electron microscopic visualization while working in a fume hood. Cells were fixed in 2.5% glutaraldehyde in sodium cacodylate buffer (pH 7.3) at 4 ^{o}C for 2 h. The supernatant fixative was aspirated, and cells washed three times in the same buffer (without glutaraldehyde). Secondary fixation of cells was done in 2% aqueous osmium tetroxide at 4 ^{o}C for 1 h. Washing was repeated using distilled water. The cells were embedded in molten agar and the agar allowed to solidify at room temperature. The agar-embedded specimens were cut into small cubes and stained with 2% aqueous uranyl acetate at 4 ^{o}C for 2 h. The specimens were dehydrated in acetone (using an increasing gradient) and embedded in a low-viscosity Spurr resin, followed by oven-polymerization at 60 ^{o}C for 24 h. Ultra-thin sections, approximately 60-90 nm sections, were cut from polymerized specimen blocks and immobilized on 300 mesh copper grids (pre-cleaned in 2% NaOH). Sections were stained in 2% aqueous uranyl acetate, followed by a second staining in Reynold's lead citrate. The cells were finally viewed and imaged using a Philips Model 410LS transmission electron microscope operating at 60 keV.

3.3.3. Transfection Mixture Preparation

For preparing the non-viral transfection formulations, it is estimated that 1 μg of plasmid DNA (i.e., 3 nmol of phosphate) combines with 1.5 nmol of dicationic molecule, such as the gemini surfactant (i.e., 1.5 nmol x 2 ammonium nitrogens) being studied to give a gemini surfactant:plasmid DNA charge ratio ($\rho_{+/-}$) of 1:1. Using this guide, separate transfection mixtures representing $\rho_{+/-}$ = 0.5:1, 1:1, 2.5:1, 5:1 and 10:1 were routinely used for cell transfection. For each preparation (representing a $\rho_{+/-}$ value), 0.2 μg of plasmid was mixed with the appropriate aliquot (in nmol) of gemini surfactant solution (1.5 mM), which was pre-diluted into 5 μL for each surfactant to eliminate volume disparities. The binary mixtures were incubated at room temperature for 15 min, after which 50 μL of the DOPE vesicles (1 mM) was added, then a final incubation of 30 min at room temperature. This order of addition of the reagents (i.e., addition of gemini surfactant to DNA, followed DOPE) has previously been demonstrated by our laboratory to give optimal transfection complexes compared with other ways of addition such as addition of the gemini surfactants to DOPE first, and then combining with the plasmid. The finished transfection mixtures were added to cells dropwise.

3.3.4. Transfection and Quantitation of Protein Expression

On the day before each transfection, 2 x 10^4 cells/well were seeded in 96-well plates (Corning Inc., Corning, NY, USA), keeping the cell types in their respective media. Volumes were kept to 100 μL per well (for 96-well plates) unless otherwise stated. One hour prior to transfection, cells were rinsed and covered with fresh serum-free culture medium. This was to avoid rapid degradation of DNA when transfection mixtures are

added to cells. The cells were then transfected with transfection mixtures representing a plasmid dose of 0.2 μg/well, which were prepared according to different preparation formulas (i.e., with different $\rho_{+/-}$ values: 10:1, 5:1, 2.5:1, 1:1, 0.5:1). Transfection mixtures that were to be added to cells were prepared using pMASIA.Luc, while the mixtures for particle size and zeta potential analysis were prepared using the pGTmCMV.IFN-GFP plasmid. This was to retain sufficient quantities of the pMASIA.Luc plasmid for routine transfections. The transfection nanoparticles formed from the complexation of the pGTmCMV.IFN-GFP plasmid using the gemini surfactants are expected to be the same and so be representative of the properties of transfection nanoparticles formed from the pMASIA.Luc plasmid. The properties are expected to be same, as the two plasmids are approximately equal in size and as the nanoparticles for the two plasmids were obtained by identical preparation steps. For size and zeta potential measurements, the transfection mixtures were prepared up to the required sample volume of 10 mL.

After 5 h incubation, the cell medium was replaced with fresh culture medium supplemented using original supplementing formula. To allow informed comparisons with results obtained in other studies using other molecular kinds of vectors, parallel transfections were run using the non-viral commercial transfection standard Lipofectamine Plus™ (Invitrogen Life Technologies, Carlsbad, CA, USA). The Lipofectamine Plus™ preparation for a plasmid dose of 0.2 μg/well followed the manufacturer's protocol. Each transfection experiment was done in triplicate. The resulting luciferase expression was quantified 12 − 72 h later, using the Promega Steady-Glo™ Luciferase Assay system and luminescence measurements (Reporter microplate luminometer, Turner Biosystems, Sunnyvale, CA, USA).

The use of Steady-Glo™ Luciferase Assay system allows the quantitation of luciferase protein (an enzyme) produced from transfection of the luciferase gene (in the form of the plasmid pMASIA.Luc) into cells. By the mode of operation of this determination method, a prepared cell lysis reagent system containing excess luciferin is added to luciferase enzyme produced *in situ* in transfected cells. This results in the action of luciferase as a catalyst for the reaction between luciferin and oxygen, a luminescent reaction (known as the luciferase reaction, Figure 3.3.4-1) with a quantum yield of 0.9, the highest for any known luminescent reaction [226]. Since luciferin and oxygen (atmospheric) are in excess, the intensity of luminescence produced and measured by a photo-detecting apparatus such as the Reporter microplate luminometer, is proportional to the quantity of luciciferase protein produced in transfected cells.

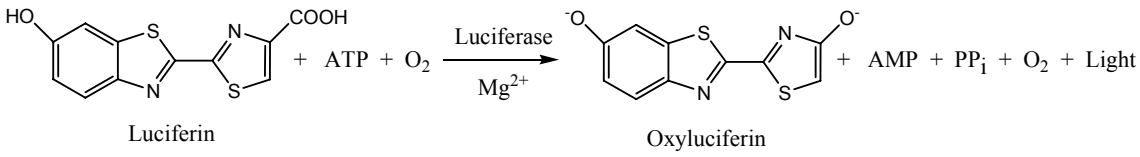

Luciferin Oxyluciferin

Figure 3.3.4-1. The luciferase reaction.
Mono-oxygenation of luciferin is catalyzed by luciferase in the presence of Mg^{2}+, ATP and molecular oxygen. This reaction provides the basis for use of luciferin-containing assays (such as Promega's Steady-Glo™ Luciferase Assay system) for determining the level of luciferase expression in cells transfected with luciferase gene-containing plasmid pMASIA.Luc. The involvement of cellular ATP in the luciferase reaction provides the basis for determing the viabilities of transfected or treated cells (Section 3.3.5-1).

3.3.5. Determination of Transfected Cell Viabilities

The experimental PAM 212 cells were prepared and transfected as described above (Section 3.3.1, 3.3.3). However, to determine the cell viabilities, that is to assess the transfection-related cytotoxicities, the transfected cells were assayed using the Promega CellTitre-Glo® luminescent cell viability assay system. The assay preparation followed the manufacturer's instructions and the emanating luminescence was monitored using a Reporter microplate luminometer (Turner).

The luminescent signal for determination of cell viability allows measurement of the amount ATP from metabolically active or viable cells and is based on the luciferase reaction (Figure 3.3.4-1). In principle, viable cells in culture maintain amounts of ATP that correlates with the number of viable (or living) cells. However, when cell death is caused through a process such as transfection, cells lose the ability to synthesize ATP, and endogenous ATPases destroy any remaining ATP, resulting in a dramatic decline in the levels of ATP. In view of this, the cell viability assay system was employed to inhibit endogenous ATPases and provide both luciferin and luciferase and other reagents necessary to measure ATP using luminescence produced from the luciferase reaction. Within a prepared assay, further ATP synthesis is ceased and the ATP molecules are released into the extracellar space (through lysis of cell membranes) for reaction with reagents (luciferin, luciferase). To ensure complete measurement of the ATP, cell viability assays must contain sufficient luciferin and luciferase as constituent reagents in order for all ATP molecules to react and generate luminescence that is proportional to the amount of ATP (Figure 3.3.4-1).

3.4. Statistics

Statistical analysis was performed by one-way ANOVA (with either SPSS 13.0 software, or using MS Excel statistical functions). Comparisons were made using Tukey's multiple comparison test, non-parametric analysis (Kruskal-Wallis test) and Pearson's correlation. Significant differences between the experimental groups were established at the $p < 0.05$ level of significance, and also at $p < 0.01$ for a number of cases where significant difference exists at only the lower probability level.

4. RESULTS

4.1. Analytical Confirmation of the Synthesized Gemini Surfactants

The results of independent analyses of the structure and purity of the surfactant products obtained from synthesis carried out in this research are given in Appendix A. These results, namely data from CH&N elemental, ^{1}H NMR and Electrospray Ionization Mass Spectrometric (ESI-MS) analyses, strongly confirm that the desired compounds were produced and well purified, there being no starting materials or intermediate monoquartenary species present.

4.2. Characteristics of the Gemini Surfactants

Important transfection-related characteristics for aqueous solutions of the gemini surfactants were obtained by measuring certain physicochemical properties of the gemini surfactant-water systems. The results are presented below.

4.2.1. Gemini Surfactant Krafft Temperatures

Generally, when a saturated gemini surfactant-in-water suspension containing excess undissolved surfactant is heated with concurrent measurement of conductivity, it reaches a point in temperature (i.e., the Krafft temperature, T_{Krafft}) at which the solubility of the surfactant increases sharply. This sharp increase, which also marks the onset of aggregation, is signaled by a rapid increase in the conductivity of the heated sample

[227]. The surge in conductivity results in an inflection in the conductance vs. temperature curve. These curves are given in Figure 4.2.1-1. Krafft temperatures for the gemini surfactants estimated from slopes of the lines before and after the inflection are tabulated in Table 4.2.1-1. The inflection points of reference are indicated by arrows.

It is important to note that while the 18-3-18, 18-7-18 and 18-7NH-18 surfactants show the typical rapid increase in conductance (i.e., sharp increase in solubility) with heating, resulting in more distinctive inflection at their Krafft temperatures (Figure 4.2.1-1B, C), the other surfactants such as 16-7-16, 16-7NH-16, 18:1-3-18:1 and 18:1-7NH-18:1 displayed less distinctive inflection points (note, the inflections referred to are indicated by arrows) (Figure 4.2.1-1A, D). The less distinctive Krafft point inflection for the latter group of gemini surfactants occurs particularly for 16-7-16 and 16-7NH-16 as a result of their fairly high solubilities at temperatures well below their Krafft temperatures. The high solubilities coupled with relatively small increases in solubility in response to rise in temperature resulted in conductance vs. temperature curves that show a gradual rise in solubility just before the Krafft temperature instead of the usual steep rise in solubility as shown for the 18-3-18 surfactant (Figure 4.2.1-1C).

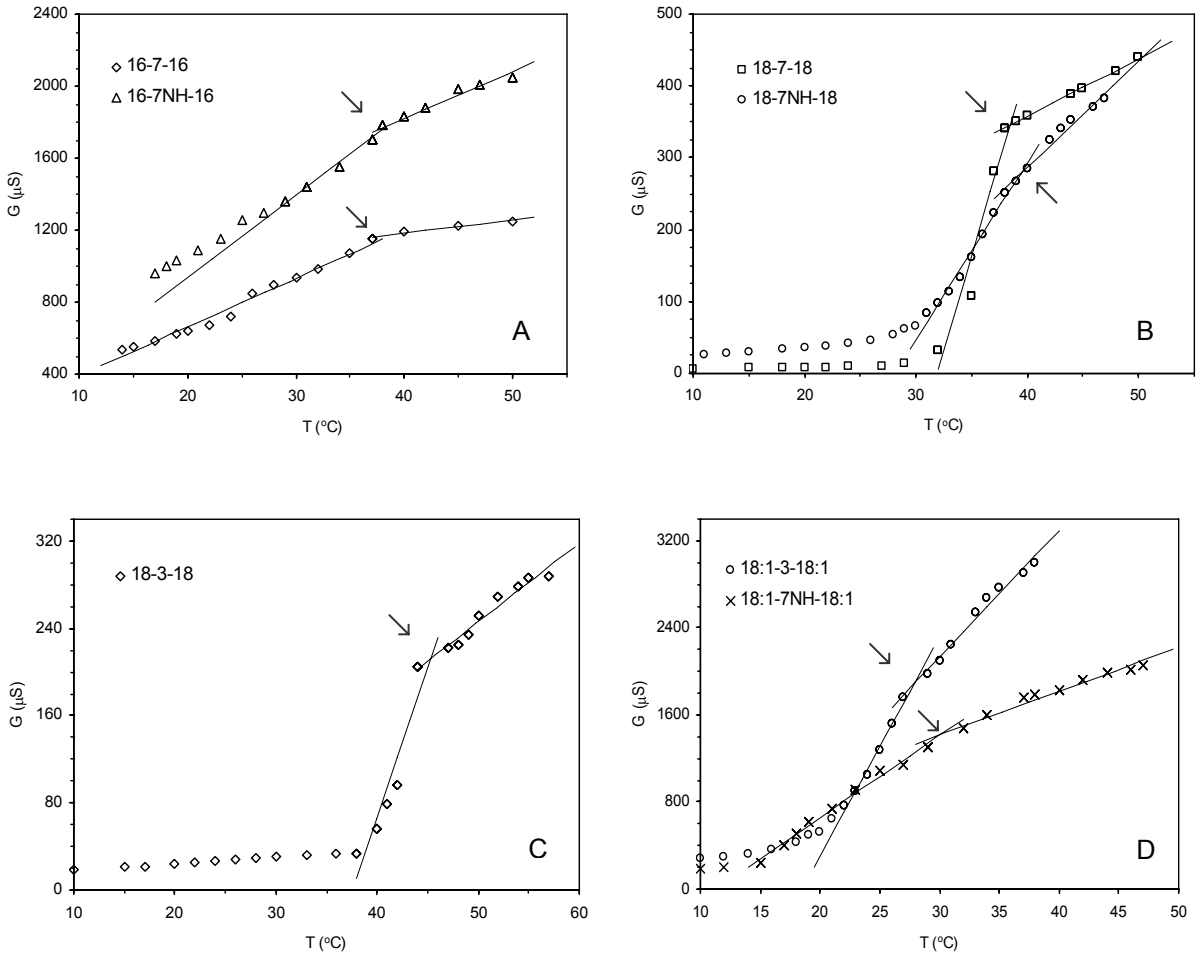

Figure 4.2.1-1. Determination of Krafft temperature for the gemini surfactants.
The point of inflection for each curve (indicated by an arrow) shows the point at which complete clarification of the saturated aqueous gemini surfactant–water system was observed. Using conductivity (G) vs. temperature (T) plots, T_{Krafft} is determined from the intersection of the regression lines for each curve. The plotted data are also given in Appendix B.

Table 4.2.1-1. Krafft temperatures (T_{Krafft}) for the gemini surfactants.

Surfactant	Molecular weight (g mol^{-1})	T_{Krafft} (^{o}C)
12-spacer-12	Various weights	DNP
m-3-m		
16-3-16	740.9	42.0[a]
18-3-18	797.0	45.3
18:1-3-18:1	793.0	28.8
m-7-m		
16-7-16	797.0	38.9
18-7-18	853.1	39.3
m-7NH-m		
16-7NH-16	798.0	38.4
18-7NH-18	854.1	39.3
18:1-7NH-18:1	850.07	30.2

DNP: determination not pursued; T_{Krafft} for the gemini surfactants with C_{12} chains falls below room temperature

[a]From ref. [228]

Krafft temperature determination for the gemini surfactants with C_{12} chains was not pursued; aqueous solutions of these surfactants did not become saturated upon addition of a large excess of the solute surfactants, implying the Krafft temperatures are lower than room temperature. On the other hand, Krafft temperature for the gemini surfactants with long, saturated carbon chains were quite higher than room temperature. High Krafft temperatures, which are usually a minimum of 39 ± 2 ^{o}C for long, saturated carbon chains ($\geq C_{16}$), are a source of potential problems in the preparation of aqueous surfactant solutions, including those with low solubilities.

The introduction of unsaturated carbon chains allowed the reduction of Krafft temperatures for the oleyl-tailed surfactants 18:1-3-18:1, 18:1-7NH-18:1 relative to their saturated C_{18} tail-bearing analogues (Table 4.2.1-1). The presence of hydrophilic groups, which generally boost solubilities of organic molecules in water, can also allow reduction of Krafft temperatures. The incorporation of an NH group, a small hydrophilic unit, did not replicate this trend in the surfactants studied. In the subsequent analysis of aqueous surfactant solutions, the solutions were prepared by dissolving the surfactant solutes at temperatures higher than the Krafft temperatures of the surfactants.

4.2.2. Surface Tension Analysis

Surface tension vs. log concentration for aqueous gemini surfactant solutions are given in Figure 4.2.2-1, below. All the curves indicated the absence of a minimum in the plateau region just above the CMC, giving additional indication of highly pure surfactants. Critical micelle concentration (CMC) values, determined from regression analysis of the pre- and post-micellar region of each curve, are given in Table 4.2.2-1.

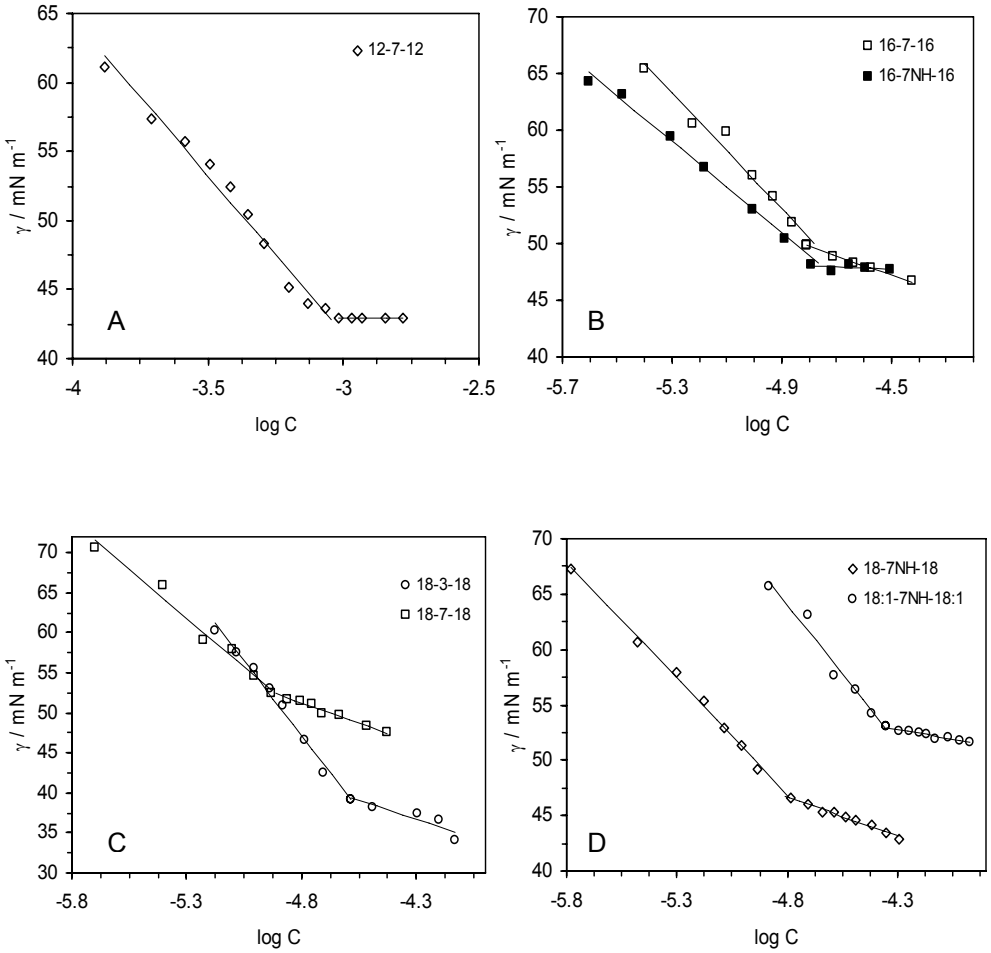

Figure 4.2.2-1. Surface tension vs. log C plots for the gemini surfactants.
Linear fits are indicated by lines; CMC values are calculated from intersections. The plotted values are also given in Appendix C.

The minimum head group area (a_0), occupied per surfactant molecule at the aqueous solution/air interface, was calculated from the surface excess concentration, Γ_{max}, according to Equation 4.2.2-1

$$a_0 = \frac{10^{18}}{N_A \Gamma_{max}} \quad (\text{unit}: \text{nm}^2\,\text{molecule}^{-1}) \qquad 4.2.2\text{-}1$$

where N_A is the Avogadro number, and Γ_{max} is derived from the Gibbs adsorption isotherm (Equation 4.2.2-2)

$$\Gamma_{max} = -\frac{1}{2.303nRT}\left(\frac{d\gamma}{d\log C}\right) \qquad 4.2.2\text{-}2$$

In Equation 4.2.2-2, R is the gas constant and T is the absolute temperature. The value for n, which is the number of species at the interface resulting from the dissociation of the surfactants, was set to 3 for the calculations in this research. This is based on the consideration that dimeric surfactants such as the type studied herein consist of one dimeric surfactant ion and two univalent counterions. Calculations using n = 2 are usually for ionic surfactants made up of one univalent surfactant ion and one counterion. Nonetheless, a value of n = 2 for dimeric surfactants is sometimes encountered in the literature, because proponents of n = 2 assume that one of the two charged groups on the surfactant ion is neutralized by a bound counterion [172-174; 229]. Consequently, while several studies have used n = 3 [182; 230-232], others have used n = 2, 3 [233; 234] for calculation of a_0 for gemini surfactants. In presence of a swamping electrolyte n is simply assigned a value of 1. Setting n = 1 indicates that the ionic strength of aqueous solution remains unchanged as surfactant concentration is varied [235].

Two general trends are observed with respect to the CMC. First, CMC values determined for the gemini surfactants, in agreement with trends reported in the literature including a work published by Zana [178], were seen to decrease as the length of the alkyl tail is increased for constant spacer length. This trend is shared by single-head-and-single-alkyl tail or monomer surfactants for which earlier studies of surface-active behaviour were focused. The distinguishing factor is that CMC values for gemini surfactants are orders of magnitude lower than for corresponding monomer surfactants of equal alkyl tail length. The second trend arises for gemini surfactants having a constant alkyl chain length and a spacer varying in both its length and elemental constitution, in a manner that eliminates simple comparison based on length. Where the spacer is a straight chain made of C and H only, 7-methylene-long spacers resulted in lower CMC values relative to 3-methylene-long spacers. But this is not to suggest any linearity between the length of spacer and CMC values. This issue is further discussed in Chapter 5.

Table 4.2.2-1. Critical micelle concentration (CMC) and head group area (a_0) of the gemini surfactants determined from surface tension measurements.

Surfactant	CMC ($\times 10^{-3}$ mol L^{-1})	a_0 (nm^2 molecule^{-1})
12-spacer-12		
12-3-13[a]	0.89 ± 0.08	1.11 ± 0.04
12-5N-12[b]	1.14 ± 0.04	1.30 ± 0.03
12-8N-12[b]	1.10 ± 0.10	1.95 ± 0.13
12-7N-12[b]	0.87 ± 0.13	2.06 ± 0.20
12-7NH-12[b]	1.29 ± 0.07	1.56 ± 0.04
m-3-m		
16-3-16[c]	0.030 ± 0.002	1.21
18-3-18	0.013 ± 0.001*	0.82 ± 0.4*
18:1-3-18:1[d]	0.0151 ± 0.0004	0.72 ± 0.05
m-7-m		
12-7-12	0.85 ± 0.07	1.24 ± 0.06
16-7-16	0.016 ± 0.009*	1.19 ± 0.08*
18-7-18	0.011 ± 0.001*	1.26 ± 0.09*
m-7NH-m		
16-7NH-16	0.16 ± 0.05*	1.44 ± 0.07*
18-7NH-18	0.013 ± 0.001*	1.36 ± 0.22*
18:1-7NH-18:1	0.044 ± 0.007*	1.22 ± 0.11*

a_0 was computed by taking n = 3 in Equation 4.2.2-2

*Experiment at 45 °C. All other values were at 25 °C including the values from the cited refs

[a]From ref. [218; 236]
[b]From ref. [219]
[c]From ref. [222]
[d]From ref. [223]

4.2.3. Specific Conductivity Analysis

The specific conductance (κ) vs. concentration (C) plots for the gemini surfactants are given in Figure 4.2.3-1. The values of CMC and the degree of micelle ionization (α) derived from the κ vs. C plots are listed in Table 4.2.3-1. Different mathematical methods are available for calculating CMC values from specific conductance vs. concentration curves. A simple one is the calculation by way of regression analysis of two intersecting linear regions above and below the CMC. But to objectively determine CMC values a different approach is needed [237], regardless whether or not experimental points distinctively show intersecting lines. As well, any errors due to manipulation of the data must be eliminated. In the determination herein, a nonlinear curve fit of the conductivity–concentration raw data has been used, in which case the first derivative of the κ vs. C curve is assumed to follow a Boltzmann-type decreasing sigmoid as follows:

$$\frac{d\kappa}{dC} = A_2 + \frac{A_1 - A_2}{1 + e^{(c-CMC)/d}} \qquad 4.2.3\text{-}1$$

where κ is the specific conductivity, c (lower case) is the total concentration of surfactant, A_1 and A_2 are the lower-premicellar and upper-postmicellar limits of sigmoid, respectively. The CMC value is the centre of the sigmoid, and d is the so-called time constant, which is directly related to the independent variable range at which the abrupt change of the dependent variable occurs. The variation of the variable κ as a function of the surfactant concentration C, is then described by the integral of Equation 4.2.3-1 [238], given by

$$\kappa = \kappa_0 + A_1 c + d(A_2 - A_1) \ln\left(\frac{1 + e^{(c-CMC)/d}}{1 + e^{-CMC/d}}\right) \qquad 4.2.3\text{-}2$$

where κ_0 (the integration constant) is the specific conductivity of the surfactant-free solvent-water. The ratio of the two parameters A_2/A_1 gives the value of the degree of micelle ionization α, with values listed in Table 4.2.3-1. The CMC values determined from conductivity analysis (Table 4.2.3-1) exhibit a decreasing trend as the hydrocarbon chain length is increased. This trend was earlier observed using surface tension analysis and is a generally known trend.

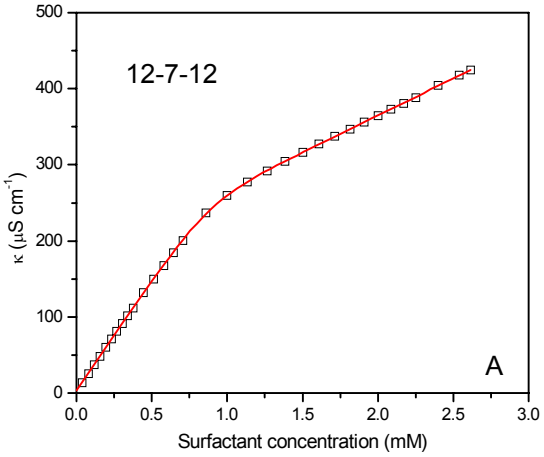
12-7-12
A
κ (μS cm-1)
Surfactant concentration (mM)
0
100
200
300
400
500
0.0
0.5
1.0
1.5
2.0
2.5
3.0

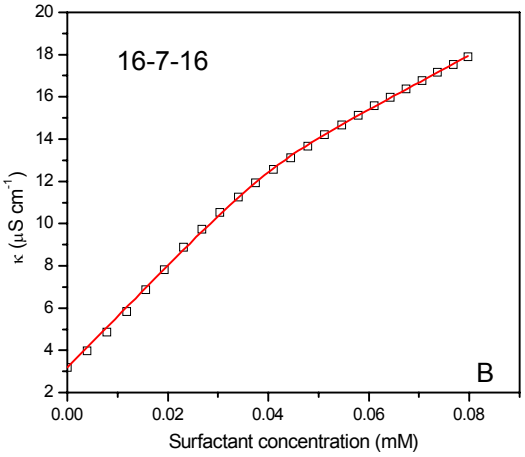
16-7-16
B
κ (μS cm-1)
Surfactant concentration (mM)
2
4
6
8
10
12
14
16
18
20
0.00
0.02
0.04
0.06
0.08

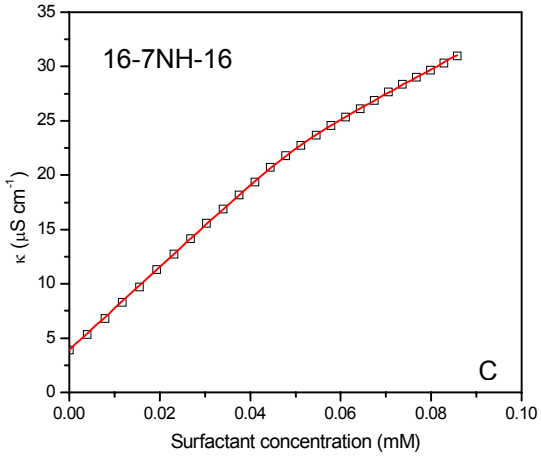
16-7NH-16
C
κ (μS cm-1)
Surfactant concentration (mM)
0
5
10
15
20
25
30
35
0.00
0.02
0.04
0.06
0.08
0.10

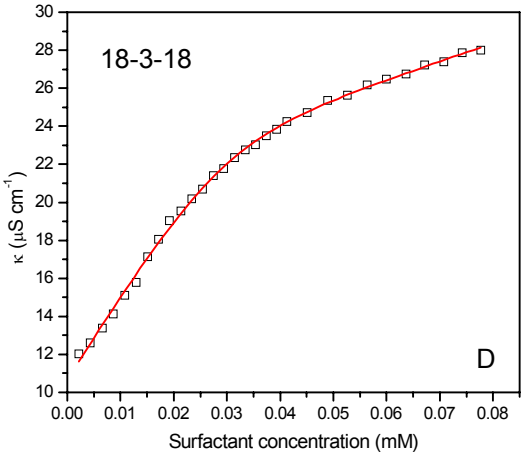
18-3-18
D
κ (μS cm-1)
Surfactant concentration (mM)
10
12
14
16
18
20
22
24
26
28
30
0.00
0.01
0.02
0.03
0.04
0.05
0.06
0.07
0.08

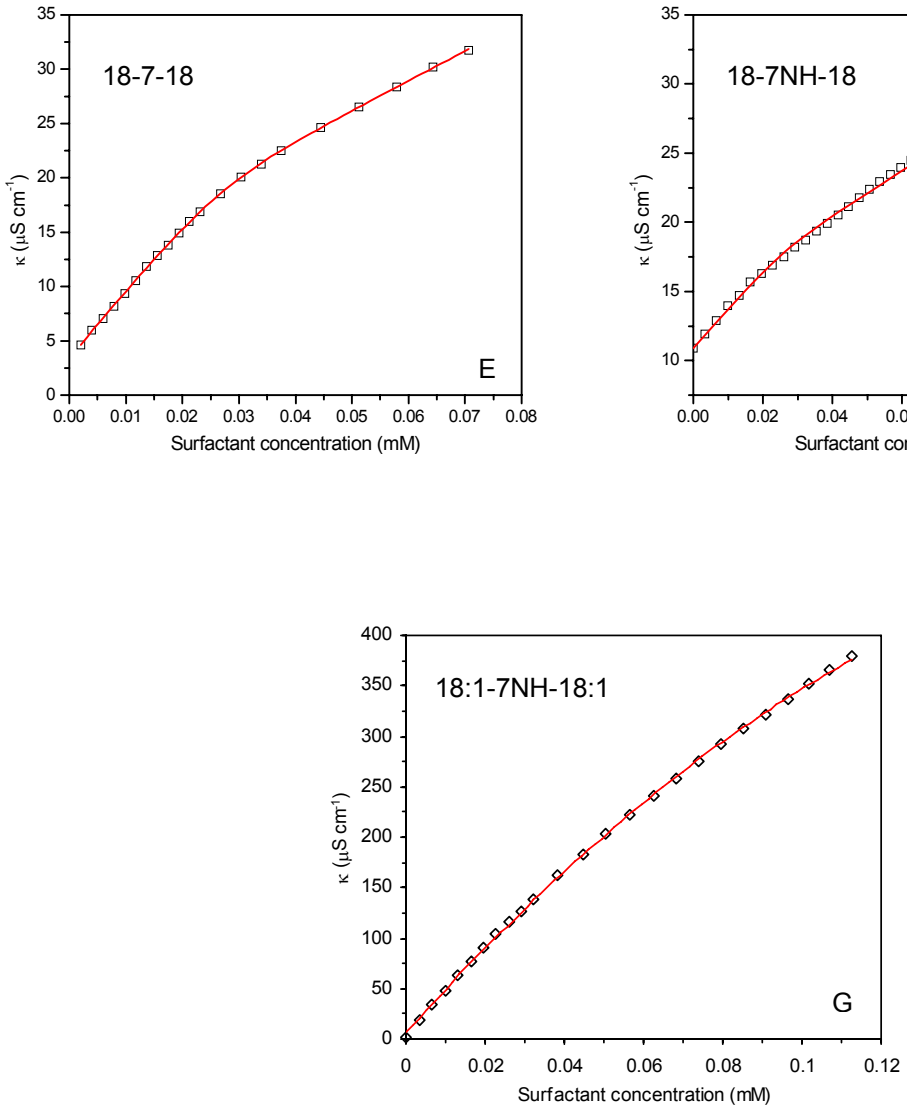

Figure 4.2.3-1. Specific conductance vs. concentration plots for the gemini surfactants. Data are graphed as sigmoids from which CMC values are determined as described (Equation 4.2.3-2). The plotted data are also given in Appendix C.

Table 4.2.3-1. Critical micelle concentration (CMC) and degree of micelle ionization (α) of the gemini surfactants determined from specific conductivity.

Surfactant	CMC ($\times 10^{-3}$ mol L^{-1})	α (no units)
12-spacer-12		
12-3-13[a]	0.98 ± 0.04	0.23 ± 0.02
12-5N-12[b]	0.97 ± 0.02	0.31 ± 0.01
12-8N-12[b]	1.22 ± 0.10	0.38 ± 0.01
12-7N-12[b]	1.17 ± 0.04	0.45 ± 0.02
12-7NH-12[b]	1.21 ± 0.04	0.42 ± 0.01
m-3-m		
16-3-16[c]	0.026 ± 0.001	0.35 ± 0.02
18-3-18	0.028 ± 0.002*	0.32 ± 0.05*
18:1-3-18:1[d]	0.0234 ± 0.0004	0.42 ± 0.06
m-7-m		
12-7-12	0.865 ± 0.005	0.334 ± 0.03
16-7-16	0.040 ± 0.01*	0.41 ± 0.16 *
18-7-18	0.026 ± 0.001*	0.44 ± 0.04*
m-7NH-m		
16-7NH-16	0.050 ± 0.001*	0.59 ± 0.06*
18-7NH-18	0.025 ± 0.002*	0.56 ± 0.02*
18:1-7NH-18:1	0.038 ± 0.008*	0.58 ± 0.06*

*Experiment at 45 °C. All other values were at 25 °C including the values from the cited refs

[a]From ref. [218]
[b]From ref. [219]
[c]From ref. [222]
[d]From ref. [223]

4.2.4. pK_a Values of the Amine-substituted Gemini Surfactants

pK_a values, obtained from pH titrations for the amine-substituted gemini surfactants, are listed in Table 4.2.4-1. pK_a analysis was not pursued for the amine-free gemini surfactants due to the expected lack of basic properties. Overall, the pK_a values obtained make the surfactants weak bases. Nonetheless, the pK_a value of a weak base gives an indication of the degree of ionization of a base; i.e., the basic strength. Lower pK_a values imply greater ability of the aza (N-CH_3) or imino (NH) groups on the surfactants to be protonated or ionized in aqueous medium and thus imply higher basic strength. The reverse is also true. With respect to cellular gene delivery, low pK_a values allow for pH buffering of endosomes during downward pH transition of these compartments. This can help protect and favour release of DNA from gemini surfactant/DNA complexes taken up by cells. In general, the protection and assisted release of DNA are considered to lead to improved transfection [239].

The pK_a values alone would suggest that 12-8N-12 and 12-7N-12 surfactants, with the lowest and second lowest pK_a values among the amine-substituted gemini surfactants, would be better in protecting and favouring the release of DNA. But any conclusion that these two surfactants will emerge as better tranfection agents relative to the other amine-subsituted gemini surfactants stands to be validated experimentally. Moreover, the level of importance of low pK_a values is relative to the effect of potentially more important factors including the demonstrated effectiveness of surfactant–DNA interactions (Table 5.1-1) and the pH-sensitivity of transfection complexes formed upon the mixing of DNA with the gemini surfactants (Section 4.3.1).

Table 4.2.4-1. pK_a values of amine-substituted gemini surfactants

Surfactant	pK_a	Surfactant	pK_a
12-5N-12[b]	5.2 ± 0.4	12-7NH-12[b]	5.0 ± 0.4
12-8N-12[b] - pK_{a1}	4.1± 0.4	16-7NH-16	5.04 ± 0.3
12-8N-12[b] - pK_{a2}*	–	18-7NH-18	5.06 ± 0.3
12-7N-12[b]	4.5 ± 0.2	18:1-7NH-18:1	4.99 ± 0.2

*Second ionization not observed under experimental conditions

[b]From ref. [219]

4.3. Characteristics of Gemini Surfactant/DNA Transfection Systems

4.3.1. Particle Size

Figure 4.3.1-1 (A – E) shows the changes in size of surfactant aggregates as a function of pH. The m-7NH-m surfactants clearly show a significant change in aggregate size on going from basic to acidic pH, as a result of protonation of their imino groups. Aggregates of the 12-7NH-12 surfactant exhibited a narrow transition in size (from ~2.5 to 3.7 nm radius, Figure 4.3.1-1A, also shown in ref [201]) compared with the vesicle-to-micelle transition observed for sugar-based gemini surfactants [52; 206; 207; 240; 241]. This observed structural change, induced by a transition from neutral to acidic pH, nonetheless holds potential importance when it comes to aiding the release of DNA once gemini surfactant-DNA complexes have been incorporated within the cell. The change in aggregate size was more pronounced for the 16-7NH-16, 18-7NH-18 and 18:1-7NH-18:1 surfactants. It is important to note the difference in hydrocarbaon tail length between these three higher m-7NH-m surfactants and the 12-7NH-12 surfactant. The hydrocarbon tails of the three higher m-7NH-m surfactants are extended by 4 to 6 C atoms (C_4 to C_6) relative to the 12-7NH-12 surfactant. This confers stronger aggregation characteristics to the three longer-tailed surfactants as evidenced by the lower CMC values of the m = 16, 18, 18:1 surfactants relative to the m = 12 surfactant. Such variation in surfactant structure helps to highlight important structural components in molecules that are designed for gene delivery.

The fact that the four m-7NH-m surfactants showed structural transition, inspite of the variation in hydrocarbon tail length (m = 12, 16, 18, 18:1, Figure 4.3.1-1A, B and C,

respectively) indicates the consistent pH-sensitivity of these surfactants. This is similar to the pH-sensitive behaviour reported for other systems [207; 242] for which the resulting size vs. pH curves, in some cases, can be said to assume a sigmoidal shape. The degree of structural change was, however, different between the 12-7NH-12 surfactant and the higher members of the series (16-7NH-16, 18-7NH-18 and 18:1-7NH-18:1). For the 12-7NH-12 surfactant, the particle size was seen to increase with acidification of the system beyond neutral pH up to a maximum at which particle size stayed constant with further acidification (decrease in pH). The accompanying change in particle size for aggregates of the 12-7NH-12 surfactant from ~2.5 to 3.7 nm (Figure 4.3.1-1A) represents an overall increase of 1.2 nm. In contrast, surfactant aggregates for the three higher members showed a more pronounced response to the downward adjustment of pH; aggregates showed size increase by 2.5 to 5 nm (Figure 4.3.1-1B, C). The particle size increase for the 16-7NH-16 and 18-7NH-18 surfactant aggrgates occurred sharply as pH was decreased below a value of 6, reaching a plateau at pH 3 or 2. The increase in particle size for the 18:1-7NH-18:1 surfactant aggregates was gradual and continuous over a wide pH range starting from 11 to around 3.5. This gave rise to an arc-shaped curve (Figure 4.3.1-1C) that somewhat departs from the classic sigmoidal shapes observed for the other surfactants within the m-7NH-m series (m = 12, 16, 18) (Figure 4.3.1-1A, B). The ‘arc-like’ structural change, nonetheless, clearly signifies the pH-senitive tendancy of the 18:1-7NH-18:1 surfactant, implying this surfactant does not fall short of the potential to aid the release of DNA once gemini surfactant–DNA complexes have been incorporated within a cell.

The difference between the 12-7NH-12 surfactant and the three higher analogues is likely due to the qualitative difference in alkyl tail length between the 12-7NH-12

surfactant and the three longer-tailed analogues. The difference hydrocarbon in tail length also stands to explain why aggregates for the three higher analogues were generally larger than aggregates for the 12-7NH-12 surfactant. Overall, the structural changes observed, which were pronounced for the three higher m-7NH-m surfactant members and less pronounced for the 12-7NH-12 surfactant, hold the potential to aid the release of complexed DNA.

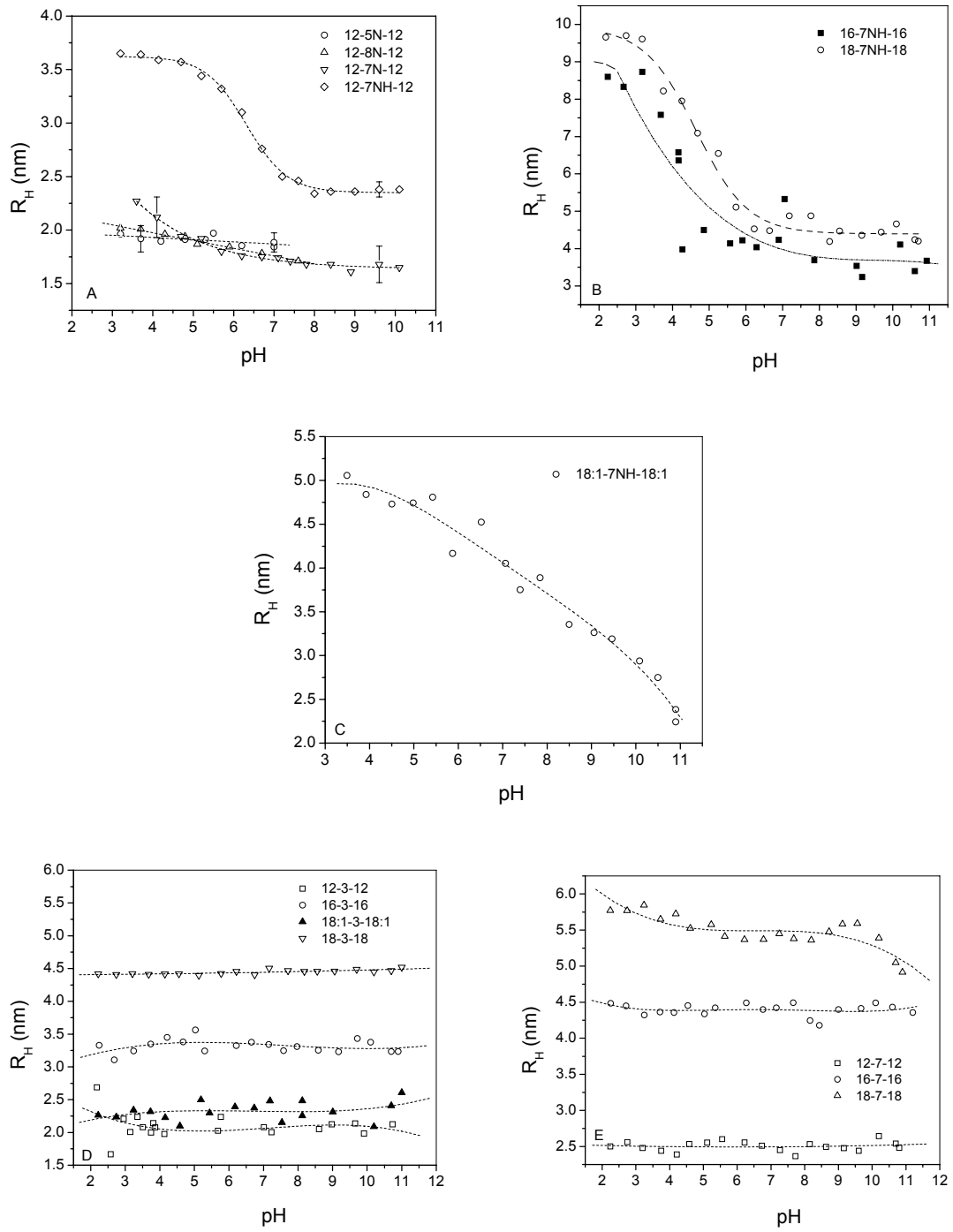

Figure 4.3.1-1. pH dependence of the size of gemini surfactant aggregates formed in aqueous solution.
Initial concentration of aqueous gemini surfactants in each case was 2 × CMC. pH was adjusted using standard acid (HCl) and base (NaOH) solutions. The results presented in part A are also published in ref [201].

Investigations for pH-dependent changes in particle size of surfactant aggregates for the rest of the surfactants involved in this study were also carried out. The aggregate size for these other surfactants, shown in Figure 4.3.1-1A (top three on the legend), Figure 4.3.1-1D (m-3-m series) and Figure 4.3.1-1E (m-7-m series), remain essentially unchanged. The lack of structural changes for these surfactants is in contrast with structural changes for the m-7NH-m surfactants and creates the scenario for one to look forward to a comparison of the two opposing traits in terms of transfection efficiency. However, in expectation that the structural changes will aid the release of complexed DNA, a higher level of transfection efficiency can be presumptuously assigned to the m-7NH-m surfactants over the other surfactants.

The aggregation of gemini surfactants (or other amphiphilic molecules) and the change in structural conformation of the aggregates from one structural phase to another, are generally gorvened by certain factors. These factors include the molecular structure of the gemini surfactant, the surfactant concentration within an aqueous solution (absolute concentration or as factor of the CMC), the ionic strength, pH and temperature of the solution. Keeping all these variables constant and varying only pH allowed the pH-sentivities already described for the gemini surfactants to be investigated. As one of the controlled variables, the gemini surfactant concentration was set to twice the CMC value (2 × CMC) of the gemini surfactants at the start of each pH-dependent size analysis. This was done to ensre proportionate aggregation for all the gemini surfactants. Under this condition, the diameter of micellar aggregates formed by each gemini surfactant can be expected to fall within the length of the fully extended tails of the gemini surfactant, with the possibility of experimental deviation. Though the use of a common concentration value, such as 2 mM, for all the gemini surfactants is sufficient

to generate surfactant aggregates for size analysis, it represents an aggregation condition that is not proportionate across all the gemini surfactants. For instance, whereas the 2 mM concentration is generally two-fold greater than the CMC values for surfactants with C_{12} tails, this concentration is far more greater than the CMC values for the surfactants with C_{16} and C_{18} tails; e.g., 2 mM is more than 100-fold greater than CMC value of the 18-3-18 surfactant which has the lowest CMC value. Further investigations could, in future, be carried out to compare the results of size analysis at a constant surfactant concentration (e.g., 2 mM) and at 2 × CMC value for each surfactant.

The influence of the molecular structure of the gemini surfactants on the surfactant aggregates was observed in two ways. First, in terms of the already described ability of aggregates of the m-7NH-m surfactants to undergo structural changes at acidic conditions due to their possession of pH-sensitive imino group. Second, in terms of the generally observed increase in aggregate size in response to increase in the hydrocarbon tail length of the surfactants (an expected trend). The larger (increasd) aggregate sizes for surfactants with longer hydrocarbon tails can be seen among the the m-7NH-m surfactants, but is particularly more obvious with the m-3-m and m-7-m surfactants. A better comparison of the surfactant aggregate size can be done at neutral or non-acidic pH. At neutral pH, the aggregates of gemini surfactants with C_{12} tails fall within a close size rang ~2.2 ± 0.2 nm. The surfactants with longer hydrocarbon tails (m = 16, 18) yielded larger aggregates, except the oleyl-tailed surfactants (m = 18:1) whose aggregates are closer in size to those of the C_{12}-tailed surfactants. The small aggregate size for the oleyl-tailed surfactants is attributable to the mono-unsaturation in the oleyl tails.

In carrying out further work on the structural changes of gemini surfactants systems, investigations were focused on m-7NH-m surfactants. The pH dependence of both particle size and zeta potential (see Section 4.3.2) was determined for ternary plasmid-gemini surfactant-lipid (PGL) transfection complexes prepared using these surfactants and the lipid DOPE. As shown in Figure 4.3.1-2 (A, B), these complexes exhibited a pH-dependent structural transition in their particle size. The initial change begins at about neutral pH, with the size of particles increasing as pH becomes more acidic, until a plateau occurs at pH lower than 4.5. The least change/increase in size (12.5 nm) within the pH range 7 to 4.5 was observed for the P-18:1-7NH-18:1-L complexes, while the rest showed an increase between 40 and 80 nm.

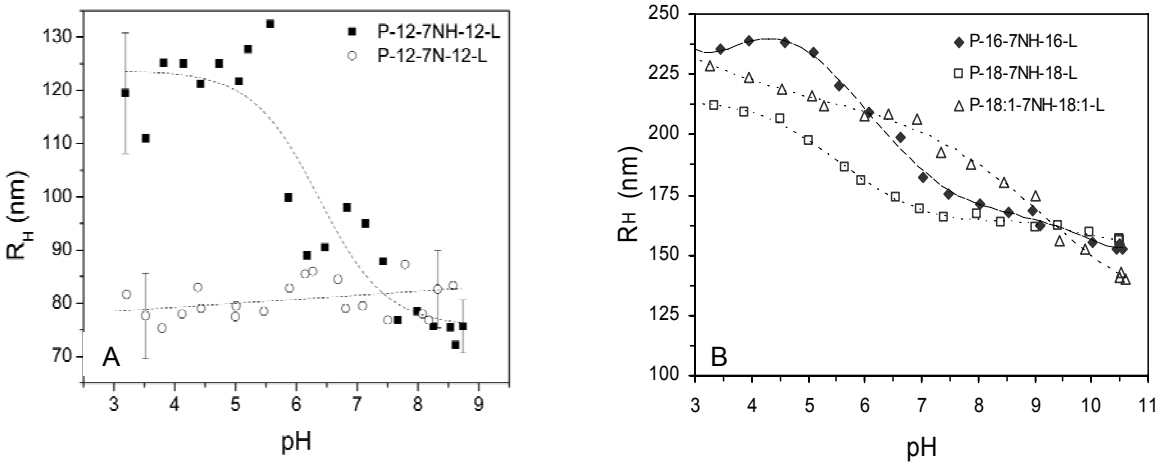

Figure 4.3.1-2. pH dependence of the size of transfection complexes formed from gemini surfactant–plasmid–DOPE mixtures.
The titrations were carried out for transfection systems with the optimal +/- charge ratio (i.e. $\rho_{+/-}$ = 10:1) in the case of each gemini surfactant to transfect cells. The results presented in part A are also published in ref [201].

With regards to the observed structural changes for both the surfactant aggregates and transfection complexes for the m-7NH-m surfactants, it is worth noting the similarity in the pattern of structural change between the aggregates and the complexes. For instance, for the 12-7NH-12 surfactant, both the complexes (Figure 4.3.1-2A) and surfactant-only aggregates (Figure 4.3.1-1A) showed an increase in their particle size in response to decreasing pH. The rest of the m-7NH-m surfactants (namely, m = 16, 18, 18:1) yielded aggregates and complexes with similar behaviour. That is, for these three higher surfactants (of the m-7NH-m series), the transfection complexes showed an increase in particle size as pH was decreased (Figure 4.3.1-2B), a trend also observed for the particle size of the surfactant aggregates (Figure 4.3.1-1B&C). These observations suggest that the transfection complexes (i.e., for all four m-7NH-m surfactants) which undergo (Figure 4.3.1-2A&B) enlargement in response to acidification, do so as a result of pH-induced expansion of the aggregated surfactant component of the transfection complexes. The disreuptive effect of such structural expansion is believed to then lead to release of DNA from its spheres of entrapment. Release of DNA is important for presenting cells with freed DNA for gene expression. The spheres of entrapment, upon endocytosis, include entrapment within the gemini surfactant–DNA complexes and within the outer endosomal membrane.

These pH-induced changes in the particle size of both the aggregates and transfection complexes, and the structural changes they indicate can be explained as follows. For the surfactants-only aggregates, the increament in particle size (for the m-7NH-m) as pH becomes increasingly acidic may suggest a swelling of the aggregates resulting from protonation and repulsion between aggregate-forming gemini surfactant molecules. This bears a similarity to observed changes from vesicular to cylindrical,

ellipsoidal or the so-called 'ribbon' entities [243], in which case the aggregate size increases at acidic pH. This is in contrast to the behaviour of other systems for which there is a reduction of the aggregate size as pH becomes increasing acidic; this is usually explained in terms of a vesicle-to-micelle transition [207]. It should, however, be noted that because the size analysis performed herein is not a 'diagnostic' analysis that determines the exact type of structural change, the changes observed for these surfactants could as well indicate other types of conformational changes. With regard to the transfection complexes, the increase in particle size is possibly the result of the dissociation of DNA from its carrier gemini surfactant molecules, an event that would allow the complexed DNA to unpack and decondense. The importance of such unpacking and decondensation of DNA after cellular uptake of complexed DNA lies in the premise that any nuclear entry should involve the freed DNA as this will permit ready protein expression. Further studies could, in future, be carried out to determine the exact type of structural changes, which in a general form, were detected in this research using pH-dependent size analysis.

4.3.2. Zeta Potential Analysis

Zeta (ζ) potential of the transfection complexes, like particle size, also displayed pH-dependence (Figure 4.3.2-1A, B), similar to previously reported systems [207]. For all the complex systems analyzed, the ζ-potential increases in response to decrease of pH within the basic range, which is consistent with the expected decrease in counterion (i.e., hydroxide) binding to the complex. The ζ-potential behaviour for the 12-7NH-12 surfactant-containing system, in the neutral to acidic pH range, was rather unique when compared with the behaviour for the three other m-7NH-m surfactants (m = 16, 18,

18:1). As the pH was decreased from a basic pH medium above pH 7, a rise in the ζ-potential curve for the 12-7NH-12 surfactant was observed, and this gave way to a plateau region beginning at around pH 7. This plateau region was followed by a sharp decrease in ζ-potential at a pH of about 5.5, becoming another plateau at lower pH (Figure 4.3.2-1A). Such behaviour could be linked to the pH-induced structural change for the 12-7NH-12 surfactant systems, which was also observed within the neutral to acidic pH range (Figure 4.3.1-1A, Figure 4.3.1-2A). For the systems containing the 16-7NH-16, 18-7NH-18 and 18:1-7NH-18:1 surfactants, increase in ζ-potential occured as the pH was decreased from a basic pH medium above pH 7. However, the ζ-potential generally plateaued or started to plateau as pH fell from pH 7 into the acidic pH range (Figure 4.3.2-1B).

As expected, the complexes for all four m-7NH-m surfactants were positively charged at neutral pH (pH = 7), with ζ-potential in the range of +40 – +45 mV (Figure 4.3.2-1). Indeed the overall positive charge at neutral pH is a result of the residual concentration of cationic gemini surfactants after DNA was neutralized and complexed with excess gemini surfactant at a gemini surfactant:DNA charge ratio of 10:1. The electrostatic interaction between the negatively charged phosphate groups of DNA and the positive charges of cationic agents has itself been routinely verified using ζ-potential analysis. The premise is that a reduction in the ζ-potential of positively charged gemini surfactant vesicles should occur after addition of negatively charged DNA (ζ-potential herein found to be -43 mV), and final charge of the mixture (in mV) should still be higher than the ζ-potential of the surfactant-free DNA [244; 245].

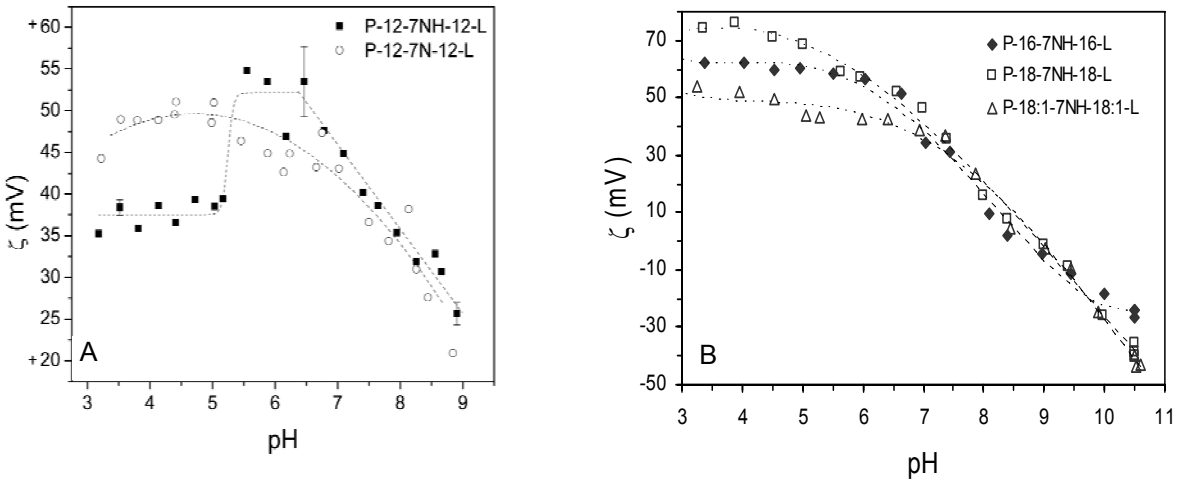

Figure 4.3.2-1. Effect of pH on the zeta potential of transfection complexes formed from gemini surfactant–plasmid–DOPE mixtures.
The titrations were carried out for transfection systems with the optimal +/- charge ratio (i.e. $\rho_{+/-}$ = 10:1) in the case of each gemini surfactant to transfect cells. Results in part A are also published in ref. [201].

4.3.3. Physical State of Transfection Complexes

The physical state of transfection complexes freshly prepared from the m-7NH-m surfactants at the +/- optimal charge ratio of 10:1 was further examined using TEM (Figure 4.3.3-1). The complex nanoparticles which showed an overall positive charge (Figure 4.3.2-1) and revealed themselves as discrete particles, in the size range of approximately 150 – 250 nm. This particle size range is particularly noteworthy because of the similarity in size of transfection complexes between TEM and pH-dependent size analysis (size range 120 – 225 nm, Figure 4.3.1-2). Such particle size agreement between analytical methods such as the pH-dependent size analysis (a method operating based on dynamic light scattering, DLS) and TEM is not commonly seen in the literature though it helps to independently confirm particle size of transfection complexes.

The physical appearance of the particles showed a very similar nature for complexes derived from the m-7NH-m surfactants regardless of the alkyl tail length (m = 12, 16, 18, 18:1). Some particles were observed to have either fused/aggregated into larger ones, reminiscent of previously reported observations [40; 187; 190; 246], or remained as single spherical entities, also consistent with previously reported studies on particles [40; 190; 247]. Apart from size, the particles were also heterogeneous in shape, with their uneven surfaces being consistent with DNA molecules being sandwiched between lipid bilayers [191; 248; 249]. Free DNA was not observed, which is clearly due to its complete neutralization, condensation and encapsulation at the optimal +/- charge ratio at which the gemini surfactant is present in excess. Also, unlike those in previous reports [40; 101; 189; 250-252], structures in the form of strands or ‘spaghetti’ were not observed. In the light of the heterogeneity observed for the complex nanoparticles, it

would be reasonable to think that such heterogeneity may well indicate the tendencies displayed by certain transfection complexes in which they adopt a number of multiple structural phases including lamellar, hexagonal and cubic phases. This hypothesis could, in future, be evaluated from small-angle X-ray scattering (SAXS) studies of the complexes and examination of the scattering pattern in relation to the physical state of complexes revealed using TEM.

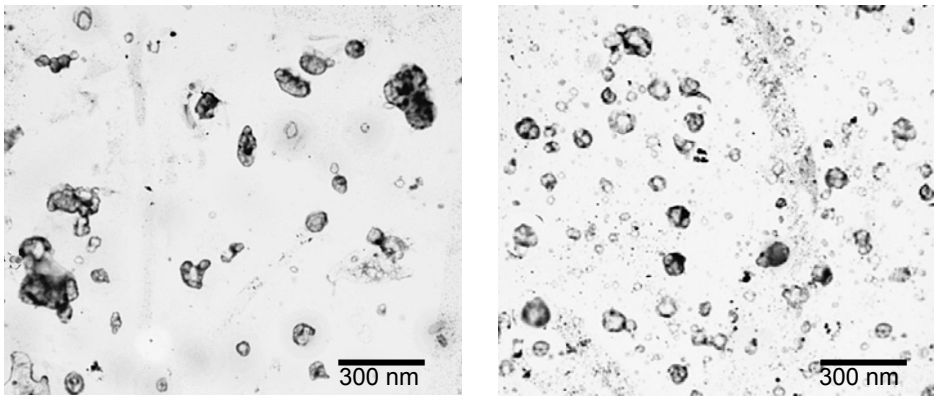

Figure 4.3.3-1. Transmission electron micrographs showing complexes derived from plasmid–gemini surfactant–lipid mixtures.
Representative selection of electron micrographs of the complex particles derived from the plasmid–m-7NH-m gemini surfactant–lipid mixtures at pH of 7.6 ± 0.4. The gemini surfactant:DNA charge ratio for the mixtures was 10:1. mag. 2400x

4.4. Ultrastructural Examination of PAM 212 Cells

The high resolution afforded by transmission electron microscopy (TEM) was employed in conjunction with TEM sample preparation techniques (described in Section 3.3.2) to study the morphology and size or other structural adaptations of the cells. The two electron micrographs in Figure 4.4-1 demonstrate a preservation of the cellular matrix and allow stereological analysis using these ultrastructural images. Morphometric measurement of several imaged cells indicates the diameter of cells falls within a range of 6-10 μm. This is assuming cells are spherical. In reality, cells were of unequal size and exhibited mixed morphologies, including nearly spherical and oval shapes.

Cell size has the potential to be important in the ability of a cell line to take up particles presented to the cells as a transfection preparation. A second factor of prime importance, in terms of efficient transfection, is the size of non-viral DNA complexes themselves being transferred into the cells. For instance, correlation has been drawn in some cases between the small size of complexes and transfection activity [253]. On the other hand, attempts seeking to explore the effects of cell size have yet to appear in the literature. The physical features, including size and morphology, of the PAM 212 cells used in this research were examined in an attempt to proceed into transfection studies with a deeper understanding of the cells' structural dimensions.

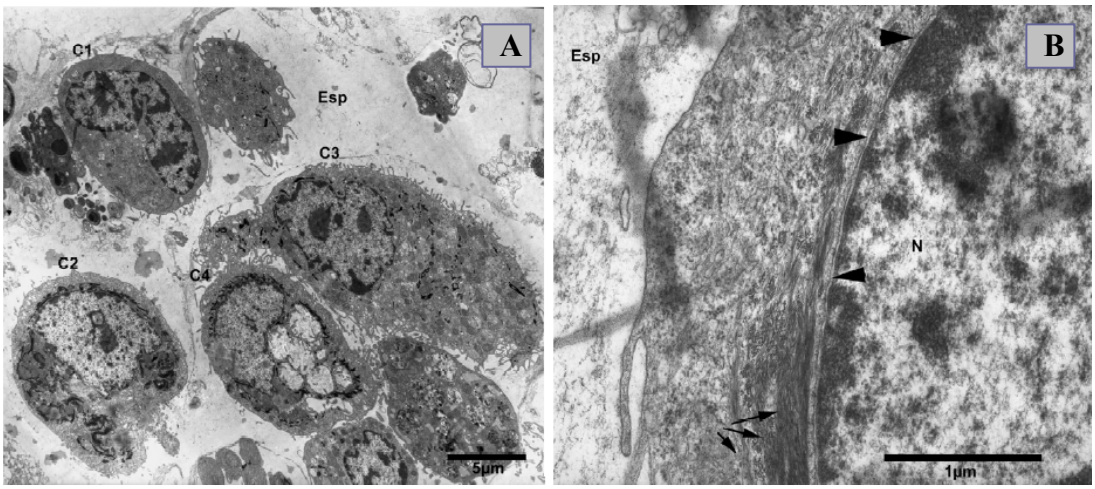

Figure 4.4-1. Transmission electron micrographs of PAM 212 cells
(A) This electron micrograph shows the extracellular background (Esp). Varying morphologies, ranging from imperfect round to elongated shapes, are revealed by the cells labeled C1, C2, C3 and C4; mag. 2400x. (B) A segment of a cell depicting the nucleus (N), and the nuclear membrane (arrowheads). Adjacent to the nuclear membrane are tonofilaments (arrows); mag. 24000x

4.5. Evaluation of Gene Expression

Assessment of the transfection abilities of the surfactants studied in this research was conducted in two phases involving two cell lines overall. COS-7 cells were used as a standard transfection cell line to perform an initial screening of surfactants for advanced testing in PAM 212 cells. Results of the two transfection phases are presented below, in Sections 4.4.2.1 and 4.4.2.2, respectively.

4.5.1. Transfection with 12-spacer-12 Gemini Surfactants

Figure 4.5.1-1 shows both transfection efficiencies and cytotoxicity results for transfection complexes prepared using the 12-spacer-12 surfactants. The experiments featured plasmid-gemini surfactant (PG) and plasmid-gemini surfactant-DOPE (PGL) complexes, which are binary and ternary systems, respectively. Increasingly, large numbers of non-viral delivery systems involving gemini surfactants are being investigated for use as transfection agents. A recent evaluation of 12-s-12 surfactants by Badea *et al*. [132] showed the highest transfection occurred with the 12-3-12 surfactant among the 12-s-12 series. For comparison, the 12-3-12 surfactant has been included in this study. Previously published results indicate that the plasmid-gemini surfactant complexes, prepared with the exclusion of DOPE, yielded weak or no transfection, while addition of DOPE to these complexes significantly increased the transfection efficiencies [39; 132; 192; 254; 255]. The results in Figure 4.5.1-1A indicate that for both PG and PGL systems, the imino-substituted 12-7NH-12 surfactant yielded the highest transfection. In this case the PG system yielded modest results, and not surprisingly, the PGL system yielded a 13-fold increase in transfection over the PG

system. Increase in transfection afforded by the addition of DOPE has been explained in terms of the ability of DOPE to stabilize cationic liposomes and to induce the destabilization of the endosomal membrane upon contact between liposome-DNA complexes and endosomes. Once destabilized, the endosomes release complexed DNA to permit its entry into the nucleus and to allow transcription to take place [254; 256] or to permit expression of the DNA while it is still in the cytosol.

The transfection efficiencies given by the aza- and imino-substituted surfactants are higher than efficiencies found for their previously reported unsubstituted counterparts [132], which do not bear any aza- and imino-substitution. These surfactants, prepared and used as amine-substituted PGL systems, also recorded greater transfection efficiencies over the plasmid-DOPE system, which yielded negligible results (Figure 4.5.1-1A). This is due to the absence of a cationic component to compact and neutralize DNA for better cellular uptake. No significant difference was observed for the 12-3-12 surfactant and 3-β-[N-(N`,N`-dimethylaminoethane)-carbamoyl] cholesterol (DC-Chol). By way of its high transfection efficiency, no significant difference in transfection was observed between the 12-7NH-12 surfactant and commercial Lipofectamine Plus™ transfection agent.

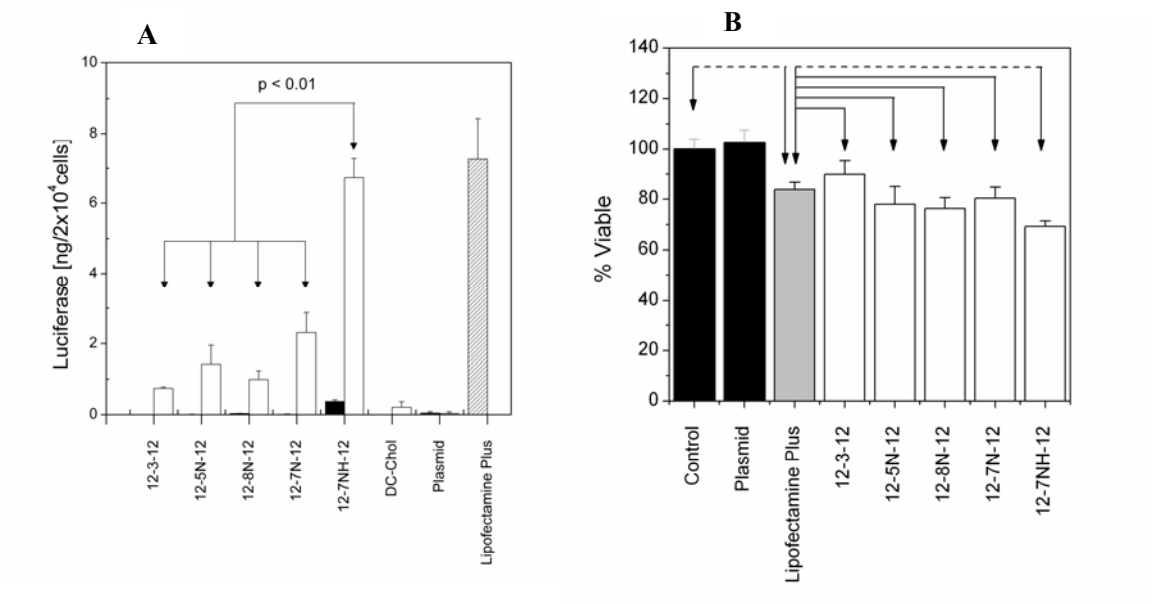

Figure 4.5.1-1. Transfection efficiency and cytotoxicity results in COS-7 cells.
(A) Transfection with plasmid-gemini surfactant complexes (PG, black bar), and gemini surfactant-DNA-DOPE nanoparticles (PGL, white bars); $\rho_{+/-}$ = 10:1 (n = 6, error = SD). Results for DC-Chol with (white) and without DOPE (black), plasmid with (white) and without DOPE (black), and Lipofectamine Plus™ (shaded), used as controls are also shown.
(B) Mean cell viability (n = 4, error bars = SD) of COS-7 cells transfected with plasmid gemini surfactant-DOPE nanoparticles (white bars) n = 4, bars = SD). Data are also presented for untransfected cells and cells transfected with plasmid only (black bars) n = 4, bars = SD), and cells transfected with Lipofectamine Plus™ (gray bar). Determination of both transfection efficiency and cell viability was done 24 h after transfecting cells. Columns connected by a solid line show no significant difference, those connected with a dashed line show a significant difference ($p < 0.01$). Results in this figure are also published in ref. [201].

As part of the assessment of surfactant suitability for use in biological hosts, transfection efficiencies were closely compared with transfection-related cytotoxicities resulting from the use of gemini surfactants and Lipofectamine Plus™ (Figure 4.5.1-1B). The surfactants 12-5N-12, 12-8N-12 and 12-7N-12 caused similar toxicity in transfected COS-7 cells as in the Lipofectamine Plus™ reagent ($p > 0.05$). Both these surfactants and Lipofectamine Plus™ reduced the viability of cells to approximately 80% of the non-transfected control or cells transfected with plasmid alone. The parent 12-3-12 surfactant recorded minimal toxicity and was not more toxic than the non-transfected control. Cell toxicity for the 12-7NH-12 surfactant was slightly higher (~70% cell viability) than for Lipofectamine Plus™ ($p < 0.01$), but not significantly different from the 12-5N-12 and 12-8N-12 surfactants ($p > 0.05$). Thus, compared with these two surfactants in the amine-substituted surfactant family, 12-7NH-12 achieved increased transfection without resulting in increased cytotoxicity.

4.5.2. Advanced Multi-surfactant Series Transfections

Following phase 1 transfections in Section 4.5.1 above, an advanced and expanded transfection phase (i.e., the ensuing section) was staged to study the best surfactants (or the structures) coming out of phase 1. These surfactants were contrasted with related but structurally different surfactant analogues for which one or more of the predicted transfection-enhancing features (based on rational molecular gene carrier design) are removed. Surfactants tested in the current transfection phase are grouped into three series; namely, m-3-m, m-7-m and m-7NH-m surfactants (Table 3.1.2-1).

4.5.2.1. Transgene Expression: Effect of Time

Protein expression following successful transfer of a reporter gene into cells or tissue can either be permanent or transient, due to a permanent or transient genetic modification, respectively, caused in the host. With permanent gene expression, the level of protein expression plateaus following an increase in the pattern of protein expression, whereas in transient gene expression, protein levels will be expected to rise and decline with time. In the particular scenario of our experiments (with PAM 212 murine keratinocytes, pMASIA.Luc plasmid and our new group of gemini surfactants), the levels of protein expression were quantified at different time points. Transfection results for plasmid–gemini–DOPE (PGL) complexes representing $\rho_{+/-}$ = 10:1 for the m-3-m surfactants are illustrated in Figure 4.5.2.1-1.

Luciferase expression rose from 12 h post-transfection to its highest level at 24 h post-transfection, and then declined through 48 h and 72 h post-transfection. Virtually no luciferase was expressed in cells transfected with two gemini surfactant-free controls; namely, plain plasmid solution (termed *naked* DNA) and plasmid combined with DOPE in a 0.1:18 weight ratio. Since the highest protein expression was detected at 24 h post-transfection, quantitation of luciferase reporter gene expression in subsequent transfections was carried out 24 h after transfection.

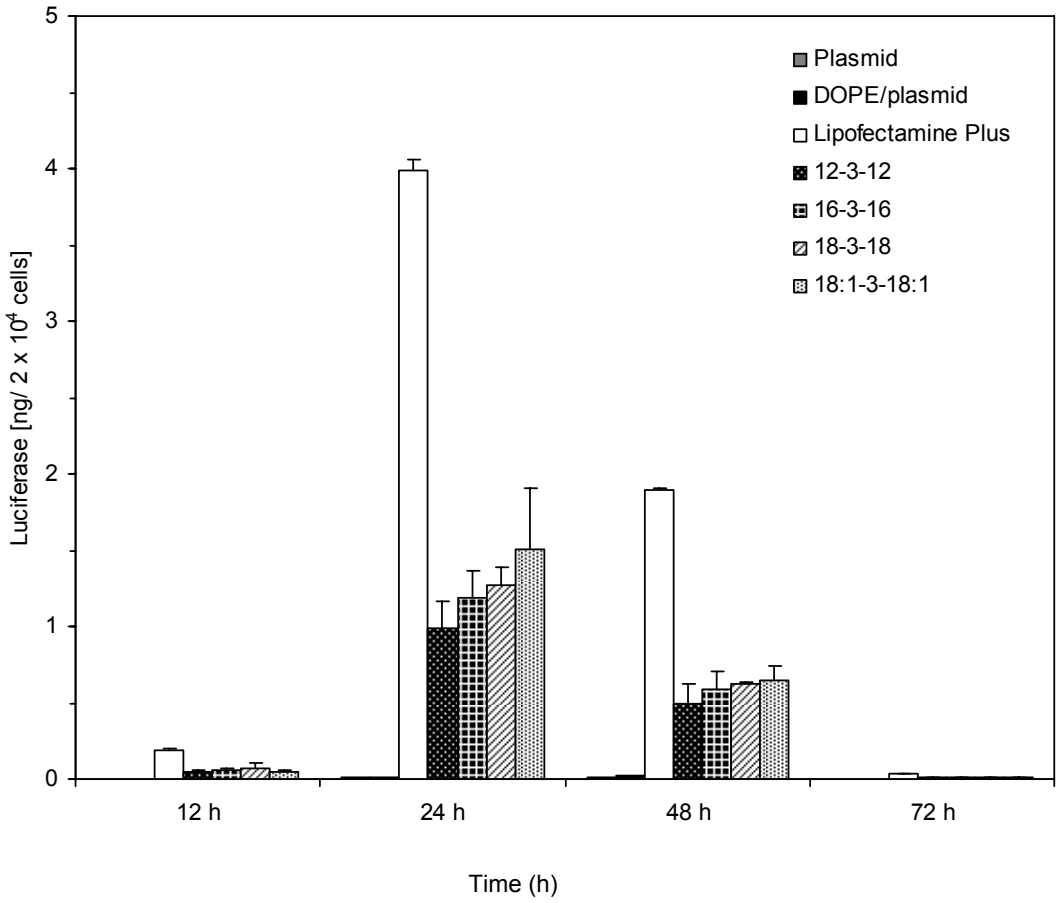

Figure 4.5.2.1-1. Luciferase reporter gene expression in PAM 212 cells measured as a function of post-transfection duration.
The PGL complexes prepared with $\rho_{+/-}$ = 10:1 featured the m-3-m surfactants. The transfections also involved three controls, namely, naked DNA (plasmid), plasmid/DOPE combination and Lipofectamine Plus reagent. The resulting protein produced within the cells was quantified after transfection at different time points: 12 h, 24 h, 48 h, 72 h. n = 4, error bars = SD.

4.5.2.2. Transgene Expression: Effect of +/- Charge Ratio

In addition to the influence of time (i.e., the post-transfection duration) on the level of expression of a reporter gene, which was shown in the previous section (Section 4.5.2.1), gene expression in host cells is also governed by how well the genetic material is packaged and presented to cells. Efficient packaging is obtained by complete neutralization, condensation and encapsulation of DNA into nanoparticles using delivery molecules containing cationic headgroups or protonatable amine groups arranged to permit close-matching interaction with DNA. In addition, the nanoparticles need an optimal +/- charge ratio to propel the nanoparticle–cell attachment and subsequent cellular uptake. In short, the efficiency of non-viral gene transfer is dependent on the +/- charge ratio and, of more interest to us, the structural features of the delivery agent. As such it was important to unify or eliminate the effect of interfering variables, including charge ratios, to create optimal conditions under which the different structural schemes exhibited by our surfactants can be fairly compared.

The first step for this was to determine the post-transfection duration leading to the highest level of gene expression (Figure 4.5.2.1-1). The next step was to determine the $\rho_{+/-}$ at which all the surfactants most effectively transfer DNA into cells (indicated by the level of gene expression). Thus, transfections were carried out involving five different charge ratio ($\rho_{+/-}$) values; namely, 10:1, 5:1, 2.5:1, 1:1, 0.5:1. The m-3-m surfactants were featured in the transfections. Figure 4.5.2.2-1 shows that the transfection efficiencies (i.e., level of luciferase expression, 24 h post-transfection) was highest in cells transfected using PGL complexes with $\rho_{+/-}$ = 10:1. Complexes with lower $\rho_{+/-}$ values recorded lower efficiencies due to reduced cell-surface binding. This observation,

using the m-3-m surfactants, led us to also conduct $\rho_{+/-}$-dependent transfections for the two analogue surfactant families, i.e., m-7-m and m-7NH-m surfactants. As expected, the $\rho_{+/-}$ = 10:1 preparation formula consistently recorded the highest transfection efficiency in both the m-7-m and m-7NH-m surfactants (Figure 4.5.2.3-1). In previous investigations by our laboratory, transfection complexes with $\rho_{+/-}$ = 10:1 also transfected cells better than complexes with higher $\rho_{+/-}$ values, including $\rho_{+/-}$ = 20:1 and 40:1 [244]. Thus, gene expression was optimal when cells were transfected using complexes with $\rho_{+/-}$ = 10:1 and the gene expression was quantitated 24 h after transfection.

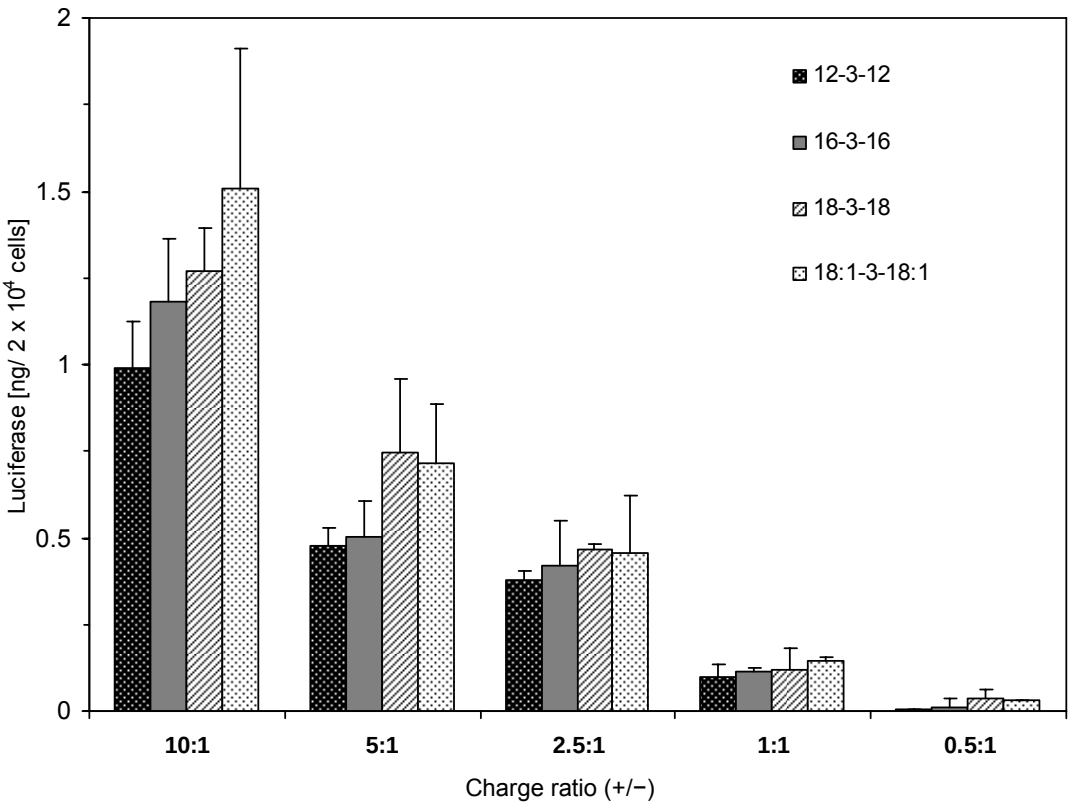

Figure 4.5.2.2-1. Luciferase reporter gene expression in PAM 212 cells measured as a function of the gemini surfactant:DNA charge ratio (i.e., the +/− charge ratio).
The PGL complexes prepared with variable $\rho_{+/-}$ values including 10:1, 5:1, 2.5:1, 1:1 and 0.5:1, featured the m-3-m surfactants. The resulting protein produced within the cells was quantified at 24 h-post transfection. n = 4, error bars = SD.

4.5.2.3. Transgene Expression: Effect of Gemini Surfactant Structure

The many variables employed in our ongoing development of optimal, potentially clinically effective gemini surfactant systems for carrying genes into cells include surfactant structural variation. So, the three series of gemini surfactants were compared under an advanced transfection phase using optimized conditions ($\rho_{+/-}$ = 10:1, 24 h post-transfection analysis). As seen in Figure 4.5.2.3-1, levels of protein expression were, overall, the highest for m-7NH-m surfactants, making them better transfection agents ($p < 0.01$) than both the m-3-m and m-7-m surfactants, which follow in that order. The level of protein expression recorded by the m-7NH-m surfactants, when compared with the commercial Lipofectamine Plus reagent, indicates that the m-7NH-m surfactants are as good transfection agents as the commercial reagent ($p < 0.01$).

The aim of studies conducted in this research was partly to determine the validity of the hypothesis that, imino-substitution in gemini surfactants induces endosomal escape, a proof of which include increased transfection efficiency. This research was to further establish the conditions necessary for imino-substitution in gemini surfactants to yield optimal effect. Together, the high transfection efficiency for the m-7NH-m surfactants and the low transfection efficiency for m-7-m surfactants (Figure 4.5.2.3-1), which serve as negative controls, uphold the hypothesis. Further more, transgene expression, which is highest 24 h post transfection, was consistently demonstrated to be optimal using transfection complexes with $\rho_{+/-}$ value of 10:1 as opposed to lower values. While noting these, it was important to conduct closer comparisons to adequately highlight key structural features of the surfactants such as imino-substituent and the level of

significance that can be attributed to them in the overall performance of gemini surfactant candidates.

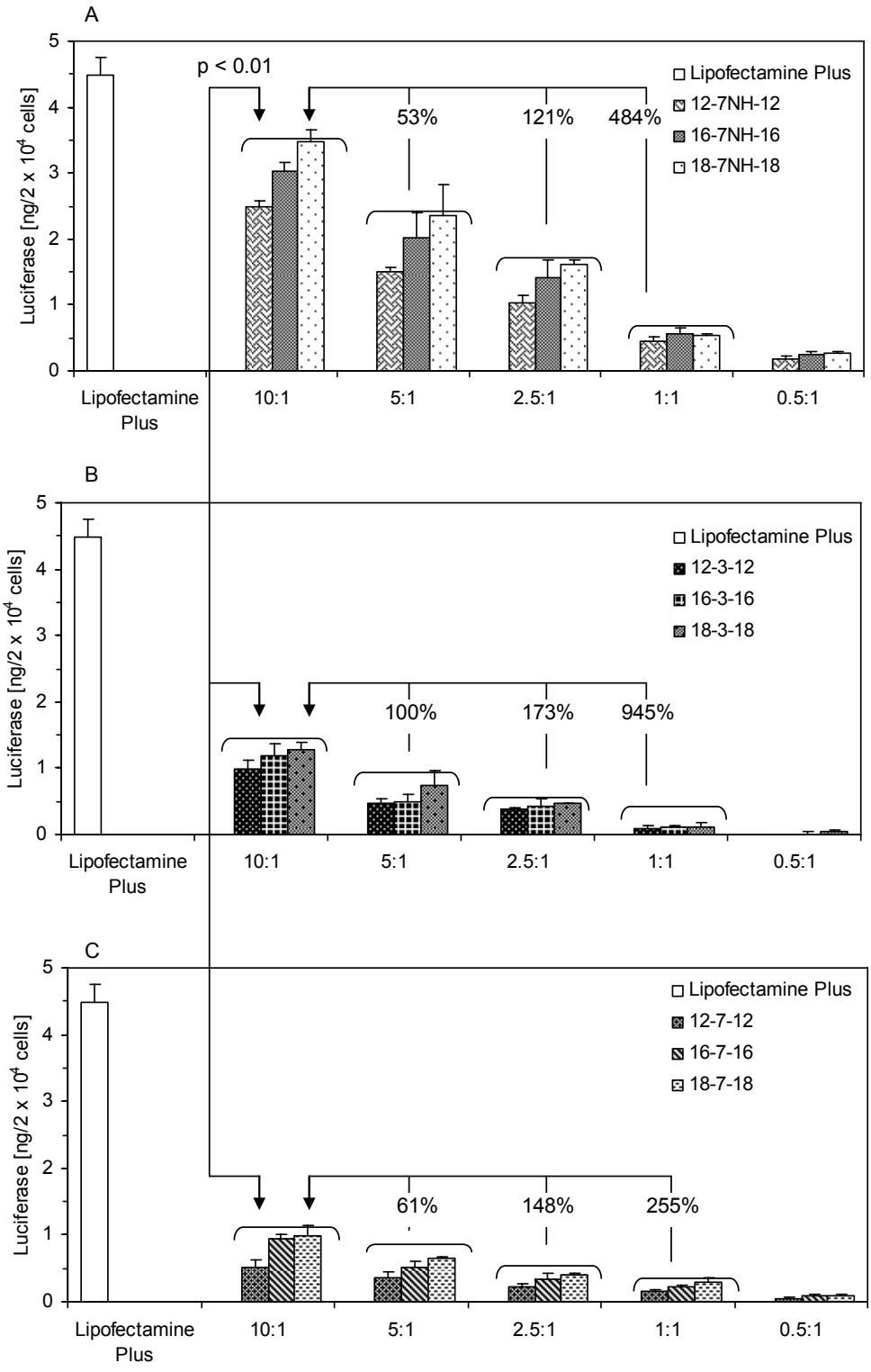
A
p < 0.01
53%
121%
484%
Lipofectamine Plus
12-7NH-12
16-7NH-16
18-7NH-18
Luciferase [ng/2 x 10^4 cells]
Lipofectamine Plus
10:1
5:1
2.5:1
1:1
0.5:1
B
100%
173%
945%
Lipofectamine Plus
12-3-12
16-3-16
18-3-18
Luciferase [ng/2 x 10^4 cells]
Lipofectamine Plus
10:1
5:1
2.5:1
1:1
0.5:1
C
61%
148%
255%
Lipofectamine Plus
12-7-12
16-7-16
18-7-18
Luciferase [ng/2 x 10^4 cells]
Lipofectamine Plus
10:1
5:1
2.5:1
1:1
0.5:1

Figure 4.5.2.3-1. Transfection efficiencies in PAM 212 cells transfected with PGL complexes prepared from gemini surfactants belonging to three different series.

(A) Transfections featuring m-7NH-m surfactants. (B) Transfections featuring m-3-m surfactants. (C) Transfections featuring m-7-m surfactants. For all (i.e., A - C), the magnitude (in percentage) by which transfection efficiencies for complexes with $\rho_{+/-}$ = 10:1 exceeds the transfection efficiencies for complexes with lower $\rho_{+/-}$ values (excluding 0.5:1) is indicated above the respective columns (taken as a group) for lower $\rho_{+/-}$values. Note that the two surfactants with m = 18:1 in the m-3-m and m-7NH-m series were excluded in this figure in order to conduct fair comparisons between these two surfactant groups and the m-7-m group with no m = 18:1 surfactant. In all cases luciferase expression was quantified after 24 h of transfection. n = 4, error bars = SD.

Comparison among surfactants for which the hydrocarbon tail length is held constant (i.e., m-3-m, m-7-m, m-7NH-m, m = 12 or 16 or 18, at a time) revealed that every surfactant from the m-7NH-m group transfected cells better than than the equal-tail surfactant from both the m-3-m and m-7-m surfactant families ($p < 0.01$) (Figure 4.5.2.3-2A, comparisons made for optimized results). Between the m-3-m and m-7-m surfactants (m = 12 or 16 or 18, at a time), the m-3-m surfactants were moderately more efficient. In fact, out of the three different tails, the m-3-m surfactant with m = 12 emerged significantly more efficient than the m-7-m surfactant with the same tail lenth. Despite these differences in transfection efficiency, only seemingly minor differences exist between the structures of the three surfactant groups (i.e., m-7NH-m, m-3-m and m-7-m surfactants). First, the m-7NH-m surfactants have an imino (NH) substitution in their spacer in place of the central methylene ($-CH_2-$) group, while the methylene group is maintained for the m-7-m surfactants. Second, the m-7NH-m surfactants have, inserted in their spacer, an imino group separated by trimethylene spacing from each of two ammonium nitrogens, whereas no imino group is present in the m-3-m surfactants whose ammonium nitrogens are also separated by trimethylene spacing (see detailed structures in Table 3.1.2-1). The m-7-m surfactants, besides not having an imino group, also lack the optimal trimethylene spacing by having a spacer (7-methylene units) that is double the optimal spacing. Thus, both the imino group and the trimethylene spacing are shown as critical structural factors for improving the transfection abilities of our gemini surfactants (this issue is further examined in the chapter 5).

The individual surfactants within surfactant groups with the same spacer type (m-7NH-m, four members; m-3-m, four members; m-7-m, three members) but with different hydrocarbon tail lengths or types were also closely examined. This included

comparison (under optimized conditions) of monounsaturated oleyl tails (m = 18:1), reported to boost transfection in some cases, with the saturated counterparts (m = 18). In one case, i.e., for the m-3-m series, the 18:1-3-18:1 surfactant with oleyl tails showed a better transfection efficiency than the 18-3-18 surfactant with saturated tails, though the difference was insignificant (Figure 4.5.2.3-2A). But within the m-7NH-m surfactant group, the transfection efficiency of the oleyl-containing 18:1-7NH-18:1 surfactant was rather lower than the saturated 18-7NH-18 analogue. Further comparisons (Figure 4.5.2.3-2B) indicated that for the m-7NH-m surfactants, increase in transfection efficiency occurred as follows: m = 12 vs. m =16, m = 12 vs. m = 18 and m = 16 vs. m = 18 (significant increase for the longer tails, $p < 0.01$). The remaining surfactant from this group, m = 18:1, which recorded the lowest efficiency (though the reverse was expected), was significantly less efficient ($p < 0.01$) than only the m = 18 and 16 surfactants, which had the highest and next highest efficiencies, respectively, within their group. For the m-3-m surfactants (m = 12, 16, 18, 18:1), the increase (or difference) in transfection efficiency was insignificant ($p < 0.01$) when any two of these surfactants were compared. This no-significant-increase (difference) observation was also true for the m-7-m surfactants (m = 12, 16, 18). Thus, using surfactant tail length as a variable largely led to insignificant statistical differences in these experiments.

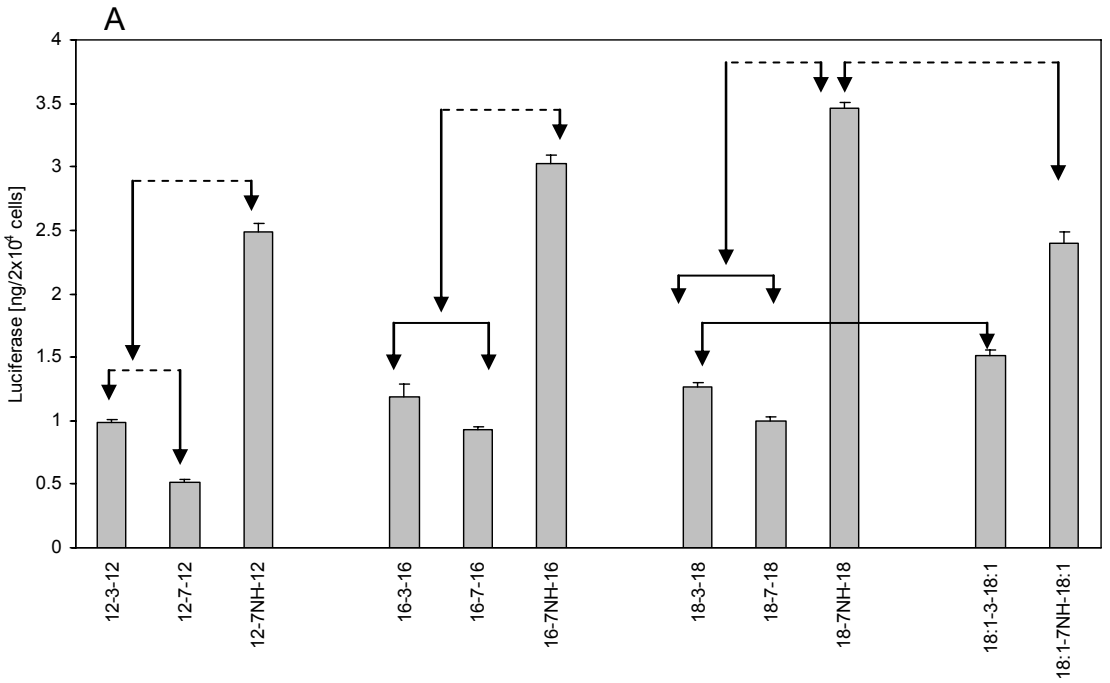
A
Luciferase [ng/2x10^4 cells]
0
0.5
1
1.5
2
2.5
3
3.5
4
12-3-12
12-7-12
12-7NH-12
16-3-16
16-7-16
16-7NH-16
18-3-18
18-7-18
18-7NH-18
18:1-3-18:1
18:1-7NH-18:1

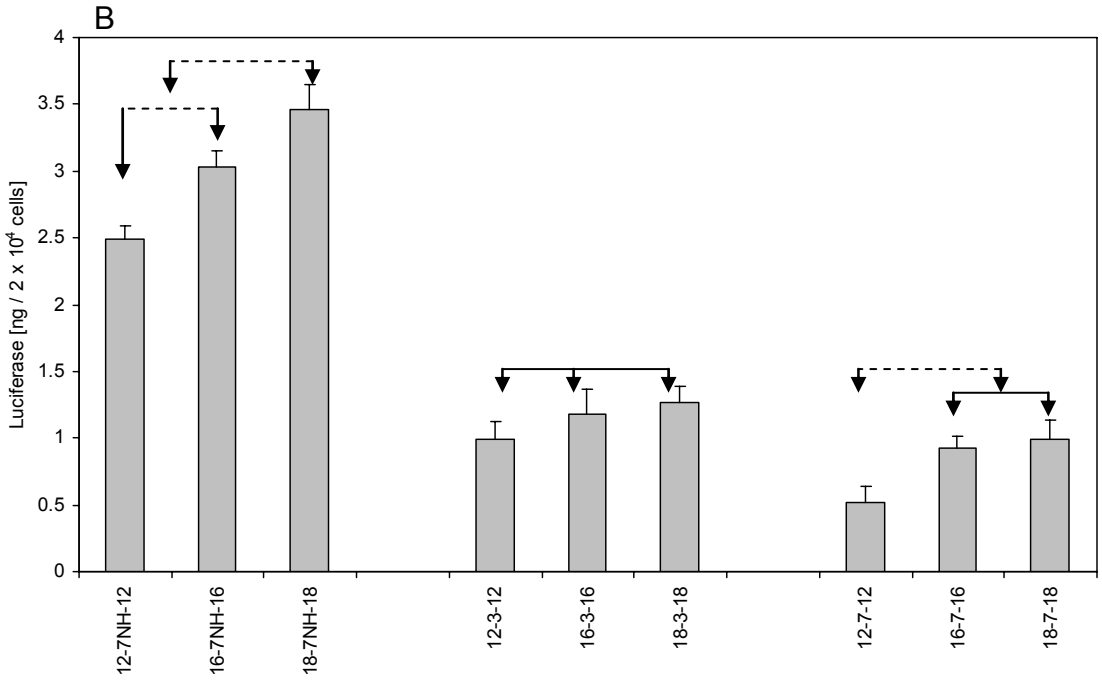
B
Luciferase [ng / 2 x 10^4 cells]
0
0.5
1
1.5
2
2.5
3
3.5
4
12-7NH-12
16-7NH-16
18-7NH-18
12-3-12
16-3-16
18-3-18
12-7-12
16-7-16
18-7-18

Figure 4.5.2.3-2. Transfection efficiencies in PAM 212 cell – comparison of underlying surfactant structures.
(A) Level of transfection efficiency compared using modifications in gemini surfactans spacer group as the changing variable, the hydrocarbon tail is held constant.
(B) Level of transfection efficiency compared using hydrocarbon tail as the changing variable, the type of spacer group is held constant.
In all cases luciferase expression was quantified 24 h after cells were transfected using complexes with $\rho_{+/-}$ = 10:1. n = 4, error bars = SD.

Legend
Solid line indicates no significant difference ($p < 0.01$) between any columns (individual or group) connected by the solid line.
Dashed line indicates a significant difference ($p < 0.01$) between columns (individual or group) connected by the dashed line.

4.5.2.4. DNA Transfection: COS-7 vs. PAM 212 Cells

The expression of a reporter gene in eukaryotic cells depends, to a large extent, on the gene's promoter region and cell type. Of interest in the present study was the effect of varying cell type. Therefore, COS-7 cells were introduced as a different cell line and the three groups of gemini surfactants were pre-assessed by way of transfection of COS-7 cells, followed by the advanced-phase transfection of PAM 212 cells. COS-7 cells are a relatively more phagocytotic cell line and thus have a higher PGL complex uptake capacity. They often serve as a standard cell line for pre-screening non-viral vectors to be used in more advanced transfection experiments. The results of pre-screening in comparison with transfection results in our chosen experimental PAM 212 cells are shown in Figure 4.5.2.4-1. The COS-7 cells showed better transfectability (ability to be transfected) than our model PAM 212 cells. This is consistent with other transfectability comparisons in which COS-7 cells were easier to transfect than other cell lines [257]. As observed with PAM 212 cells, results of $\rho_{+/-}$-dependent transfections in COS-7 cells (Figure D-I, Appendix D) were the best for PGL complexes with $\rho_{+/-}$ = 10:1, and decreased as $\rho_{+/-}$ decreased.

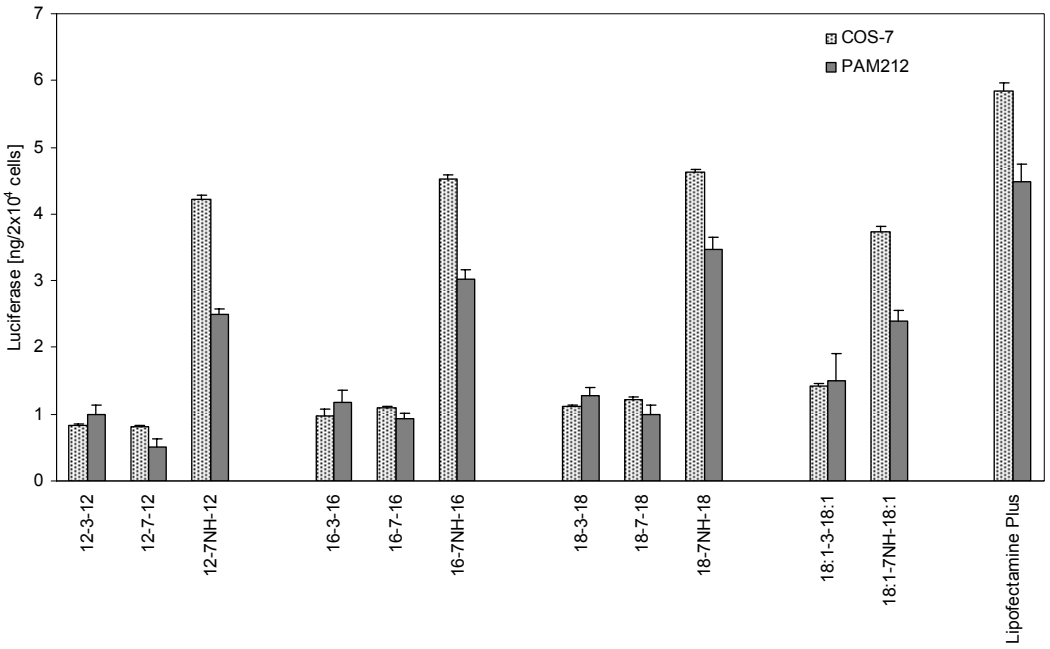

Figure 4.5.2.4-1. Comparison of gemini surfactant-mediated transfection in COS-7 and PAM 212 cells for m-3-m, m-7-m and m-7NH-m surfactants.
Origins of cell lines: COS-7, monkey kidney; PAM 212, epidermis of newborn BALB/C mice. The transfections were carried out using optimized conditions (PGL complexes with $\rho_{+/-}$ = 10:1; the luciferase expression was quantified after 24 h of transfection).

4.5.3. Evaluation of Transfection-related Toxicological Effects

The efficacy of any medication or benefit of the ingredients therein is particularly important when comparing the therapeutic benefit realized on the one hand, with the toxicity effects on tissues or cells on the other hand. Ultimately, the efficacy/toxicity balance must fall within safe limits to not put the life of organisms being genetically treated in more danger and for a promoted molecular delivery system to successfully pass through regulatory steps. We therefore determined cytotoxicities in our transfections using the optimal conditions. The cytotoxicity results for transfections in both COS-7 and PAM 212 cells are shown in Figure 4.5.3-1.

For both cell lines, the individual gemini surfactants recorded cell viability within the 75 – 80% range, which is statistically similar to the 80% cell viability level recorded by Lipofectamine Plus reagent. The cell viability of both the surfactants and Lipofectamine Plus reagent contrasts with the control surfactant-free transfections (Control, Plasmid, DOPE/plasmid, Figure 4.5.3-1) for which the cell viability was 100% due to the absence of any toxic surfactants or Lipofectamine components. Not withstanding the statistical similarity in the toxicity effects posed by the gemini surfactants, the m-7NH-m and m-3-m surfactants recorded the lower and upper edge of cell viability values, respectively, whereas the m-7-m surfactants were placed in between. Thus, the cytotoxicities generally increased in the following order: m-3-m < m-7-m < and m-7NH-m surfactants. However, neither cell line was particularly more susceptible to toxic effects as there was no indicating trend to suggest cell type susceptibility. This is against the premise that COS-7 cells are more phagocytotic and may have taken up more gemini surfactant-containing complexes, thus expressing more

protein than PAM 212 cells under the same conditions (Figure 4.5.3-1). In short, despite the probability of higher intake of toxicity-causing transfection complexes, the COS-7 cells did not show higher toxicity than the PAM 212 cells. This is likely due to the fast cell division (growth) mechanism that is in-built in COS-7 cells. The fast cell division mechanism would allow living cells to divide and quickly replenish cells dying as a result of transfection-related toxicity. The result will be a high survival rate as if to discount the higher particle uptake capacity of the COS-7 cells compared to the PAM 212 cells.

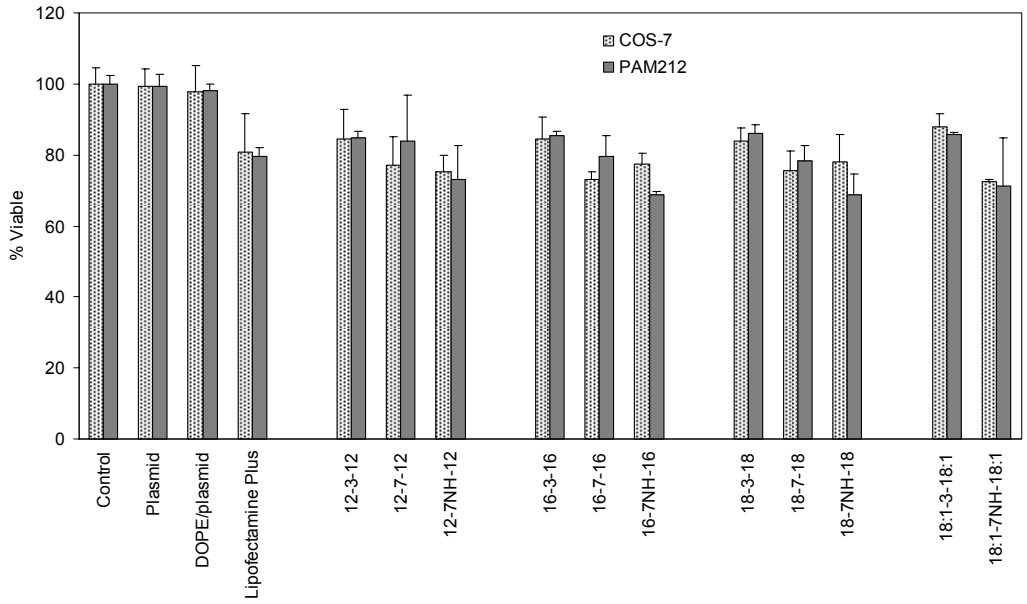

Figure 4.5.3-1. Comparison of cell viabilities in COS-7 and PAM 212 cells transfected using m-3-m, m-7-m and m-7NH-m surfactants.
Also included are results for non-transfected cells (Control), *naked* DNA (Plasmid), plasmid combined with DOPE (DOPE/plasmid) and Lipofectamine Plus™ reagent. Transfections were carried out using optimized conditions (i.e., PGL complexes with $\rho_{+/-}$ = of 10:1, with luciferase quantitation 24 h after transfection). n = 4, error bars = SD.

To evaluate the effect of different doses of gemini surfactants on the level of transfection-related toxicities, as a complementary investigation to the $\rho_{+/-}$-dependent gene expression (shown in Figure 4.5.2.2-1), cytotoxicities in both COS-7 and PAM 212 cells were determined following cell transfections. The transfections were carried out using PGL complexes containing varying concentrations of gemini surfactants, and with $\rho_{+/-}$ values corresponding to the values in previous transfections (Figure 4.5.2.2-1). The results displayed in Figure 4.5.3-2 were obtained for the m-7NH-m surfactants, and is representative of the dose-dependent cytotoxicity trends also for the m-3-m and m-7-m surfactants. Since cell viability of transfected cells is inversely related to cytotoxicity (% Mortality = 100 - % cell viability), a decline in cell viability indicates an increase in cytotoxicity. As such, the observed increase in cell viability of transfected cells in response to reduction of the gemini concentration used for transfection corresponds to a decrease in cytotoxicity as the gemini surfactant concentration is decreased.

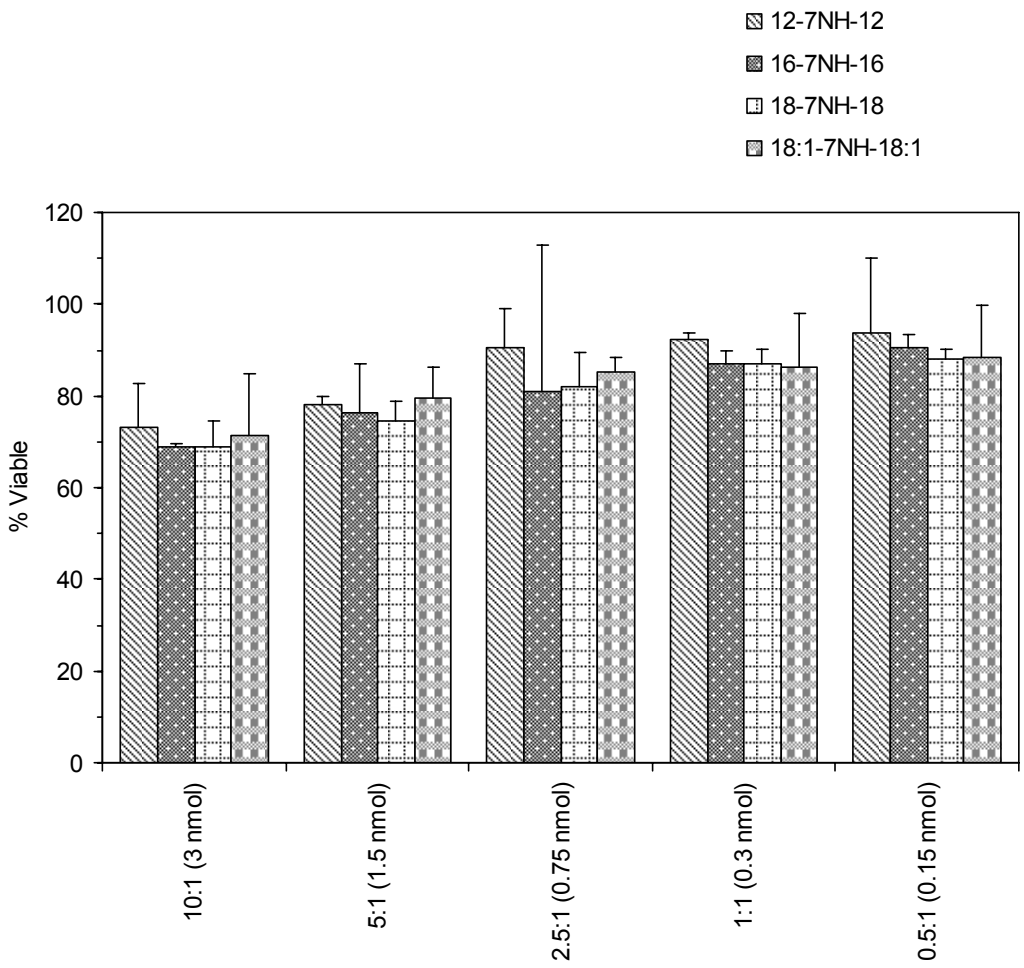

Figure 4.5.3-2. Dose-dependent toxicities for gemini surfactants in PAM 212 cells. Cells were transfected with PGL complexes prepared using varying concentration of m-7NH-m surfactants (i.e., complexes had values of $\rho_{+/-}$ ranging from 10:1 to 0.5:1. The numbers in parentheses next to each $\rho_{+/-}$ value represent the amount of surfactant used for preparing complexes based on a uniform plasmid dose of 0.2 μg). Cell viabilities were quantified after 24 h of transfection. The figure inset shows the level of cytotoxicity or motility in transfected cells (% Mortality = 100 - % cell viability). n = 4, errors bars = SD.

In our pre-screening tests for the surfactants, cell viability experiments were also carried out for COS-7 cells covering the three gemini surfactant groups and the five different gemini surfactant dose variations (i.e., using PGL complexes with variable $\rho_{+/-}$ values: 10:1, 5:1, 2.5:1, 1:1, 0.5:1). The results for these experiments (Figure D-2, Appendix D) were consistent with the surfactant concentration–toxicity proportionality trend, reiterated by the results of our present transfections of PAM 212 cells (Figure 4.5.3-2).

5. DISCUSSION

5.1. Design Scheme and Properties of the Gemini Surfactants

The research on gemini surfactants in general is currently being led by studies focusing on the m-s-m or N,N-bis(dimethylalkyl)-α,ω-alkanediammonium surfactants (Figure 1.4.3-1), an example of which is the 12-3-12 gemini surfactant having two C_{12} alkyl tails (dodecyl tails, m = 12) and a trimethylene spacer (s = 3). Through modification of the m-s-m gemini surfactant structure, with many manipulations centred on the headgroup-spacer region (the hub of major modifications), other types of gemini surfactants have evolved. The application of gemini surfactants, in general, in gene therapy research is in part driven by the safety issues surrounding the more effective viral alternatives, and of significant surfactant research interest, also driven by the remarkable suitability of molecular characteristics displayed by gemini surfactants. For instance, the critical micelle concentration (CMC) of gemini surfactants is generally some orders of magnitude lower than it is for comparable monomer surfactants, making gemini surfactants greatly superior over monomer surfactants in the encapsulation of DNA for delivery to cells. Because lower CMCs permit lower concentrations of gemini surfactants to effectively encapsulate DNA for cellular delivery, toxicity levels are greatly minimized in biological hosts.

The gemini surfactants studied herein include both normal m-s-m types and amine-substituted gemini surfactants that are based on the m-s-m general structure. For the m-

3-m, m-7-m and m-7NH-m series of surfactants, with a fixed spacer group for each series (Table 3.1.2-1), an increase in the alkyl tail length resulted in an increase in the Kraft temperature (Table 4.2.1-1) and a decrease in the CMC (Tables 4.2.2-1, 4.2.3-1), conformant with the linear decrease in the natural logarithm of CMC, which correlates with increase in alkyl tail length [258]. Two types of C_{18} hydrocarbon chains, which are the longest alkyl tails used for the gemini surfactants, resulted in different Kraft temperatures. Saturated C_{18} tails resulted in the highest Kraft temperatures, regardless of the nature of spacer group, while in contrast, unsaturated C_{18} tails (oleyl chains) reduced these Kraft temperatures by 9 – 16 ^{o}C (Table 4.2.1-1), underscoring the purpose of their use. As compared to saturated hydrocarbon tails, unsaturation in hydrocarbon tails introduces 'bends' in unsaturated tails. The bends results in poor stacking of the tails and lead to intermolecular forces that are much weaker than for saturated tails, consequently leading to reduced Kraft temperatures for surfactants with unsaturated tails.

As noted earlier, the trend of CMC values resulting from variations in the gemini surfactant spacer groups differs from the generally inverse relationship between CMC values and length of alkyl tail. Changes in the CMCs as a result of variations in the gemini surfactant spacer groups are in themselves small compared with the effect of variation in the tail length. The CMC values, determined from both surface tension and specific conductivity analysis (Tables 4.2.2-1, 4.2.3-1, respectively), are slightly lower for the m-s-m gemini surfactants (m = constant) having s = 7 than for those with s = 3. This observation for the two different polymethylene spacers is consistent with results previously reported in literature in which the CMC goes through maximum at s = 4–5, observed in an investigation of polymethylene spacers ranging from 2–16 methylene units for 12-s-12 gemini surfactants [218]. The reasons for such behaviour and the

potential of spacer variations to induce a rich array of aggregate structures for drug encapsulation, made possible by a number of steric, electrostatic and hydrophobic interactions, has been recently reviewed [86]. The rise in CMC up to its maximum value at s = 4–5 has been explained in terms of the conformational changes that gemini surfactants with short spacers ($1 \leq s \leq 4$) have to undergo in order to pack the alkyl tails into the core of micelles. But as the spacer chain extends beyond s = 6, its hydrophobic character as well as folding into the core of the micelles increases, thus favouring micelle formation and decreasing the CMC [178; 179].

The amine-substitution of gemini surfactants, which exploits the small changes that spacer variations generally cause to the CMC, was employed to impart other physicochemical properties while maintaining fairly constant CMCs. Some of the properties relate to changes including the insertion of pH-active aza- ($N\text{-}CH_3$) and imino- (N-H) groups in the polymethylene spacers of m-s-m gemini surfactant structures. This is demonstrated in the 12-spacer-12 and m-7NH-m surfactant groups (Table 3.1.2-1). The slight increase in CMC resulting from these more hydrophilic spacers (aza- and imino-substituted) relative to their equivalent length polymethylene counterparts can be linked to diminished or lack of spacer incorporation within the core of the micelle due to increased solubility, and this is less favourable to micelle formation [86].

The headgroup area (a_0), another characteristic of gemini surfactants central to their interaction with DNA, was also varied through changes in the spacer group of surfactants. The values of a_0 were higher for spacer species containing 8 or 7 atoms in the spacer chain and decreased as the spacer length decreased (Tables 4.2.2-1). The trend in literature indicates an increase in a_0 with an increase in length of spacer chain up

to s = 10 - 12, at which point there is a maximum, and then a decrease in a_0 beyond s = 10 - 12 [218; 234]. The decrease of a_0 after s = 10 - 12 is taken as evidence of the folding of longer spacers away from the water-side of the water-oil interface, which then brings the interconnected quaternary ammonium headgroups close to one another [86]. But whether a spacer is long or short, the ability of gemini surfactants to interact with or compact DNA is governed by the characteristics of the two distinct structural elements of gemini surfactants; namely, the headgroup-spacer region and the hydrophobic tail.

The gemini surfactants studied herein (Table 3.1.2-1) can be rated in terms of the characteristics referred to above, which are, for the headgroup-spacer region: equilibrium N-to-N distance, value of a_0, and available positive charges for neutralizing DNA phosphates; and for the hydrocarbon tail: tail length and whether it is saturated or unsaturated. A mathematical approach that relates these surfactant characteristics to the optimal morphology these surfactants form upon self-aggregation is given by Equation 5.1-1 below,

$$N_s = \frac{v}{la_0} \qquad 5.1\text{-}1$$

where v = volume of alkyl tail, l = length of alkyl tail, and a_0 = surface area occupied by the head-group. The magnitude of N_s indicates the preferred curvature of the aggregate structure. An N_s value of 0.3 favours spherical micelle organization (highly curved), whereas N_s = 1 and N_s > 1 favours planar bilayer formation and inverted micelles, respectively. Efficient DNA compaction using gemini surfactants is achieved when the spacer length s is <4 or >10, but not for intermediate lengths, and the compaction is enhanced when increasing the alkyl tail length from C_{12} - C_{18} [259]. One report [202] in which the 16-6-16 surfactant gave a higher transfection in cells than both the 16-2-16

and 16-3-16 surfactants is somewhat contrary to the positive correlation between efficient DNA compaction and high transfection. In other words, for the m-s-m surfactants herein, the m-3-m series is expected to compact DNA better than the m-7-m series; a similar trend in their transfection could also be expected. The use of unsaturated alkyl tails (oleyl tails) for one of the m-3-m surfactants could be more beneficial since oleyl tails have been suggested to form mixed structures, including micellar, while, for instance, saturated C_{16} tails form lamellar structures alone [202].

The equilibrium N-to-N distance ($d_{N\text{-}to\text{-}N}$) between nitrogen centres in the gemini surfactants (Table 5.1-1), especially for the gemini surfactants with aza- and imino-groups incorporated within their spacers, have been examined and previously published by our laboratory [201]. When the N-to-N distances, calculated from energy minimized models of the surfactants molecules, are said to allow a closer match with adjacent phosphates on DNA spaced by 6.5 - 7.1 Å [260], more favourable electrostatic interactions can occur between the gemini surfactants and DNA [261]. A study examining the interaction of DNA with the polyamine spermine [261], which has a trimethylene spacing of 4.9 Å between its adjacent nitrogen centres [262-264], has shown the trimethylene spacing to be suitable for electrostatic interactions between DNA and the polyamine agent. Calculations of N-to-N distances have also been reported specifically for gemini surfactants. The calculations for gaseous 18-s-18 are reported to be 5.23 Å, 6.21 Å and 7.76 Å, for s = 3, 4, and 5, respectively [182]. Stronger transfections have been demonstrated for surfactants with short N-to-N distances, such as s = 3 and 4, supporting the hypothesis that these spacings allow surfactants to optimally interact with DNA [265]. The implications of these findings with respect to the gemini surfactants (Table 5.1-1) being studied in this research are as follows: the m-

3-m, m-7NH-m and 12-spacer-12 group of surfactants, which have N-to-N distance of around 5.1 - 5.25 Å, are well placed for optimal interaction with DNA and transfection of cells [201]. The m-7-m surfactants, on the other hand, seem to have a spacer (10.08 Å) that is longer than required for optimal interactions and culminates in weak transfection. The folding of spacers that leads to enhanced transfection efficiencies has been clearly observed only for very long spacers, e.g., s = 16 [132], suggesting that the spacer for the m-7-m surfactants might be incapable of such folding.

Table 5.1-1. Distance between nitrogen centres for the gemini surfactants

Surfactants	Atoms	$d_{N\text{-to-}N}$ (Å)	Model
m-3-m series 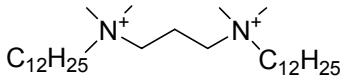 Others: m = 16, 18, 18:1	N1 – N2	5.25	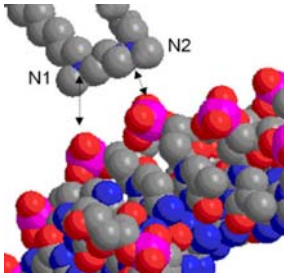
12-5N-12 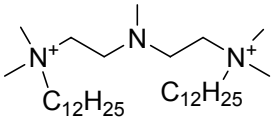	N1 – N2 N1 – N3 N2 – N3	3.90 7.52 3.88	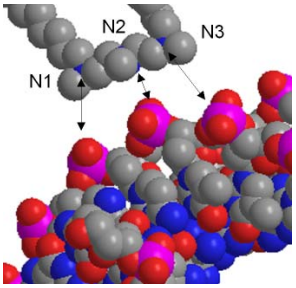
12-8N-12 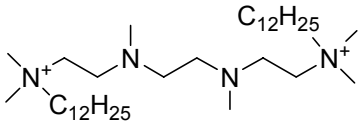	N1 – N2 N1 – N3 N1 – N4 N2 – N3 N2 – N4 N3 – N4	3.86 7.40 11.17 3.86 7.42 3.86	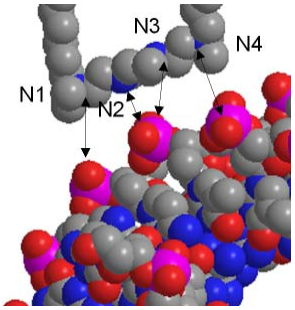

Note: Table continued on next page.

Table 5.1-1 (cont'd).
Distance between nitrogen centres for the gemini surfactants

Surfactants	Atoms	$d_{N\text{-}to\text{-}N}$ (Å)	Model
m-7NH-m series 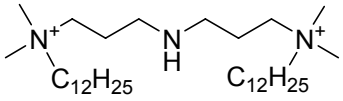 Others: m = 16, 18, 18:1	N1 – N2 N1 – N3 N2 – N3	5.08 10.15 5.08	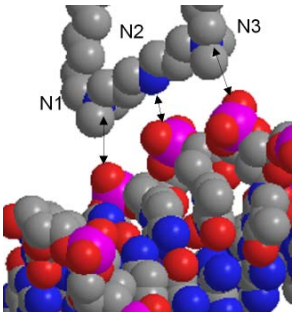
12-7N-12 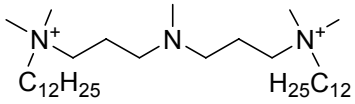	N1 – N2 N1 – N3 N2 – N3	5.14 10.18 5.14	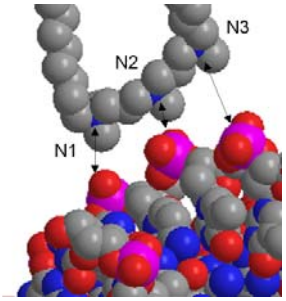
m-7-m series 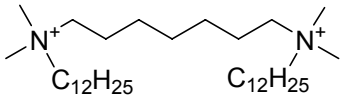 Others: m = 16, 18	N1 – N2	10.08	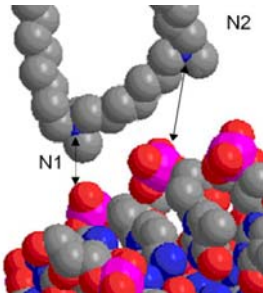

Calculated from Energy Minimized Model of Molecules using ChemOffice Chem 3D Pro Software. Molecules were energy minimized (MM2 force field) in the gas phase to a minimum root-mean-square gradient of 0.05. ref. [201].

In summary, the design scheme applied to the gemini surfactants varied the surfactant alkyl tail length and the degree of alkyl tail saturation, with alkyl tail varieties including C_{12}, C_{16}, C_{18} (all saturated) and *cis*-oleyl tail (monounsaturated C_{18}). The different spacers used for the gemini surfactants also varied in length (number of methylene units) and allowed for the type of amine-substituents in the spacer as well as the spacing between nitrogen centres in the gemini surfactant spacer to be varied. The solution properties of the gemini surfactants (Tables 4.2.2-1, 4.2.3-1) responded to applied modifications as expected. The differences among the gemini surfactants in terms of both the solution properties and structure of the gemini surfactants introduce differences in the levels of transfection efficiency achievable by the various compounds. The sections that follow examine transfection results in detail in order to answer the question of the correlation between transfection and properties of the investigated surfactants.

5.2. Transfection Abilities of the 12-spacer-12 Surfactants

Cellular gene delivery or transfection studies involving five 12-spacer-12 gemini surfactants, combined with complementary analysis of transfection-related cytotoxicities, marked the start of investigations of the transfection abilities of the gemini surfactants (Table 3.1.2-1). Results for the 12-spacer-12 surfactants in COS-7 cells (Figure 4.4.2.1-1) provided an initial platform for correlating the efficiency of transfection to the characteristics of the gemini surfactants. The fact that the 12-7NH-12 surfactant matched the commercial transfection agent Lipofectamine Plus™ in transfection efficiency, and is followed by the significantly less efficient surfactants in the order 12-7N-12, 12-5N-12, 12-8N-12, 12-3-12, makes the 12-7NH-12 surfactant the

focus of discussion. Table 5.2-1 summarizes transfection results (Luciferase expression - highest values at the bottom of table, cell viabilities) from the charts in Figure 4.4.2.1-1 to illustrate the trend in transfection.

Table 5.2-1. Transfection and cell viability levels for the 12-spacer-12 surfactants

Surfactant or agent	Luciferase expression (ng/2 × 10^4 cells)	% Viable (treated cells)
Plasmid	0.06 ± 0.01	100 ± 4
12-3-12	0.80 ± 0.03	90 ± 4
12-8N-12	1.01 ± 0.21	77 ± 2
12-5N-12	1.41 ± 0.55	78 ± 5
12-7N-12	2.30 ± 0.60	80 ± 2
12-7NH-12*	0.40 ± 0.01	ND
12-7NH-12	6.70 ± 0.50	70 ± 1
Lipofectamine Plus™	7.40 ± 1.12	82 ± 2

Results for surfactants are for PGL preparations of the surfactants; however, 12-7NH-12* is for a preparation without the lipid DOPE component. Values for plasmid are representative of both plasmid-only and plasmid-DOPE systems. ND: not determined

In relating the levels of transfection to the composition or characteristics of various transfection systems, it is important to first note that the addition of DOPE to the binary surfactant–plasmid systems (i.e., 12-7NH-12*, Table 5.2-1) caused a significant increase in transfection. Such a finding has been reported in previous studies [39; 132; 192; 254; 255]. Explanations offered for this beneficial effect are that helper lipids such as DOPE are able to stabilize liposomes and facilitate the release of complexed DNA through membrane fusion and/or destabilization of the endosomal membrane [254; 256]. A similar boosting effect was also evidenced by the addition, or absence, of a cationic component in systems with plasmid, and either with or without DOPE (Table 5.2-1). A clear demonstration is the significant increase in transfection for all nitrogen-substituted PGL systems relative to the plasmid–DOPE system (≈Plasmid, Table 5.2-1; $p < 0.05$). This stresses the need for negatively charged macromolecular DNA to be neutralized, condensed and complexed or encapsulated into small (nanometre-scale) particles to improve uptake by cells. Indeed, if a high DNA condensation beyond an average minimum is needed for efficient transfection, then the more efficient condensation of DNA reported for the 12-7NH-12 surfactant [201] may provide some explanation for its high transfection efficiency (i.e., the surfactant's PGL system).

One of the foremost indications from transfection results for the 12-spacer-12 surfactants is that amine-substitution is the factor responsible for the increased transfection for the four amine-substituted surfactants over the base 12-3-12 surfactant structure. But to create another level of interest, the amine-substituted gemini surfactants are in two types: the aza- and the imino-substituted surfactants. The most efficient aza-substituted surfactant 12-7N-12 (one N-CH_3), compared with family members, has a spacer that is two methylene units longer relative to 12-5N-12 (one N-CH_3) and one

methylene unit shorter relative to 12-8N-12 (two N-CH_3) (efficiencies being in that order). Clearly, the decline in transfection for 12-8N-12, which has double the number of aza substituents relative to its two family members, removes any expectation that transfection efficiency will correlate with a mere multiplicity of the aza substituents. Rather, other factors are necessary to adequately account for the observed difference. First, the increase in aza substituents for the 12-8N-12 surfactant creates an increased steric effect within the spacer group that affects the ability of the surfactant to form aggregates and/or bind DNA. Second, and as noted earlier (Table 5.1-1), optimal surfactant–DNA interactions are allowed by, for instance, an equilibrium inter-nitrogen spacing of 3-methylene units. This separation provides a closer match and electrostatic interaction between nitrogen groups on the surfactants and phosphate units on DNA. The condition is met by 12-7N-12 but not its two family members, which both have a rather short dimethylene spacing between their nitrogen centres. The trimethylene separation between the nitrogen centres in the imino-substituted surfactant 12-7NH-12 would, in part, account for the high transfection efficiency observed for this surfactant.

The 12-7NH-12 surfactant presents a clear contrast to 12-7N-12 and the other aza-substituted surfactants. Its increased transfection relative to 12-7N-12 may be in part due to decreased steric hindrance. A more important factor to account for the wide difference in transfection between the two surfactants is the increased pH activity owing to the imino substituent versus the aza substituent. By monitoring the changes in size of surfactant aggregates and the plasmid–gemini surfactant–lipid complexes as function of pH, a significant change in size for both the aggregates and the complexes was observed on going from a basic to acidic pH for samples involving the 12-7NH-12 surfactant (Figures 4.3.1-1A, 4.3.1-2A, respectively). The change results from the protonation of

the imino group. As earlier noted, even though the transition in size for the surfactant aggregates in particular is not as wide as the kind of vesicle to micelle transitions reported for sugar-based gemini surfactants [52; 206; 207; 240; 241; 266], the relevance to increased transfection is still clear. The transitions, due to their structural perturbation effect, aid in the endosomal release of DNA taken up by cells in the form of complexed DNA. The fact that the 12-7N-12 surfactant shows no change in the size of complexes containing it, and is also less efficient in transfection than the 12-7NH-12 surfactant, strongly supports the link between increased pH-activity and increased transfection. Unlike the 12-7N-12 surfactant, which only shows an increase in zeta potential with a decrease in pH (in response to decreasing amount of OH^- ions available to bind to its complexes), 12-7NH-12-containing complexes exhibited a transition in zeta potential as pH turns more acidic, in addition to the noted pH-induced structural transition. Such pH-sensitivity (shown by 12-7NH-12) and its potential to cause structural change, which will lead to increased transfection, can be placed in the context of previous reports. For example, pH-induced transitions from lamellar to the more fusogenic inverse hexagonal structure for DNA-carbohydrate gemini surfactant complexes are hypothesized to facilitate membrane fusion, and thus promote increased transfection at that level [52; 205]. Similar pH-induced transitions could be expected for the Lipofectamine Plus™ system based on the structure of component DOSPA, as well as in other polyamine-based molecules for gene delivery.

The morphological characteristics of transfection complexes involving DNA and either lipids or gemini surfactants present another level for explaining transfection patterns. These characteristics of the 12-spacer-12 gemini surfactant–plasmid–DOPE complexes, including small-angle X-ray scattering (SAXS) data, are presented in

recently published work [201]; a summary of the salient points are given in Table 5.2-2 (below). Transfection complexes, in general, display various structural forms, including the more common lamellar structures [39; 256; 267], and also inverse hexagonal [39] and cubic structures [268]. Inverse hexagonal bilayer complexes had earlier been associated with increased transfection, but later reports have shown that other structures such as lamellar (including multilamellar [269]) yield high transfection provided their membrane charge density (σ_M) exceeds a critical minimum of 1.04×10^{-2} e/Å^2 [39; 270]. But since the computed value of σ_M is less than the minimum value for all the 12-spacer-12 surfactants except 12-3-12 and 12-5N-12 (Table 5.2-2), there has to have been other structural forms apart from lamellar to explain the efficient transfection, especially for the 12-7NH-12 surfactant. σ_M calculation is based on Equation 5.2-1;

$$\sigma_M = \frac{eZN_{cl}}{N_{nl}A_{nl} + N_{cl}A_{cl}} \qquad 5.2\text{-}1$$

where Z = 2 = valency of gemini surfactant, A_{nl} and A_{cl} are the headgroup areas for DOPE (= 46 Å^2 [271]) and the gemini surfactants, respectively, and N_{nl} and N_{cl} are the number of moles of DOPE and the gemini surfactant.

Table 5.2-2. Membrane charge densities (σM), scattering peak positions (q) and d-spacing for the plasmid–gemini surfactant–DOPE nanoparticles (complexes) obtained from SAXS measurements (all previously published [201]).

Surfactant	σ_M ($\times 10^{-2}$ e/Å^2)	q (Å^{-1})	d-spacing (Å)
12-3-12[a]	1.15	Previous	Previous
12-5N-12	1.05	**0.107** (L), 0.173 (DNA), 0.207 (L)	58.6
12-8N-12	0.780	**0.105** (L), 0.119, 0.170 (DNA), 0.210 (L)	59.6
12-7N-12	0.748	0.083, 0.097, **0.105**, 0.117, 0.134, 0.174	59.6
12-7NH-12	0.920	0.083, 0.094, **0.106**, 0.116, 0.171	59.4

[a]Previously reported by our group [272; 273]: complexes for 12-3-12 form lamellar (L), inverse hexagonal and cubic structures. Calculation – d-spacing = 2π/q. Numbers in bold indicate main scattering peaks.

As indicated in Table 5.2-2, complexes formed with 12-3-12, 12-5N-12 and 12-8N-12 surfactants exhibit a lamellar (L) phase (peaks, d-spacing given). However, 12-3-12 has been noted in earlier reports to also form inverse hexagonal and cubic phase complexes, making it possible that the additional peak for 12-8N-12 is a sign of an additional phase. For both 12-7N-12 and 12-7NH-12, a main peak (bold) and several additional peaks exist. Research has yet to name the structural phases that these peaks correspond to. The presence of multiple scattering peaks for complexes of the 12-7N-12 and 12-7NH-12 surfactants (increased transfection) is consistent with complexes for 12-3-12, 16-3-16 and 18:1-3-18:1 for which multiple phases have been identified [272; 273]. Thus, these three surfactants display structural polymorphism. Therefore, the suggestion that complexes of gemini surfactants capable of polymorphism fuse readily with endosomal lipids and assist the release of DNA [201] could explain the increased transfection for the 12-7N-12 and 12-7NH-12 surfactants.

The importance of the level of transfection achieved by the 12-spacer-12 surfactants gains significant emphasis when factored together with cell toxicities caused by the surfactants (Table 5.2-1). The 12-7NH-12 surfactant was slightly more toxic to cells, reducing cell viability to 70%, relative to its equally efficient-transfection counterpart (agent) Lipofectamine Plus™, which resulted in 80% cell viability ($p < 0.01$). These cell viabilities are relative to the 100% viable control cells. The aza-gemini surfactants (12-5N-12, 12-8N-12 and 12-7N-12), however, showed similar toxicity to the cells relative to Lipofectamine Plus, while the parent gemini surfactant 12-3-12 was also similar to the control. But, more importantly, the 12-7NH-12 surfactant was not significantly more toxic relative to its amine-substituted analogues (12-5N-12, 12-8N-12) ($p < 0.01$). This implies that the remarkable increase in transfection efficiency for the 12-7NH-12

surfactant does not result in a corresponding rise in cell toxicity. Thus, this surfactant has emerged as a suitable candidate or base structure for further modification and testing, with the anticipation that the resulting modified structures would be more efficient transfection agents.

5.3. Transfection with Multi-series Gemini Surfactants

5.3.1. The Gemini Surfactant Series and Structures

As elaborated in Section 5.2, investigation of the 12-spacer-12 surfactants (with variable spacers) led to the discovery of significantly different transfection abilities that split the surfactants into two subgroups [201]. The 12-7NH-12 surfactant recorded the highest transfection efficiency and was significantly similar to the commercial Lipofectamine Plus reagent. The rest of the surfactants, including 12-3-12, gave significantly lower efficiencies. In advancing this initial work, additional gemini surfactants were generated through molecular design and synthesis, giving rise to an expanded gemini surfactant library. The expanded library of gemini surfactants can be grouped into three series; namely, m-3-m, m-7-m and m-7NH-m surfactants (Table 3.1.2-1). The surfactants within any of the series vary only in the length or nature of their hydrocarbon tail while the difference between any two series occurs in both the tail length and spacer type. Thus, a different chemistry and architecture of the head–spacer region is encountered on moving from one series of gemini surfactants to the other. Transfection results for these gemini surfactants, altogether, would provide information on structure–activity correlations that are important to the delivery of nucleic acids by the surfactants. An insight into such structure–activity correlations will pave the way for

design of new and more effective compounds. As significant contribution to the development of non-viral gene delivery, transfection studies for the m-7-m surfactants and three of the m-7NH-m surfactants (those with m = 16, 18, 18:1) are being reported for the first time.

5.3.2. Structure – Activity Relationship

The extensive investigation carried out for the 12-spacer-12 gemini surfactants allowed the transfection efficiencies recorded (in COS-7 cells) by these surfactants to be rationalized in terms of the surfactant molecular structure and properties of the resultant gemini surfactant–plasmid–DOPE complexes. In brief, the high transfection efficiency for the 12-7NH-12 surfactant is attributable to its ability to engage in close-matching or more favourable interactions with DNA phosphate groups, as well as its ability to induce the endosomal release of complexed DNA to allow nuclear entry and protein expression. This integrated ability is attributable to the trimethylene spacing between nitrogen centres and the more pH-sensitive imino group, both of which are important features for transfection [201; 263; 274]. Thus, quite expectedly, transfection results for the multi-series gemini surfactants show the highest transfection efficiencies for the m-7NH-m surfactants, even though in this instance the use of PAM 212 cells led to a general reduction in the level of protein expression compared to COS-7 cells. This reduction in protein expression could account for the slightly wider difference in transfection efficiency between the m-7NH-m surfactant group (lower) and Lipofectamine Plus™ reagent (higher). The slight difference (found in PAM 212 cells), however, is statistically insignificant.

The distinctively higher transfection abilities for the m-7NH-m surfactants (Figure 4.5.2.2-1) reinforce earlier indications of the special functionality conferred on these surfactants by the pH-active imino group (Section 5.2), and is consistent with recent reports [201; 263; 274]. First, the positive effect of the imino group is made manifest by the fact that the m-7-m surfactants, which in comparison lack only the imino group, resulted in rather low overall transfection. Second, even though the m-3-m surfactants also have trimethylene spacing between their nitrogen centres for close-matching interactions with DNA phosphates, they nonetheless recorded low transfection results. Between the m-3-m and m-7-m surfactants, the former recorded slightly higher (though statistically insignificant) transfection efficiency over the later (Figure 4.5.2.2-1). This emphasizes the important role of trimethylene spacings in the spacer for optimal gemini surfactant interaction with DNA as against the rather long heptamethylene spacing. The heptamethylene spacer, at the same time, is not long enough compared with, for instance, 16-methylene spacers, which are able to fold into the bilayer membranes, restoring the required optimal spacing and leading to enhanced transfections [132]. Published work on polyamine–DNA interactions supports this conclusion by showing that trimethylene and tetramethylene spacings are required for a tight binding interaction between polyamines and double helical DNA [261; 275; 276]. Such high affinity binding was later linked to higher transfection in CHO cells [277].

Also on the subject of interactions, recently published work has indicated that the use of dimethylene spacings weaken or perturb cationic liposome–DNA interactions. While such non-optimal transfection agent–DNA interactions have been shown to negatively affect (or, at the least, not to enhance transfection ability) [277], as found for both 12-5N-12 and 12-8N-12 herein, other reports have correlated similar significantly

weak transfection agent–DNA interactions to increased transfection [274]. But, as a contributory factor to reduced transfection ability, the 12-5N-12 and 12-8N-12 surfactants have methyl group(s) on the tertiary amino functional group(s), for which the resulting steric hindrance further limits their interactions with DNA. The opposing reports with regards to the influence of non-optimal or weak transfection agent–DNA interactions on transfection efficiency clearly poses a question of what level of interactions is required for enhanced cellular gene transfer. That is, which of 'high affinity binding' or 'loose/weak binding' interactions are preferable? The use of amphiphile agents for gene delivery in part rest upon their ability to neutralize, condense and encapsulate DNA into nano-complexes, and release the DNA inside a cell at the needed time. Thus, while the need to neutralize, condense and encapsulate calls for a reasonable amount of 'high affinity binding', the need also to release DNA has led to the rationalization of high transfection efficiency in terms of weak interactions. For these reasons, emphasis in non-viral gene delivery is shifting toward both optimal 'high affinity binding' and incorporation of functional groups to help engineer DNA release once complexes are incorporated in a cell [52; 205] – as demonstrated in the use of the N-H group in the m-7NH-m surfactants.

The difference in transfection between the three series of surfactants can be explained at yet another level using the pK_a values. The importance of pK_a is made more evident by the fact that m-7NH-m surfactants have amino groups that exhibit basic character while both the m-3-m and m-7-m surfactants possess no amino groups. The pK_a values for the m-7NH-m surfactants, listed on Table 4.2.4-1, are all approximately 5. Such low pK_a values in relation to the final pH range of 7.6 ± 0.4 for the optimal transfection complexes ($\rho_{+/-}$ = 10:1) prepared for transfection imply that the excess

amino functional group in the finished complexes would remain unprotonated. The presence of such an unprotonated amino functional group further supports the proposition of assisted endosomal release of complexed DNA following entry of complexes into the cell [274]. Amino functional groups with low pK_a values in polyethylenimine (PEI) have been suggested to have the capacity to buffer intracellular endosomal compartments after cellular uptake of complexes, thereby promoting osmotic shock of the endosomal membranes and release of DNA into the cytosol [239; 257].

In other words, the m-7NH-m surfactants have outperformed both the m-3-m and m-7-m surfactant groups by possessing a low pK_a-conferred capacity to release DNA from endosomes following cellular uptake or endocytosis. The potential availability of unprotonated amino functional groups for this purpose is supported by the fact that the amino functional groups have pK_a values (around 5) that are lower than both the pH of finished transfection complexes (found to be 7.6 ± 0.4) and the physiological pH of host cells (excluding cells' endosomal compartments). It should, however, be pointed out that, among the 12-spacer-12 surfactants, both 12-8N-12 and 12-7N-12 had pK_a values lower than 5 (implying greater buffering capacity). But these two were outperformed by the 12-7NH-12 surfactant either because the two surfactants are limited by the lack of suitable separation between the nitrogen centres (Table 5.1-1), the steric hindrance from the amino-containing methyl group or both factors.

Of the overall dependence of transfection activity on the structural elements of the gemini surfactants investigated, the hydrophobic moiety accounted for a small to statistically insignificant portion of it. This is relative to the effect of varying the headgroup–spacer region as described above. Also, at the narrower level of alkyl tail vs. alkyl tail comparison, difference in transfection was insignificant in the majority of

cases. For both the m-3-m and m-7-m surfactants, the trend of increased transfection in response to the increase in the alkyl tail length, though evident and consistent with some reports [198], was insignificant. Increase in transfection was only statistically significant in the m-7NH-m surfactants, being slightly statistically higher for m = 16, 18 relative to m = 12, 18:1 ($p < 0.01$). The former pair was equivalently efficient as was the later. The occurrence of sharper differences in transfection in a number of cases has stemmed from comparisons of transfection agents having alkyl tails with a single digit number of C atoms with agents whose alkyl tails fall within the much more transfection-efficient range (12 to 18 C atoms) [210]. But, in general, the question of whether there is a best length of alkyl tail (saturated or unsaturated, asymmetric or not) has been answered with split experimental findings, ruling out any linear correlation between tail length and transfection [185; 278]. For instance, a study of phospholipids indicated that shorter alkyl tails allowed for better *in vitro* transfection, whereas longer tails were needed for better *in vivo* transfection [279]. In broader studies of collections of alkyl tails in the range C_{12} – C_{18}/$C_{18:1}$, each of them namely, C_{12} [280; 281], C_{14} [282; 283], C_{18} [73; 210; 284] and $C_{18:1}$ [52; 73; 282; 285] has emerged the best out of the rest in one study or the other.

With regard to unsaturated alkyl tails, the 18:1-3-18:1 surfactant, made by incorporation of mono-unsaturated oleyl tails in the m-3-m template, yielded the highest transfection for that series, whereas 18:1-7NH-18:1 created from m-7NH-m template dropped in its series (Figure 4.5.2.2-1). This apparent paradox is placed in the context of recent reports: oleyl tails were found to perform less than the optimal C_{18} counterparts in studies of spermine-based gemini surfactants [210] and biodegradable pyridinium amphiphiles [284]; other studies involving carbohydrate-based and peptide-substituted

gemini surfactants as well as other amphiphile molecules have found oleyl tails to be more effective relative to their saturated analogues [52; 73; 282; 285]. Oleyl tails when they result in higher transfection are believed to do so through their enhancement of the membrane fluidity of transfection complexes, an effect correlated to endosomal escape [281]. On the other hand, the susceptibility of the double bond to oxidation, either during transfection complex preparation or during a storage duration, may constitute the potential to cause reduced transfection yield [185].

5.4. Transfection Complexes: Particle Characteristics vs. Transfection

The presence of different forms of particle structure observed in transfection systems involving the m-7NH-m surfactants have been noted using TEM, Section 4.3.3. The observed heterogeneity may well indicate the polymorphic tendencies displayed by transfection complexes whereby they adopt a number of multiple structural phases including lamellar, hexagonal and cubic phases. A number of studies have been reported in which SAXS studies of DNA/gemini surfactant complexes revealed multiple structural phases and these phases were matched with different structural forms observed using TEM [205]. The positive correlation between structural polymorphism and higher transfection has already been underscored [272; 273]. For instance, the m-3-m surfactants (m = 12, 16, 18:1), which are known for their ability to form polymorphic complexes with DNA, are observed to mediate effective transfections both in this research and previously [272; 273]. In line with the link between polymorphism and effective transfection, it is reasonable to ascribe the increased transfection of the m-7NH-m surfactants in part to their polymorphism, which is being proposed based on TEM studies (Figure 4.3.3-1). The proposition of polymorphism could, in future, be

evaluated using SAXS studies and an examination of the SAXS scattering pattern in relation to electron micrographical studies for the m-7NH-m surfactant/DNA transfection systems.

The increase in transfection efficiency observed for the amine-substituted m-7NH-m surfactants relative to the unsubstituted m-3-m and m-7-m surfactants is also in part related to the ability to undergo pH-induced structural transition. Unlike the m-3-m and m-7-m surfactants, the m-7NH-m surfactants displayed a structural change in response to a neutral to acidic pH transition for both the gemini surfactant-only aggregates or vesicles and the transfection complexes formed from these surfactants and DNA (Figures 4.3.1-1, 4.3.1-2). The occurrence of such structural change together with the increased transfection observed for the m-7NH-m surfactants is consistent with reports in which either vesicle-to-micelle [52] or lamellar-to-hexagonal [205] structural changes have been correlated with increased transfection. For the purpose of increasing transfection, these structural changes are believed to mediate the release of DNA from endosomes through the membrane perturbation or fusion that results from the change of structural conformation [52; 205]. The changes also reflect the ability of certain types of gemini surfactants to interface with and take advantage of the progressive acidification process associated with lysosomal/endosomal degradation through which cells conduct their internal natural recycling and foreign particle destruction [33].

The pH-induced structural changes for transfections systems prepared from the m-7NH-m surfactants, described above, and the potential for this behaviour to cause the release of DNA trapped in endosomal compartments fit with proposed diagrammatic models [33; 205; 247; 286]. Such step-specific models (for endosomal release or escape) give precise illustration and throw more light on the overall process of DNA transfection

presented in Figure 1.3.4-1. Asokan and Cho in their recent report presented a simplified description of the release or escape of complexed DNA from endosomal compartments in terms of a shift of the compartmental pH to an acidic state by the action of cells' internal machinery (Figure 5.4-1) [286].

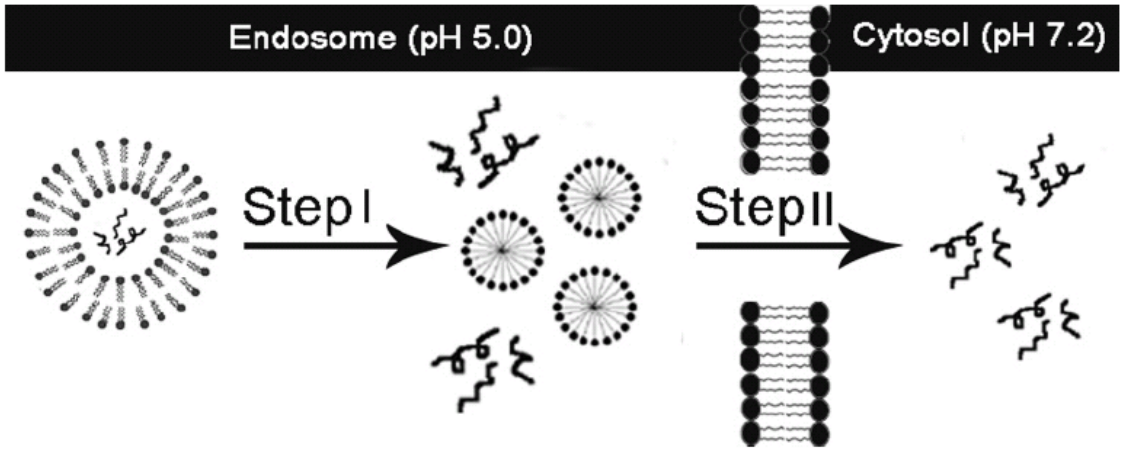

Figure 5.4-1. Illustration of the proposed 'endosomal release or escape' of complexed DNA during cellular transfection with pH-sensitive gene delivery molecules.
The release mechanism is summarized into two steps and explained as follows:

In **Step I**, the endosomal compartment and its contents turn acidic, presumably as the cell prepares to naturally digest and/or recycle the internalized foreign material. Spontaneously, the surfactant-containing DNA complexes absorb protons through protonation of the m-7NH-m surfactants, which as found in pH-controlled particle size analysis (Figures 4.3.1-1, 4.3.1-2), results in a change of the original complex structure. The type of structural change depicted here is a vesicle-to-micelle transition, but the possible structural changes for complexes also include a potential lamellar-to-hexagonal transition. Both of these would cause a disruption to the endosomal membrane and trigger a dissociation of the DNA from the surfactants either immediately or subsequently.

In **Step II**, the contents of the endosomal compartment including the DNA (bold black coils) are released into the cytosol through pores created in the disrupted endosomal membrane. The DNA is shown to have already dissociated from the micelles before the release, but the possibility for post-release dissociations have also been expressed [33],

and could readily occur for lamellar-to-hexagonal transitions. The release of freed DNA or surfactant-associated DNA into the cytosol allows the DNA to avoid imminent destruction through endosomal digestion. The step also brings DNA to the final phase of its journey, i.e., passage into the nucleus. Alternatively, the DNA can be directly involved in protein expression in the cytosol without the need for an additional transport into the nucleus. The two step mechansim was proposed by Asokan and Cho [286].

Another characteristic that potentially indicates a change in the nature of transfection complexes, i.e., zeta potential, was observed to undergo a transition in response to acidification for the 12-7NH-12 surfactant. But the surfactants with longer alkyl tails lacked a clear transition in zeta potential, showing rather a decrease in zeta potential as a function of decreasing pH consistent with the expected decrease in hydroxide ion concentration (Figure 4.3.2-1). This nonetheless still allows the increased transfection efficiency for the m-7NH-m surfactants to be explained in terms of the pH-induced changes in the complex structures that are inferred through acidification vs. size measurements (Figures 4.3.1-1, 4.3.1-2).

5.5. Non-Transfectant-related Factors Affecting Transfection

The complex multi-step process of DNA transfection is governed by not only the structural elements of delivery molecules (the transfectants) but also by biological as well as other factors. This is supported by the findings herein, including the fact that luciferase gene expression was time-dependent (Figure 4.5.2.1-1), rising to a peak at 24 h after transfection and then declining. The transgene expression was also affected by the cell type (Figure 4.5.2.4-1) and the dose of gemini surfactant (Figure 4.5.2.2-1). This might suggest that simple relationships between transfection efficiency and any of these factors, particularly structure of delivery molecules, are not to be expected. But the implications of any set of variables, whether they arise regularly, circumstantially or both, can inform the development process of non-viral gene medications. With regard to the time-dependent decline of luciferase expression, future genetic medications working in a similar fashion can be applied repeatedly as already practiced for an overwhelming number of non-genetic medications.

The fact that COS-7 cells displayed higher transfectability (ability to be transfected) than PAM 212 cells might suggest that evolving non-viral gene medicines based on gemini surfactants will need to be specialized for use in specific cell types or range of cell types. In other words, one type of medication built with a certain kind of gemini surfactant vector might not be effective for application in all cell/tissue types or via all routes of administration. The need to specialize medications could also result from nucleic acids meant for delivery to the cell nucleus as against those meant for cytosolic delivery. Antisense oligonucleotides usually destined for cell cytoplasm complete their journey upon crossing the cell plasma membrane into the cytoplasm. But transfer of plasmid DNA to the nuclei calls for additional transport processes for the DNA to make it through the cytoplasm and across nuclear membrane into the nucleus.

A scarcely investigated but potentially very important factor affecting the uptake of transfection complexes by cells is the size and morphology of the cells themselves. Understandably, the fact that the size and morphology of cells evolve as the cells grow in culture and cannot be routinely controlled limit investigations involving the exploitation of cell size and morphology as manipulatable variables. Furthermore, given a good level of control over the life mechanisms of living cells, it would be possible to artificially program or induce cell division to occur while cell transfection is being carried out. Cell division provides a special opportunity for increased nuclear entry of DNA during transfection, as there is transient opening of the cell nucleus. Thus, clearly, a step beyond the general lack of control over the above-mentioned cellular attributes, including cell division and the size and morphology naturally adopted by cells, could prove to be very important in cellular gene delivery. But in the meantime, examination of the natural size and morphologies adopted by cultured PAM 212 cells was carried out

in this research using stereological-TEM analysis (Figure 4.4-1). Cells on average measured 6 – 10 μm in diameter when taken as circular or spherical entities, and were 24 – 40-fold larger than the transfection complexes (measuring 250 nm, maximum), which were presented to the cells for uptake. Some studies have recently reported that active uptake of complexes through endocytosis is achieved for complexes in the small size range of around 100 nm [287]. If small size of the complexes is required, then the herein-found size ratios, which confer relative small and large sizes to the complexes and cells, respectively, place the cells in a position to effectively engulf or endocytose the complexes. Such examination of size ratios could be continued in future transfection studies to obtain accumulated data for a more comprehensive cell-to-transfection complex size ratio analysis.

5.6. Toxicological Evaluation

The incorporation of amphiphile transfection agents, which in many cases are non-natural and non-biodegradable, into cells through uptake of transfection complexes creates cell membrane pores and disrupts the cellular signalling mechanism by inhibition of protein kinase C [288]. Whether synthesized or developed from natural components and subunits, the efficacy of any molecular gene delivery system is particularly important when comparing its optimal gene delivery record with the cytotoxicity associated with it. Upon toxicological investigations, both the m-3-m and m-7-m surfactant groups (unsubstituted) were found to cause lower toxicities to cells relative to the imino-substituted m-7NH-m surfactants (comparison done under optimal transfection conditions: $\rho_{+/-}$ = 10:1, 24 h post-transfection evaluation, Figure 4.5.3-1). However, because of the level of similarity, no significant distinction ($p > 0.05$) was

observed between the m-3-m and m-7-m surfactants (which have closer similarity) or between either of the unsubstituted gemini surfactant groups and the m-7NH-m surfactants. Altogether, although the m-7NH-m surfactants emerged narrowly more toxic to cells, they transfected the cells at much higher efficiencies than their less efficient m-3-m and m-7-m counterparts. Thus, their kind of headgroup–spacer moiety yielded remarkably higher transfections without a correspondent increase in their cytotoxicity effects. This ranks them high in terms of good efficacy/toxicity balance.

When viewed in the light of two other variables, which are the length of alkyl tail and level of gemini surfactant usage (i.e., concentration) the cytotoxicities either showed no correlation at all or correlated rather weakly. But in general the cytotoxicities varied insignificantly ($p > 0.01$) in response to both variables within the range investigated. In response to increase in gemini surfactant dose, cytotoxicities rose insignificantly in most of the cases. This trend is illustrated in Figure 4.5.3-2 using results for the m-7NH-m surfactants. For the gemini surfactant dose corresponding to $\rho_{+/-} = 10:1$ (which yielded the best transfection for all surfactants) the cytotoxicity was insignificantly higher than for lower $\rho_{+/-}$ values. However the $\rho_{+/-} = 10:1$ dose showed more than 50% greater transfection efficiency than the lower doses (Figure 4.5.2.2-1) was also significantly more efficient than previously reported doses exceeding $\rho_{+/-} = 10:1$ [244]. Thus, the higher transfection for the $\rho_{+/-} = 10:1$ dose coupled with its low dose-related toxicity makes it the optimum condition for transfection complex preparation using the investigated gemini surfactants. It was only at this dose that the m-7NH-m surfactants transfected cells at a level as high as Lipofectamine Plus™ (Figure 4.5.2.2-1), while maintaining a high level of cell viability comparable to Lipofectamine Plus™ (Figure 4.4.3-1) ($p < 0.01$ in both cases).

5.7. Concluding Remarks

The investigations conducted over the entire research and described in this thesis included the rational design and synthesis of novel gemini surfactants, and the fitting of these surfactants within a library of gemini surfactants (totaling 14 different compounds) for *in vitro* gene delivery studies. A significant amount of ^{1}H NMR, ESI-MS and CH&N analytical data were generated that confirmed the targeted synthetic gemini surfactant products and their high-grade purities. Characteristics of the gemini surfactants that are important to gene delivery were determined; these include Krafft temperatures, CMC values, headgroup areas, pK_a values and the pH-dependencies of size and zeta potential of the aqueous gemini surfactants. Transfection complexes, prepared from mixtures of gemini surfactants, plasmid and DOPE, were also analyzed to determine their size and zeta potential pH-dependencies, as well as their morphological attributes. Transfection studies, staged in two phases and involving two cell lines, were ultimately carried out using fresh transfection complexes. In brief, the m-7NH-m surfactants emerged as the most efficient in transfecting cells, and as potential or suitable candidates for non-viral gene delivery at high levels including *in vivo*. The results also demonstrate that the transfection efficiencies of the surfactants studied could be improved by stepwise optimization of the surfactant structures, including lengthening the alkyl tails from C_{12} to either C_{18} or $C_{18:1}$. The specific conclusions of the research are given in Sections 5.7.1 to 5.7.3.

5.7.1. Important Structural Features Emerging from Transfection Studies

The following specific conclusions can be drawn in relation to beneficial structural features:

- The gemini surfactants built from chosen headgroup–spacer and hydrocarbon tail moieties and displaying various structures, exhibited controlled properties and also properties that varied naturally.
- A strong correlation between structure of the gemini surfactants and their transfection ability is noted. Incorporation of amino functional groups generally accentuated transfection ability; however, the use of an N-H group showed a stronger impact than an N-CH_3 group (12-7NH-12 better than 12-7N-12). This difference relates to limitations imposed by the N-CH_3 group, which include reduced pH-activity, on one hand, and steric hindrance against optimal surfactant–DNA interactions, on the other hand.
- Also, in relation to the impact of the gemini surfactant structure, optimal equilibrium distance (corresponding to tri-methylene separation) between adjacent nitrogen centres was also important, although the impact was found to be modest. Also, with both N-H group and optimal inter-nitrogen separation, transfection ability could still be enhanced by lengthening the alkyl tails from C_{12} to either C_{18} or $C_{18:1}$.

5.7.2. Morphology of Transfection Complexes or Nanoparticles

The characteristics of transfection complexes derived from plasmid–gemini surfactant–DOPE mixtures constitute yet another dimension determining the level of transfection. Complexes capable of adopting polymorphic structural phases and which

undergo pH-induced structural transition demonstrated high transfection efficiencies. Endosomal release of DNA can be staged by both characteristics. Ability to exhibit both characteristics (e.g., 12-7NH-12-based complexes are both polymorphic and pH-sensitive) led to higher transfection compared with the ability to exhibit only one characteristic (e.g., 12-3-12-based complexes are only polymorphic).

5.7.3. Toxicological Effects

Evaluated toxicological effects associated with the gemini surfactants show that the most efficient m-7NH-m surfactants imposed no higher toxicity on cells relative to the less efficient surfactants. Thus, the rational design of the m-7NH-m surfactants to enhance their transfection abilities also ensured that their toxicity to cells was kept minimal. These surfactants have thus emerged as suitable candidates for non-viral gene delivery at *in vivo* or higher levels.

5.7.4. Future Directions of Research

As indicated above, gene delivery abilities of the m-7NH-m surfactants could be further investigated *in vivo*, for instance using a mouse gene delivery model. The *in vivo* delivery could be targeted to the epidermal keratinocytes using topical administration since the model PAM 212 cell line used herein are themselves developed from murine epidermal keratinocytes primary cultures. Such an investigation will, in combination with the *in vitro* results presented herein, provide direction as to the next steps forward for designing efficient gemini surfactants for non-viral gene delivery. In the meantime, results at the *in vitro* level suggest that incorporation of additional imino (N-H) groups could make the resulting m-$(NH)_{X+1}$-m surfactants more efficient transfection agents

since the use of a single imino group resulted in increased transfection for the m-7NH-m surfactants (Figure 5.7.4-1). The variable x is the number of additional imino groups separated by trimethylene spacings; $x \geq 1$. Similarly, variations in length of hydrocarbon chain ranging from C_{12} to either C_{18} or $C_{18:1}$ can be introduced. The gene delivery assessment of these further-designed surfactants could be complemented by evaluation of their toxicological effects.

m-$(NH)_{X+1}$-m surfactants • Simple schemes, quick and easy synthesis	Peptide-based gemini surfactants [73; 289] • Complex schemes, synthetic challenges to be expected
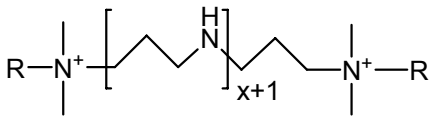	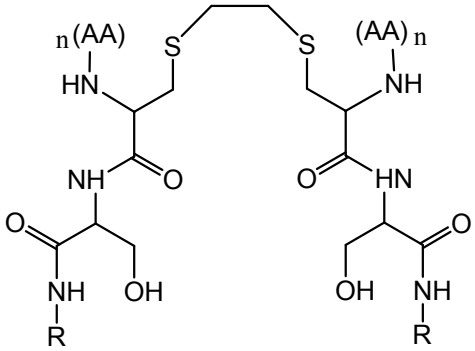
R = C_mH_{2m+1} m = 12, 16, 18, 18:1 (oleyl) x = number of extra NH groups	R = C_mH_{2m+1} m = 12, 14, 16, 18, 18:1 (oleyl) AA = amino acid, n = number of amino acids

Figure 5.7.4-1. Schematic difference between m-$(NH)_{X+1}$-m (left) and peptide-based (right) gemini surfactants.
The m-$(NH)_{X+1}$-m surfactant structural template proposes the next level of molecular design of gemini surfactant structures within the framework of further increasing the transfection efficiencies demonstrated in this research.

Within the context of routine production of gene delivery molecules for practical application, it is important for these molecules to be produceable in sizeable quantites to meet demands of a possible pharmaceutical non-viral genetic medicine industry. This particularly requires that the current research of gene delivery molecules, including gemini surfactants, lead to the design of efficient but simple candidates for which optimal and large-scale industrial manufacture can be easily attained. Such optimal and large-scale manufacture is necessary for obtaining gemini surfactants with high-grade purity, as required for any pharmaceutical ingredient, and for reducing cost of production. Even though a number of complex molecular structures such as the peptide-based gemini surfactant structure shown in Figure 5.7.4-1 have been demonstrated to fall into the same class or a higher class of transfection efficiency than the commercial transfection Lipofectamine Plus™ reagent [33; 73; 289], the synthesis of this surfactant falls within inherent limitations. In general, synthetic methods for generating compounds with multiple functional groups or moieties (such as the peptide-based gemini surfactant, Figure 5.7.4-1) are less efficient. As a comparative advantage, the m-7NH-m surfactants designed in this research are simple, allow quick and easy synthesis and yet yield transfection efficiencies as high as Lipofectamine Plus™. By expectation, this advantage should, at the minimum, hold for the m-$(NH)_{X+1}$-m surfactants (Figure 5.7.4-1), with the possibility that these surfactants could prove to be better than Lipofectamine Plus™.

6. REFERENCES

1. **T. Friedmann** (1996). Human gene therapy - an immature genie, but certainly out of the bottle. *Nature Medicine (New York)* **2**, 144.

2. **E. H. Chowdhury, and T. Akaike** (2005). Advances in fabrication of calcium phosphate nano-composites for smart delivery of DNA and RNA to mammalian cells. *Current Analytical Chemistry* **1**, 187-192.

3. **A. D. Miller** (1998). Cationic liposomes for gene therapy. *Angewandte Chemie, International Edition* **37**, 1769-1785.

4. **A. Bout** (1996). Prospects for human gene therapy. *European Journal of Drug Metabolism and Pharmacokinetics* **21**, 175-179.

5. **S. D. Patil, D. G. Rhodes, and D. J. Burgess** (2005). DNA-based therapeutics and DNA delivery systems: A comprehensive review. *AAPS Journal* **7**, E61-E77.

6. **W. F. Anderson** (1984). Prospects for human gene therapy. *Science (Washington, DC, United States)* **226**, 401-409.

7. **R. J. Desnick, and E. H. Schuchman** (1998). Gene therapy for genetic diseases. *Acta Paediatrica Japonica* **40**, 191-203.

8. **C. M. Lynch** (1997). New prospects for cardiovascular gene therapy. *Expert Opinion on Investigational Drugs* **6**, 1691-1696.

9. **A. Darji, C. A. Guzman, B. Gerstel, P. Wachholz, K. N. Timmis, J. Wehland, T. Chakraborty, and S. Weiss** (1997). Oral somatic transgene vaccination using attenuated S. typhimurium. *Cell (Cambridge, Massachusetts)* **91**, 765-775.

10. **D. R. Sizemore, A. A. Branstrom, and J. C. Sadoff** (1995). Attenuated Shigella as a DNA delivery vehicle for DNA-mediated immunization. *Science (Washington, D C)* **270**, 299-302.

11. **G. Dietrich, A. Bubert, I. Gentschev, Z. Sokolovic, A. Simm, A. Catic, S. H. E. Kaufmann, J. Hess, A. A. Szalay, and W. Goebel** (1998). Delivery of antigen-encoding plasmid DNA into the cytosol of macrophages by attenuated suicide Listeria monocytogenes. *Nature Biotechnology* **16**, 181-185.

12. **P. Paglia, E. Medina, I. Arioli, C. A. Guzman, and M. P. Colombo** (1998). Gene transfer in dendritic cells, induced by oral DNA vaccination with Salmonella typhimurium, results in protective immunity against a murine fibrosarcoma. *Blood* **92**, 3172-3176.

13. **C. Grillot-Courvalin, S. Goussard, F. Huetz, D. M. Ojcius, and P. Courvalin** (1998). Functional gene transfer from intracellular bacteria to mammalian cells. *Nature Biotechnology* **16**, 862-866.

14. **C. Grillot-Courvalin, S. Goussard, and P. Courvalin** (1999). Bacteria as gene delivery vectors for mammalian cells. Commentary. *Current Opinion in Biotechnology* **10**, 477-481.

15. **H. Loessner, and S. Weiss** (2004). Bacteria-mediated DNA transfer in gene therapy and vaccination. *Expert Opinion on Biological Therapy* **4**, 157-168.

16. **G. Vassaux, J. Nitcheu, S. Jezzard, and N. R. Lemoine** (2006). Bacterial gene therapy strategies. *Journal of Pathology* **208**, 290-298.

17. **D. D. Lasic** (1997). Liposomes in gene delivery (Boca Raton, CRC Press).

18. **M. Stribley John, S. Rehman Khurram, H. Niu, and M. Christman Gregory** (2002). Gene therapy and reproductive medicine. *Fertility and sterility* **77**, 645-657.

19. **J. C. Davies, D. M. Geddes, and E. W. Alton** (2001). Gene therapy for cystic fibrosis. *journal of gene medicine* **3**, 409-417.

20. **K. Yoshimura, M. A. Rosenfeld, H. Nakamura, E. M. Scherer, A. Pavirani, J. P. Lecocq, and R. G. Crystal** (1992). Expression of the human cystic fibrosis transmembrane conductance regulator gene in the mouse lung after in vivo intratracheal plasmid-mediated gene transfer. *Nucleic Acids Research* **20**, 3233-3240.

21. **N. J. Caplen, E. W. F. W. Alton, P. G. Middleton, J. R. Dorin, B. J. Stevenson, X. Gao, S. R. Durham, P. K. Jeffery, M. E. Hodson, and et al.** (1995). Liposome-mediated CFTR gene transfer to the nasal epithelium of patients with cystic fibrosis. *Nature Medicine (New York)* **1**, 39-46.

22. **M. K. Chuah, D. Collen, and T. VandenDriessche** (2001). Gene therapy for hemophilia. *journal of gene medicine* **3**, 3-20.

23. **T. Shimada** (1993). Present status and future prospects of human gene therapy. *Nihon Kyobu Shikkan Gakkai zasshi* **31 Suppl**, 1-4.

24. **I. S. Blagbrough, A. J. Geall, and A. P. Neal** (2003). Polyamines and novel polyamine conjugates interact with DNA in ways that can be exploited in non-viral gene therapy. *Biochemical Society Transactions* **31**, 397-406.

25. **H. C. Chiou, M. A. Lucas, C. C. Coffin, M. G. Banaszczyk, C. R. Ill, and C. P. Lollo** (2001). Gene therapy strategies for the treatment of chronic viral hepatitis. *Expert Opinion on Biological Therapy* **1**, 629-639.

26. **M. E. Evans, C. T. Jordan, S. M. Chang, C. Conrad, J. L. Gerberding, H. L. Kaufman, C. G. Mayhall, J. A. Nolta, A. M. Pilaro, S. Sullivan, D. J. Weber, and N. A. Wivel** (2000). Clinical infection control in gene therapy: a multidisciplinary conference. *Infection control and hospital epidemiology : official journal of the Society of Hospital Epidemiologists of America* **21**, 659-673.

27. **T. Bettinger, and M. L. Read** (2001). Recent developments in RNA-based strategies for cancer gene therapy. *Current opinion in molecular therapeutics* **3**, 116-124.

28. **G. J. Nabel, E. G. Nabel, Z. Y. Yang, B. A. Fox, G. E. Plautz, X. Gao, L. Huang, S. Shu, D. Gordon, and A. E. Chang** (1993). Direct gene transfer with DNA-liposome complexes in melanoma: Expression, biologic activity, and lack of toxicity in humans. *Proceedings of the National Academy of Sciences of the United States of America* **90**, 11307-11311.

29. (2008). The internet site of Shenzhen SiBiono GeneTech Co.,Ltd, a pioneer developer of commercial gene therapeutic products, headquarters based in China. Official release titled, "Brief Introduction". In http://www.sibiono.com/en.

30. **H. Jia** (2006). Gene therapy finds welcoming environment in China. *Nature Medicine (New York, NY, United States)* **12**, 263-264.

31. **P. N. Rangarajan, and G. Padmanaban** (1996). Gene therapy: Principles, practice, problems and prospects. *Current Science* **71**, 360-368.

32. **M. T. Lin, L. Pulkkinen, and J. Uitto** (2000). Cutaneous gene therapy. Principles and prospects. *Dermatologic clinics* **18**, 177-188, xi.

33. **A. J. Kirby, P. Camilleri, J. B. F. N. Engberts, M. C. Feiters, R. J. M. Nolte, O. Soderman, M. Bergsma, P. C. Bell, M. L. Fielden, C. L. Garcia Rodriguez, P. Guedat, A. Kremer, C. McGregor, C. Perrin, G. Ronsin, and M. C. P. van Eijk** (2003). Gemini surfactants: New synthetic vectors for gene transfection. *Angewandte Chemie, International Edition* **42**, 1448-1457.

34. **J. Wolff, D. L. Lewis, H. Herweijer, J. Hegge, and J. Hagstrom** (2005). Non-viral approaches for gene transfer. *Acta Myologica* **24**, 202-208.

35. **F. M. Menger, and C. A. Littau** (1991). Gemini-surfactants: synthesis and properties. *Journal of the American Chemical Society* **113**, 1451-1452.

36. **F. M. Menger, and C. A. Littau** (1993). Gemini surfactants: a new class of self-assembling molecules. *Journal of the American Chemical Society* **115**, 10083-10090.

37. **P. L. Felgner, T. R. Gadek, M. Holm, R. Roman, H. W. Chan, M. Wenz, J. P. Northrop, G. M. Ringold, and M. Danielsen** (1987). Lipofection: a highly efficient, lipid-mediated DNA-transfection procedure. *Proceedings of the National Academy of Sciences of the United States of America* **84**, 7413-7417.

38. **S. Lehrman** (1999). Virus treatment questioned after gene therapy death (ENGLAND: United Kingdom), pp. 517-518.

39. **K. Ewert, N. L. Slack, A. Ahmad, H. M. Evans, A. J. Lin, C. E. Samuel, and C. R. Safinya** (2004). Cationic lipid-DNA complexes for gene therapy: Understanding the relationship between complex structure and gene delivery pathways at the molecular level. *Current Medicinal Chemistry* **11**, 133-149.

40. **J. Zabner, A. J. Fasbender, T. Moninger, K. A. Poellinger, and M. J. Welsh** (1995). Cellular and molecular barriers to gene transfer by a cationic lipid. *Journal of Biological Chemistry* **270**, 18997-19007.

41. **J. A. Zasadzinski** (1997). Novel approaches to lipid based drug delivery. *Current Opinion in Solid State & Materials Science* **2**, 345-349.

42. **D. J. Segalman, and W. R. Witkowski** (1995). Two-dimensional finite element analysis of a polymer gel drug delivery system. *Materials Science & Engineering, C: Biomimetic Materials, Sensors and Systems* **C2**, 243-249.

43. **S. Kawakami, F. Yamashita, and M. Hashida** (2005). Liposomal in vivo gene delivery. *Modern Biopharmaceuticals* **4**, 1507-1519.

44. **E. Raz, D. A. Carson, S. E. Parker, T. B. Parr, A. M. Abai, G. Aichinger, S. H. Gromkowski, M. Singh, D. Lew, and M. A. Yankauckas** (1994). Intradermal gene immunization: the possible role of DNA uptake in the induction of cellular immunity to viruses. *Proceedings of the National Academy of Sciences of the United States of America* **91**, 9519-9523.

45. **J. A. Wolff, R. W. Malone, P. Williams, W. Chong, G. Acsadi, A. Jani, and P. L. Felgner** (1990). Direct gene transfer into mouse muscle in vivo. *Science (Washington, DC, United States)* **247**, 1465-1468.

46. **J.-P. Behr** (1994). Gene Transfer with Synthetic Cationic Amphiphiles: Prospects for Gene Therapy. *Bioconjugate Chemistry* **5**, 382-389.

47. **J. Y. Legendre, and F. C. Szoka, Jr.** (1992). Delivery of plasmid DNA into mammalian cell lines using pH-sensitive liposomes: comparison with cationic liposomes. *Pharmaceutical Research* **9**, 1235-1242.

48. **M. Colin, R. P. Harbottle, A. Knight, M. Kornprobst, R. G. Cooper, A. D. Miller, G. Trugnan, J. Capeau, C. Coutelle, and M. C. Brahimi-Horn** (1998). Liposomes enhance delivery and expression of an RGD-oligolysine gene transfer vector in human tracheal cells. *Gene Therapy* **5**, 1488-1498.

49. **C. L. Cepko, B. E. Roberts, and R. C. Mulligan** (1984). Construction and applications of a highly transmissible murine retrovirus shuttle vector. *Cell (Cambridge, MA, United States)* **37**, 1053-1062.

50. **P. Hug, and R. G. Sleight** (1991). Liposomes for the transformation of eukaryotic cells. *Biochimica et Biophysica Acta, Molecular Basis of Disease* **1097**, 1-17.

51. **D. C. Litzinger, and L. Huang** (1992). Phosphatidylethanolamine liposomes: drug delivery, gene transfer and immunodiagnostic applications. *Biochimica et Biophysica Acta, Reviews on Biomembranes* **1113**, 201-227.

52. **M. L. Fielden, C. Perrin, A. Kremer, M. Bergsma, M. C. Stuart, P. Camilleri, and J. B. F. N. Engberts** (2001). Sugar-based tertiary amino gemini surfactants with a vesicle-to-micelle transition in the endosomal pH range mediate efficient transfection in vitro. *European Journal of Biochemistry* **268**, 1269-1279.

53. **A. D. Miller** (1992). Human gene therapy comes of age. *Nature* **357**, 455-460.

54. **E. Marshall** (1995). Clinical research: Less hype, more biology needed for gene therapy. *Science (Washington, D C)* **270**, 1751.

55. **B. Abdallah, L. Sachs, and B. A. Demeneix** (1995). Non-viral gene transfer: Applications in developmental biology and gene therapy. *Biology of the Cell* **85**, 1-7.

56. **M. C. Papadopoulos, R. G. Giffard, and B. A. Bell** (2000). Principles of gene therapy: potential applications in the treatment of cerebral ischaemia. *British journal of neurosurgery* **14**, 407-414.

57. **Y. Hong, K. Lee, S. S. Yu, S. Kim, J.-G. Kim, H. Y. Shin, and S. Kim** (2004). Factors affecting retrovirus-mediated gene transfer to human CD34+ cells. *Journal of Gene Medicine* **6**, 724-733.

58. **P. Grandi, M. Spear, X. O. Breakefield, and S. Wang** (2004). Targeting HSV amplicon vectors. *Methods (San Diego, CA, United States)* **33**, 179-186.

59. **V. W. Van Beusechem, and D. Valerio** (1992). Prospects for human gene therapy. *Transgenesis*, 283-323.

60. **V. Matti, J. Saily, S. J. Ryhanen, J. M. Holopainen, S. Borocci, G. Mancini, and P. K. J. Kinnunen** (2001). Characterization of mixed monolayers of

phosphatidylcholine and a dicationic gemini surfactant SS-1 with a Langmuir balance: effects of DNA. *Biophysical Journal* **81**, 2135-2143.

61. **S. Zhang, Y. Xu, B. Wang, W. Qiao, D. Liu, and Z. Li** (2004). Cationic compounds used in lipoplexes and polyplexes for gene delivery. *Journal of Controlled Release* **100**, 165-180.

62. **D. Teichler Zallen** (2000). US gene therapy in crisis. *Trends in Genetics* **16**, 272-275.

63. **J. A. Heinemann, and G. F. Sprague, Jr.** (1989). Bacterial conjugative plasmids mobilize DNA transfer between bacteria and yeast. *Nature (London, United Kingdom)* **340**, 205-209.

64. **M. Lessl, and E. Lanka** (1994). Common mechanisms in bacterial conjugation and Ti-mediated T-DNA transfer to plant cells. *Cell (Cambridge, MA, United States)* **77**, 321-324.

65. **L. De Laporte, J. Cruz Rea, and L. D. Shea** (2006). Design of modular non-viral gene therapy vectors. *Biomaterials* **27**, 947-954.

66. **M. J. Cline, H. Stang, K. Mercola, L. Morse, R. Ruprecht, J. Browne, and W. Salser** (1980). Gene transfer in intact animals. *Nature (London, United Kingdom)* **284**, 422-425.

67. **F. L. Graham, and A. J. Van der Eb** (1973). New technique for the assay of infectivity of human adenovirus 5 DNA. *Virology*, 456-467.

68. **D. Luo, and W. M. Saltzman** (2000). Synthetic DNA delivery systems. *Nature Biotechnology* **18**, 33-37.

69. **L. Huang, M.-C. Hung, E. Wagner, and Editors** (1999). Nonviral Vectors for Gene Therapy).

70. **D. V. McAllister, M. G. Allen, and M. R. Prausnitz** (2000). Microfabricated microneedles for gene and drug delivery. *Annual Review of Biomedical Engineering* **2**, 289-313.

71. **V. Regnier, A. Tahiri, N. Andre, M. Lemaitre, T. Le Doan, and V. Preat** (2000). Electroporation-mediated delivery of 3'-protected phosphodiester oligodeoxynucleotides to the skin. *Journal of Controlled Release* **67**, 337-346.

72. **I. Badea, R. Verrall, M. Baca-Estrada, S. Tikoo, A. Rosenberg, P. Kumar, and M. Foldvari** (2005). In vivo cutaneous interferon-g gene delivery using novel dicationic (gemini) surfactant-plasmid complexes. *Journal of Gene Medicine* **7**, 1200-1214.

73. **C. McGregor, C. Perrin, M. Monck, P. Camilleri, and A. J. Kirby** (2001). Rational approaches to the design of cationic gemini surfactants for gene delivery. *Journal of the American Chemical Society* **123**, 6215-6220.

74. **E. Fisicaro, C. Compari, E. Duce, G. Donofrio, B. Rozycka-Roszak, and E. Wozniak** (2005). Biologically active bisquaternary ammonium chlorides: physicochemical properties of long chain amphiphiles and their evaluation as non-viral vectors for gene delivery. *Biochimica et Biophysica Acta, General Subjects* **1722**, 224-233.

75. **A. D. Miller** (2004). Nonviral liposomes. *Methods in Molecular Medicine* **90**, 107-137.

76. **D. Kirpotin, K. Hong, N. Mullah, D. Papahadjopoulos, and S. Zalipsky** (1996). Liposomes with detachable polymer coating: destabilization and fusion of dioleoylphosphatidylethanolamine vesicles triggered by cleavage of surface-grafted poly(ethylene glycol). *FEBS Letters* **388**, 115-118.

77. **K. Ohtani, M. Nakamura, S. Saito, K. Nagata, K. Sugamura, and Y. Hinuma** (1989). Electroporation: application to human lymphoid cell lines for stable introduction of a transactivator gene of human T-cell leukemia virus type I. *Nucleic Acids Research* **17**, 1589-1604.

78. **Y. Onishi, Y. Eshita, A. Murashita, M. Mizuno, and J. Yoshida** (2005). Synthesis and characterization of 2-diethyl-aminoethyl-dextran-methyl methacrylate graft copolymer for nonviral gene delivery vector. *Journal of Applied Polymer Science* **98**, 9-14.

79. **J. Haensler, and F. C. Szoka, Jr.** (1993). Polyamidoamine cascade polymers mediate efficient transfection of cells in culture. *Bioconjugate Chemistry* **4**, 372-379.

80. **L. Qin, D. R. Pahud, Y. Ding, A. U. Bielinska, J. F. Kukowska-Latallo, J. R. Baker, Jr., and J. S. Bromberg** (1998). Efficient transfer of genes into murine cardiac grafts by starburst polyamidoamine dendrimers. *Human Gene Therapy* **9**, 553-560.

81. **E. Serres, P. Vicendo, E. Perez, T. Noel, and I. Rico-Lattes** (1999). DNA Condensation and Transfection of Cells in Culture by a New Polynorbornane Polycationic Polymer. *Langmuir* **15**, 6956-6960.

82. **O. Boussif, F. Lezoualc'h, M. A. Zanta, M. D. Mergny, D. Scherman, B. Demeneix, and J.-P. Behr** (1995). A versatile vector for gene and oligonucleotide transfer into cells in culture and in vivo: polyethylenimine. *Proceedings of the National Academy of Sciences of the United States of America* **92**, 7297-7301.

83. **Y. Barenholz** (2001). Liposome application: problems and prospects. *Current Opinion in Colloid & Interface Science* **6**, 66-77.

84. (September 2008). The Journal Gene Medicine Clinical trials internet site. www.wiley.co.uk/genetherapy/clinical/. Navigation: "Charts & Tables", then "Vectors".

85. **C. M. Varga, R. Langer, and D. A. Lauffenburger** (2003). Quantitative comparison of nonviral gene delivery vectors: Model analysis of intracellular trafficking events. *Abstracts of Papers, 225th ACS National Meeting, New Orleans, LA, United States, March 23-27, 2003*, BIOT-125.

86. **S. D. Wettig, R. E. Verrall, and M. Foldvari** (2008). Gemini surfactants: a new family of building blocks for non-viral gene delivery systems. *Current Gene Therapy* **8**, 9-23.

87. **T. Friedmann** (1997). Overcoming the obstacles to gene therapy. *Scientific American* **276**, 96-101.

88. **J. J. Harrington, G. Van Bokkelen, R. W. Mays, K. Gustashhaw, and H. F. Willard** (1997). Formation of de novo centromeres and construction of first-generation human artificial microchromosomes. *Nature Genetics* **15**, 345-355.

89. **H. F. Willard** (2000). Perspectives: Genomics and gene therapy: Artificial chromosomes coming to life. *Science (Washington, D C)* **290**, 1308-1309.

90. **F. M. Menger, and J. S. Keiper** (2000). Gemini surfactants. *Angewandte Chemie, International Edition* **39**, 1907-1920.

91. **O. Zelphati, and F. C. Szoka, Jr.** (1996). Intracellular distribution and mechanism of delivery of oligonucleotides mediated by cationic lipids. *Pharmaceutical research* **13**, 1367-1372.

92. **D. R. Lu, and S. Øie** (2004). Cellular drug delivery : principles and practice (Totowa, Humana Press).

93. **L. Stamatatos, R. Leventis, M. J. Zuckermann, and J. R. Silvius** (1988). Interactions of cationic lipid vesicles with negatively charged phospholipid vesicles and biological membranes. *Biochemistry* **27**, 3917-3925.

94. **N. Duzgunes, J. A. Goldstein, D. S. Friend, and P. L. Felgner** (1989). Fusion of liposomes containing a novel cationic lipid, N-[2,3-(dioleyloxy)propyl]-N,N,N-trimethylammonium: induction by multivalent anions and asymmetric fusion with acidic phospholipid vesicles. *Biochemistry* **28**, 9179-9184.

95. **J. P. Behr, B. Demeneix, J. P. Loeffler, and J. Perez-Mutul** (1989). Efficient gene transfer into mammalian primary endocrine cells with lipopolyamine-

coated DNA. *Proceedings of the National Academy of Sciences of the United States of America* **86**, 6982-6986.

96. **J. P. Behr** (1993). Synthetic gene-transfer vectors. *Accounts of Chemical Research* **26**, 274-278.

97. **D. D. Lasic** (1997). Recent developments in medical applications of liposomes: sterically stabilized liposomes in cancer therapy and gene delivery in vivo. *Journal of Controlled Release* **48**, 203-222.

98. **H. Farhood, N. Serbina, and L. Huang** (1995). The role of dioleoyl phosphatidylethanolamine in cationic liposome mediated gene transfer. *Biochimica et Biophysica Acta, Biomembranes* **1235**, 289-295.

99. **D. S. Friend, D. Papahadjopoulos, and R. J. Debs** (1996). Endocytosis and intracellular processing accompanying transfection mediated by cationic liposomes. *Biochimica et Biophysica Acta, Biomembranes* **1278**, 41-50.

100. **L. Parker Alan, C. Newman, S. Briggs, L. Seymour, and J. Sheridan Paul** (2003). Nonviral gene delivery: techniques and implications for molecular medicine. *Expert Rev Mol Med FIELD Full Journal Title:Expert reviews in molecular medicine* **5**, 1-15.

101. **F. Labat-Moleur, A. M. Steffan, C. Brisson, H. Perron, O. Feugeas, P. Furstenberger, F. Oberling, E. Brambilla, and J. P. Behr** (1996). An electron microscopy study into the mechanism of gene transfer with lipopolyamines. *Gene Therapy* **3**, 1010-1017.

102. **K. A. Mislick, and J. D. Baldeschwieler** (1996). Evidence for the role of proteoglycans in cation-mediated gene transfer. *Proceedings of the National Academy of Sciences of the United States of America* **93**, 12349-12354.

103. **J. G. Smith, R. L. Walzem, and J. B. German** (1993). Liposomes as agents of DNA transfer. *Biochimica et Biophysica Acta, Reviews on Biomembranes* **1154**, 327-340.

104. **P. L. Felgner, and G. M. Ringold** (1989). Cationic liposome-mediated transfection. *Nature* **337**, 387-388.

105. **P. Pires, S. Simoes, S. Nir, R. Gaspar, N. Duzgunes, and M. C. Pedroso de Lima** (1999). Interaction of cationic liposomes and their DNA complexes with monocytic leukemia cells. *Biochim Biophys Acta* **1418**, 71-84.

106. **J. Smisterova, A. Wagenaar, M. C. A. Stuart, E. Polushkin, G. ten Brinke, R. Hulst, J. B. F. N. Engberts, and D. Hoekstra** (2001). Molecular shape of the cationic lipid controls the structure of cationic lipid/dioleylphosphatidylethanolamine-DNA complexes and the efficiency of gene delivery. *Journal of Biological Chemistry* **276**, 47615-47622.

107. **A. J. Verkleij** (1984). Lipidic intramembranous particles. *Biochimica et Biophysica Acta, Reviews on Biomembranes* **779**, 43-63.

108. **H. Ellens, J. Bentz, and F. C. Szoka** (1986). Destabilization of phosphatidylethanolamine liposomes at the hexagonal phase transition temperature. *Biochemistry* **25**, 285-294.

109. **J. Zabner, A. J. Fasbender, T. Moninger, K. A. Poellinger, and M. J. Welsh** (1995). Cellular and molecular barriers to gene transfer by a cationic lipid. *The Journal of biological chemistry* **270**, 18997-19007.

110. **K. Byrnes Colman, H. Nass Petra, D. Duncan Mark, and W. Harmon John** (2002). A nuclear targeting peptide, M9, improves transfection efficiency in fibroblasts. *The Journal of surgical research* **108**, 85-90.

111. **L. Vaysse, R. Harbottle, B. Bigger, A. Bergau, O. Tolmachov, and C. Coutelle** (2004). Development of a Self-assembling Nuclear Targeting Vector System Based on the Tetracycline Repressor Protein. *Journal of Biological Chemistry* **279**, 5555-5564.

112. **B. Gopalan, I. Ito, D. Branch Cynthia, C. Stephens, A. Roth Jack, and R. Ramesh** (2004). Nanoparticle based systemic gene therapy for lung cancer: molecular mechanisms and strategies to suppress nanoparticle-mediated inflammatory response. *Technology in cancer research & treatment* **3**, 647-657.

113. **R. Ramesh, T. Saeki, N. Smyth Templeton, L. Ji, L. C. Stephens, I. Ito, D. R. Wilson, Z. Wu, C. D. Branch, J. D. Minna, and J. A. Roth** (2001). Successful treatment of primary and disseminated human lung cancers by systemic delivery of tumor suppressor genes using an improved liposome vector. *Molecular Therapy* **3**, 337-350.

114. **R. Ramesh, I. Ito, Y. Saito, Z. Wu, A. M. Mhashikar, D. R. Wilson, C. D. Branch, J. A. Roth, and S. Chada** (2004). Local and systemic inhibition of lung tumor growth after nanoparticle-mediated mda-7/IL-24 gene delivery. *DNA and Cell Biology* **23**, 850-857.

115. **Y.-H. H. Lien, and L.-W. Lai** (2002). Gene therapy for renal disorders: what are the benefits for the elderly? *Drugs & Aging* **19**, 553-560.

116. **J. S. Chamberlain** (2002). Gene therapy of muscular dystrophy. *Human Molecular Genetics* **11**, 2355-2362.

117. **S. Dokka, D. Toledo, X. Shi, J. Ye, and Y. Rojanasakul** (2000). High-efficiency gene transfection of macrophages by lipoplexes. *International journal of pharmaceutics* **206**, 97-104.

118. **R. J. Akhurst** (1989). Prospects for gene therapy now and in the future. *Journal of inherited metabolic disease* **12 Suppl 1**, 191-201.

119. **R. C. Hoeben, M. P. Einerhand, E. Briet, H. van Ormondt, D. Valerio, and A. J. van der Eb** (1992). Toward gene therapy in haemophilia A: retrovirus-mediated transfer of a factor VIII gene into murine haematopoietic progenitor cells. *Thrombosis and haemostasis* **67**, 341-345.

120. **R. M. Hoffman** (2000). The hair follicle as a gene therapy target. *Nature biotechnology* **18**, 20-21.

121. **E. S. Fenjves** (1994). Approaches to gene transfer in keratinocytes. *The Journal of investigative dermatology* **103**, 70S-75S.

122. **L. Li, and R. M. Hoffmann** (1997). Topical liposome delivery of molecules to hair follicles in mice. *Journal of Dermatological Science* **14**, 101-108.

123. **V. Preat, and N. Dujardin** (2001). Topical delivery of nucleic acids in the skin. *STP Pharma Sciences* **11**, 57-68.

124. **J. C. Birchall** (2005). Cutaneous gene delivery. *Polymeric Gene Delivery*, 573-588, 571 plate.

125. **S. H. Yuspa, P. Hawley-Nelson, J. R. Stanley, and H. Hennings** (1980). Epidermal Cell Culture. *Transplantion Proceedings* **XII, Suppl. 1**, 114-122.

126. **W. D. Osborne, and A. H. Arnton** (1990). Topical Drug Formulations, **Vol 42** (New York, Marcel Dekker, Inc).

127. **M. Malmsten** (2002). Surfactants and Polymers in Drug Delivery, **Vol 122** (New York, Marcel Dekker, Inc.).

128. **J. W. Hopewell** (1990). The skin: its structure and response to ionizing radiation. *Int J Radiat Biol* **57**, 751-773.

129. **N. Weiner, N. Williams, G. Birch, C. Ramachandran, C. Shipman, Jr., and G. Flynn** (1989). Topical delivery of liposomally encapsulated interferon evaluated in a cutaneous herpes guinea pig model. *Antimicrob Agents Chemother* **33**, 1217-1221.

130. **L. Li, V. Lishko, and R. M. Hoffman** (1993). Liposome targeting of high molecular weight DNA to the hair follicles of histocultured skin: a model for gene therapy of the hair growth processes. *In vitro cellular & developmental biology Animal* **29A**, 258-260.

131. **H. Deng, Q. Lin, and P. A. Khavari** (1997). Sustainable cutaneous gene delivery. *Nature Biotechnology* **15**, 1388-1391.

132. **I. Badea, R. Verrall, M. Baca-Estrada, S. Tikoo, A. Rosenberg, P. Kumar, and M. Foldvari** (2005). In vivo cutaneous interferon-gamma gene delivery

using novel dicationic (gemini) surfactant-plasmid complexes. *J Gene Med* **7**, 1200-1214.

133. **F. Jacobsen, T. Hirsch, D. Mittler, M. Schulte, M. Lehnhardt, D. Druecke, H. H. Homann, H. U. Steinau, and L. Steinstraesser** (2006). Polybrene improves transfection efficacy of recombinant replication-deficient adenovirus in cutaneous cells and burned skin. *Journal of Gene Medicine* **8**, 138-146.

134. **M. C. N. Marchetto, A. R. Muotri, D. K. Burns, E. C. Friedberg, and C. F. M. Menck** (2004). Gene transduction in skin cells: Preventing cancer in xeroderma pigmentosum mice. *Proceedings of the National Academy of Sciences of the United States of America* **101**, 17759-17764.

135. **J. Jacoby** (2004). Gene therapy: Cornerstone of modern medicine in the new millennium? *Gene Therapy* **11**, 427-428.

136. **J. E. Cleaver** (1968). Defective repair replication of DNA in xeroderma pigmentosum. *Nature* **218**, 652-656.

137. **K. H. Kraemer, M. M. Lee, and J. Scotto** (1987). Xeroderma pigmentosum. Cutaneous, ocular, and neurologic abnormalities in 830 published cases. *Archives of dermatology* **123**, 241-250.

138. **J. H. J. Hoeijmakers** (2001). Genome maintenance mechanisms for preventing cancer. *Nature (London, United Kingdom)* **411**, 366-374.

139. **M. Berneburg, and A. R. Lehmann** (2001). Xeroderma pigmentosum and related disorders: Defects in DNA repair and transcription. *Advances in Genetics* **43**, 71-102.

140. **R. M. A. Costa, V. Chigancas, R. d. S. Galhardo, H. Carvalho, and C. F. M. Menck** (2003). The eukaryotic nucleotide excision repair pathway. *Biochimie* **85**, 1083-1099.

141. **S. Horiki, H. Miyauchi-Hashimoto, K. Tanaka, O. Nikaido, and T. Horio** (2000). Protective effects of sunscreening agents on photocarcinogenesis, photoaging, and DNA damage in XPA gene knockout mice. *Archives of Dermatological Research* **292**, 511-518.

142. **K. H. Kraemer, J. J. DiGiovanna, A. N. Moshell, R. E. Tarone, and G. L. Peck** (1988). Prevention of skin cancer in xeroderma pigmentosum with the use of oral isotretinoin. *The New England journal of medicine* **318**, 1633-1637.

143. **D. Yarosh, J. Klein, A. O'Connor, J. Hawk, E. Rafal, and P. Wolf** (2001). Effect of topically applied T4 endonuclease V in liposomes on skin cancer in xeroderma pigmentosum: a randomized study. *Lancet* **357**, 926-929.

144. **K. Atabay, C. Celebi, S. Cenetoglu, N. K. Baran, and Z. Kiymaz** (1991). Facial resurfacing in xeroderma pigmentosum with monoblock full-thickness skin graft (United States, Department of Plastic and Reconstructive Surgery, Gazi University School of Medicine, Ankara, Turkey), pp. 1121-1125.

145. **A. R. Harrop, A. Ghahary, P. G. Scott, N. Forsyth, A. Uji-Friedland, and E. E. Tredget** (1995). Regulation of collagen synthesis and mRNA expression in normal and hypertrophic scar fibroblasts in vitro by interferon-g. *Journal of Surgical Research* **58**, 471-477.

146. **S. A. Jimenez, E. Hitraya, and J. Varga** (1996). Pathogenesis of scleroderma. Collagen. *Rheumatic diseases clinics of North America* **22**, 647-674.

147. **R. Paus, and G. Cotsarelis** (1999). The biology of hair follicles. *The New England journal of medicine* **341**, 491-497.

148. **L. Li, and R. M. Hoffman** (1995). The feasibility of targeted selective gene therapy of the hair follicle. *Nature Medicine (New York)* **1**, 705-706.

149. **V. Alexeev, and K. Yoon** (1998). Stable and inheritable changes in genotype and phenotype of albino melanocytes induced by an RNA-DNA oligonucleotide. *Nature Biotechnology* **16**, 1343-1346.

150. **N. Sato, P. L. Leopold, and R. G. Crystal** (1999). Induction of the hair growth phase in postnatal mice by localized transient expression of sonic hedgehog. *Journal of Clinical Investigation* **104**, 855-864.

151. **V. Alexeev, O. Igoucheva, A. Domashenko, G. Cotsarelis, and K. Yoon** (2000). Localized in vivo genotypic and phenotypic correction of the albino mutation in skin by RNA-DNA oligonucleotide. *Nature Biotechnology* **18**, 43-47.

152. **N. Sato, P. L. Leopold, and R. G. Crystal** (2001). Effect of adenovirus-mediated expression of sonic hedgehog gene on hair regrowth in mice with chemotherapy-induced alopecia. *Journal of the National Cancer Institute* **93**, 1858-1864.

153. **W. Ahmad, M. Faiyaz ul Haque, V. Brancolini, H. C. Tsou, S. ul Haque, H. Lam, V. M. Aita, J. Owen, M. deBlaquiere, J. Frank, P. B. Cserhalmi-Friedman, A. Leask, J. A. McGrath, M. Peacocke, M. Ahmad, J. Ott, and A. M. Christiano** (1998). Alopecia universalis associated with a mutation in the human hairless gene. *Science (Washington, D C)* **279**, 720-724.

154. **S. H. Yuspa, P. Hawley-Nelson, B. Koehler, and J. R. Stanley** (1980). A survey of transformation markers in differentiating epidermal cell lines in culture. *Cancer Research* **40**, 4694-4703.

155. **W. M. McDonnell, and F. K. Askari** (1996). Molecular medicine: DNA vaccines. *New England Journal of Medicine* **334**, 42-45.

156. **C. Condon, S. C. Watkins, C. M. Celluzzi, K. Thompson, and L. D. Falo, Jr.** (1996). DNA-based immunization by in vivo transfection of dendritic cells. *Nature Medicine (New York)* **2**, 1122-1128.

157. **M. A. Liu** (2003). DNA vaccines: An overview. *Journal of Internal Medicine* **253**, 402-410.

158. **I. K. Srivastava, and M. A. Liu** (2003). Gene vaccines. *Annals of Internal Medicine* **138**, 550-559.

159. **J. J. Donnelly, B. Wahren, and M. A. Liu** (2005). DNA Vaccines: Progress and Challenges. *Journal of Immunology* **175**, 633-639.

160. **H. Fan, Q. Lin, G. R. Morrissey, and P. A. Khavari** (1999). Immunization via hair follicles by topical application of naked DNA to normal skin. *Nat Biotechnol* **17**, 870-872.

161. **J. D. Watson, and F. H. C. Crick** (1953). Genetical implications of the structure of deoxyribose nucleic acid. *Nature (London, United Kingdom)* **171**, 964-967.

162. **J. D. Watson, and F. H. C. Crick** (1953). Molecular structure of nucleic acids. A structure for deoxyribose nucleic acid. *Nature (London, United Kingdom)* **171**, 737-738.

163. **M. H. F. Wilkins, A. R. Stokes, and H. R. Wilson** (1953). Molecular structure of deoxypentose nucleic acids. *Nature (London, United Kingdom)* **171**, 738-740.

164. **R. E. Franklin, and R. G. Gosling** (1953). Evidence for 2-chain helix in crystalline structure of sodium deoxyribonucleate. *Nature (London, United Kingdom)* **172**, 156-157.

165. **R. E. Franklin, and R. G. Gosling** (1953). Molecular configuration in sodium thymonucleate. *Nature (London, United Kingdom)* **171**, 740-741.

166. (May 2008). The internet site of Wikedia Encyclopedia, with a featured article titled "DNA". In http://en.wikipedia.org/wiki/DNA.

167. **J. M. Butler** (2001). Forensic DNA Typing: Biology and Technology Behind STR Markers).

168. **M. A. Fox, and J. K.Whitesell** (1994). Organic Chemistry (Boston, Jones and Bartlett Publishers).

169. **N. S. Templeton, and Editor** (2004). Gene and Cell Therapy: Therapeutic Mechanisms and Strategies Second Edition, Revised and Expanded).

170. **S. G. Gregory, K. F. Barlow, K. E. McLay, R. Kaul, D. Swarbreck, A. Dunham, C. E. Scott, K. L. Howe, K. Woodfine, C. C. A. Spencer, M. C. Jones, C. Gillson, S. Searle, Y. Zhou, F. Kokocinski, L. McDonald, R. Evans, K. Phillips, A. Atkinson, R. Cooper, C. Jones, R. E. Hall, T. D. Andrews, C. Lloyd, R. Ainscough, J. P. Almeida, K. D. Ambrose, F. Anderson, R. W. Andrew, R. I. S. Ashwell, K. Aubin, A. K. Babbage, C. L. Bagguley, J. Bailey, R. Banerjee, H. Beasley, G. Bethel, C. P. Bird, S. Bray-Allen, J. Y. Brown, A. J. Brown, S. P. Bryant, D. Buckley, D. C. Burford, W. D. H. Burrill, J. Burton, J. Bye, C. Carder, J. C. Chapman, S. Y. Clark, G. Clarke, C. Clee, S. M. Clegg, V. Cobley, R. E. Collier, N. Corby, G. J. Coville, J. Davies, R. Deadman, P. Dhami, O. Dovey, M. Dunn, M. Earthrowl, A. G. Ellington, H. Errington, L. M. Faulkner, A. Frankish, J. Frankland, L. French, P. Garner, J. Garnett, L. Gay, M. R. J. Ghori, R. Gibson, L. M. Gilby, W. Gillett, R. J. Glithero, D. V. Grafham, S. M. Gribble, C. Griffiths, S. Griffiths-Jones, R. Grocock, S. Hammond, E. S. I. Harrison, E. Hart, E. Haugen, P. D. Heath, S. Holmes, K. Holt, P. J. Howden, A. R. Hunt, S. E. Hunt, G. Hunter, J. Isherwood, R. James, C. Johnson, D. Johnson, A. Joy, M. Kay, J. K. Kershaw, M. Kibukawa, A. M. Kimberley, A. King, A. J. Knights, H. Lad, G. Laird, C. F. Langford, S. Lawlor, D. A. Leongamornlert, D. M. Lloyd, J. Loveland, J. Lovell, M. J. Lush, R. Lyne, S. Martin, M. Mashreghi-Mohammadi, L. Matthews, N. S. W. Matthews, S. McLaren, S. Milne, S. Mistry, M. J. F. M. Moore, T. Nickerson, C. N. O'Dell, K. Oliver, A. Palmeiri, S. A. Palmer, R. D. Pandian, A. Parker, D. Patel, A. V. Pearce, A. I. Peck, S. Pelan, K. Phelps, B. J. Phillimore, R. Plumb, K. M. Porter, E. Prigmore, J. Rajan, C. Raymond, G. Rouse, C. Saenphimmachak, H. K. Sehra, E. Sheridan, R. Shownkeen, S. Sims, C. D. Skuce, M. Smith, C. Steward, S. Subramanian, and et al.** (2006). The DNA sequence and biological annotation of human chromosome 1. *Nature (London, United Kingdom)* **443**, 1013.

171. **S. G. Gregory, K. F. Barlow, K. E. McLay, R. Kaul, D. Swarbreck, A. Dunham, C. E. Scott, K. L. Howe, K. Woodfine, C. C. A. Spencer, M. C. Jones, C. Gillson, S. Searle, Y. Zhou, F. Kokocinski, L. McDonald, R. Evans, K. Phillips, A. Atkinson, R. Cooper, C. Jones, R. E. Hall, T. D. Andrews, C. Lloyd, R. Ainscough, J. P. Almeida, K. D. Ambrose, F. Anderson, R. W. Andrew, R. I. S. Ashwell, K. Aubin, A. K. Babbage, C. L. Bagguley, J. Bailey, H. Beasley, G. Bethel, C. P. Bird, S. Bray-Allen, J. Y. Brown, A. J. Brown, D. Buckley, J. Burton, J. Bye, C. Carder, J. C. Chapman, S. Y. Clark, G. Clarke, C. Clee, V. Cobley, R. E. Collier, N. Corby, G. J. Coville, J. Davies, R. Deadman, M. Dunn, M. Earthrowl, A. G. Ellington, H. Errington, A. Frankish, J. Frankland, L. French, P. Garner, J. Garnett, L. Gay, M. R. J. Ghori, R. Gibson, L. M. Gilby, W. Gillett, R. J. Glithero, D. V. Grafham, C. Griffiths, S. Griffiths-Jones, R. Grocock, S. Hammond, E. S. I. Harrison, E. Hart, E. Haugen, P. D. Heath, S. Holmes, K. Holt, P. J.**

Howden, A. R. Hunt, S. E. Hunt, G. Hunter, J. Isherwood, R. James, C. Johnson, D. Johnson, A. Joy, M. Kay, J. K. Kershaw, M. Kibukawa, A. M. Kimberley, A. King, A. J. Knights, H. Lad, G. Laird, S. Lawlor, D. A. Leongamornlert, D. M. Lloyd, J. Loveland, J. Lovell, M. J. Lush, R. Lyne, S. Martin, M. Mashreghi-Mohammadi, L. Matthews, N. S. W. Matthews, S. McLaren, S. Milne, S. Mistry, M. J. F. Moore, T. Nickerson, C. N. O'Dell, K. Oliver, A. Palmeiri, S. A. Palmer, A. Parker, D. Patel, A. V. Pearce, A. I. Peck, S. Pelan, K. Phelps, B. J. Phillimore, R. Plumb, J. Rajan, C. Raymond, G. Rouse, C. Saenphimmachak, H. K. Sehra, E. Sheridan, R. Shownkeen, S. Sims, C. D. Skuce, M. Smith, C. Steward, S. Subramanian, N. Sycamore, A. Tracey, A. Tromans, Z. Van Helmond, M. Wall, J. M. Wallis, S. White, S. L. Whitehead, J. E. Wilkinson, D. L. Willey, H. Williams, L. Wilming, P. W. Wray, Z. Wu, A. Coulson, M. Vaudin, J. E. Sulston, R. Durbin, T. Hubbard, R. Wooster, I. Dunham, N. P. Carter, G. McVean, M. T. Ross, J. Harrow, M. V. Olson, S. Beck, J. Rogers, and D. R. Bentley (2006). The DNA sequence and biological annotation of human chromosome 1. *Nature (London, United Kingdom)* **441**, 315-321.

172. **F. Devinsky, and I. Lacko** (1990). Quaternary ammonium salts. Part XV. Micelle formation of bisquaternaries. *Tenside, Surfactants, Detergents* **27**, 344-349.

173. **F. Devinsky, I. Lacko, F. Bittererova, and L. Tomeckova** (1986). Relationship between structure, surface activity, and micelle formation of some new bisquaternary isosteres of 1,5-pentanediammonium dibromides. *Journal of Colloid and Interface Science* **114**, 314-322.

174. **F. Devinsky, L. Masarova, and I. Lacko** (1985). Surface activity and micelle formation of some new bisquaternary ammonium salts. *Journal of Colloid and Interface Science* **105**, 235-239.

175. **C. A. Bunton, L. B. Robinson, J. Schaak, and M. F. Stam** (1971). Catalysis of nucleophilic substitutions by micelles of dicationic detergents. *Journal of Organic Chemistry* **36**, 2346-2350.

176. **Y. P. Zhu, A. Masuyama, and M. Okahara** (1990). Preparation and surface active properties of amphipathic compounds with two sulfate groups and two lipophilic alkyl chains. *Journal of the American Oil Chemists' Society* **67**, 459-463.

177. **R. Zana** (2002). Alkanediyl-a,w-bis(dimethylalkylammonium bromide) Surfactants. *Journal of Colloid and Interface Science* **246**, 182-190.

178. **R. Zana, M. Benrraou, and R. Rueff** (1991). Alkanediyl-a,w-bis(dimethylalkylammonium bromide) surfactants. 1. Effect of the spacer chain length on the critical micelle concentration and micelle ionization degree. *Langmuir* **7**, 1072-1075.

179. **R. Zana** (2002). Dimeric (gemini) surfactants: effect of the spacer group on the association behavior in aqueous solution. *Journal of Colloid and Interface Science* **248**, 203-220.

180. **F. M. Menger, and B. N. A. Mbadugha** (2001). Gemini Surfactants with a Disaccharide Spacer. *Journal of the American Chemical Society* **123**, 875-885.

181. **F. M. Menger, and A. V. Peresypkin** (2001). A Combinatorially-Derived Structural Phase Diagram for 42 Zwitterionic Geminis. *Journal of the American Chemical Society* **123**, 5614-5615.

182. **F. M. Menger, J. S. Keiper, and V. Azov** (2000). Gemini Surfactants with Acetylenic Spacers. *Langmuir* **16**, 2062-2067.

183. **B. S. Sekhon** (2004). Gemini (dimeric) surfactants: the two-faced molecules. *Resonance* **9**, 42-49.

184. **N. S. Templeton** (2001). Developments in liposomal gene delivery systems. *Expert Opinion on Biological Therapy* **1**, 567-570.

185. **D. Niculescu-Duvaz, J. Heyes, and C. J. Springer** (2003). Structure-activity relationship in cationic lipid mediated gene transfection. *Current Medicinal Chemistry* **10**, 1233-1261.

186. **D. S. Friend, D. Papahadjopoulos, and R. J. Debs** (1996). Endocytosis and intracellular processing accompanying transfection mediated by cationic liposomes. *Biochimica et biophysica acta* **1278**, 41-50.

187. **S. W. Hui, M. Langner, Y. L. Zhao, P. Ross, E. Hurley, and K. Chan** (1996). The role of helper lipids in cationic liposome-mediated gene transfer. *Biophys J* **71**, 590-599.

188. **M. Ruponen, S. Yla-Herttuala, and A. Urtti** (1999). Interactions of polymeric and liposomal gene delivery systems with extracellular glycosaminoglycans: physicochemical and transfection studies. *Biochimica et Biophysica Acta, Biomembranes* **1415**, 331-341.

189. **H. Gershon, R. Ghirlando, S. B. Guttman, and A. Minsky** (1993). Mode of formation and structural features of DNA-cationic liposome complexes used for transfection. *Biochemistry* **32**, 7143-7151.

190. **S. J. Eastman, C. Siegel, J. Tousignant, A. E. Smith, S. H. Cheng, and R. K. Scheule** (1997). Biophysical characterization of cationic lipid:DNA complexes. *Biochimica et Biophysica Acta, Biomembranes* **1325**, 41-62.

191. **D. D. Lasic, H. Strey, M. C. A. Stuart, R. Podgornik, and P. M. Frederik** (1997). The Structure of DNA-Liposome Complexes. *Journal of the American Chemical Society* **119**, 832-833.

192. **J. O. Radler, I. Koltover, T. Salditt, and C. R. Safinya** (1997). Structure of DNA-cationic liposome complexes: DNA intercalation in multilamellar membranes in distinct interhelical packing regimes. *Science* **275**, 810-814.

193. **D. D. Dunlap, A. Maggi, M. R. Soria, and L. Monaco** (1997). Nanoscopic structure of DNA condensed for gene delivery. *Nucleic Acids Research* **25**, 3095-3101.

194. **K. Kunath, A. von Harpe, D. Fischer, H. Petersen, U. Bickel, K. Voigt, and T. Kissel** (2003). Low-molecular-weight polyethylenimine as a non-viral vector for DNA delivery: comparison of physicochemical properties, transfection efficiency and in vivo distribution with high-molecular-weight polyethylenimine. *Journal of controlled release : official journal of the Controlled Release Society* **89**, 113-125.

195. **I. Tranchant, B. Thompson, C. Nicolazzi, N. Mignet, and D. Scherman** (2004). Physicochemical optimisation of plasmid delivery by cationic lipids. *Journal of Gene Medicine* **6**, S24-S35.

196. **K. Baraldo, N. Leforestier, M. Bureau, N. Mignet, and D. Scherman** (2002). Sphingosine-Based Liposome as DNA Vector for Intramuscular Gene Delivery. *Pharmaceutical Research* **19**, 1144-1149.

197. **S. Even-Chen, and Y. Barenholz** (2000). DOTAP cationic liposomes prefer relaxed over supercoiled plasmids. *Biochimica et Biophysica Acta, Biomembranes* **1509**, 176-188.

198. **G. Byk, C. Dubertret, V. Escriou, M. Frederic, G. Jaslin, R. Rangara, B. Pitard, J. Crouzet, P. Wils, B. Schwartz, and D. Scherman** (1998). Synthesis, Activity, and Structure-Activity Relationship Studies of Novel Cationic Lipids for DNA Transfer. *Journal of Medicinal Chemistry* **41**, 224-235.

199. **S. Bhattacharya, and S. De** (1999). Synthesis and vesicle formation from dimeric pseudoglyceryl lipids with (CH2)m spacers: pronounced m-value dependence of thermal properties, vesicle fusion, and cholesterol complexation. *Chemistry--A European Journal* **5**, 2335-2347.

200. **J. Gaucheron, T. Wong, K. F. Wong, N. Maurer, and P. R. Cullis** (2002). Synthesis and Properties of Novel Tetraalkyl Cationic Lipids. *Bioconjugate Chemistry* **13**, 671-675.

201. **S. D. Wettig, I. Badea, M. Donkuru, R. E. Verrall, and M. Foldvari** (2007). Structural and transfection properties of amine-substituted gemini surfactant-based nanoparticles. *Journal of Gene Medicine* **9**, 649-658.

202. **H. S. Rosenzweig, V. A. Rakhmanova, and R. C. MacDonald** (2001). Diquaternary Ammonium Compounds as Transfection Agents. *Bioconjugate Chemistry* **12**, 258-263.

203. **E. Fisicaro, C. Compari, E. Duce, G. Donofrio, B. Rozycka-Roszak, and E. Wozniak** (2005). Biologically active bisquaternary ammonium chlorides: physico-chemical properties of long chain amphiphiles and their evaluation as non-viral vectors for gene delivery. *Biochim Biophys Acta* **1722**, 224-233.

204. **S. D. Wettig, I. Badea, M. Donkuru, R. E. Verrall, and M. Foldvari** (2008). Substitution Effects in Gemini Surfactants: Application to DNA Transfecction. *Manuscript in Preparation*.

205. **P. C. Bell, M. Bergsma, I. P. Dolbnya, W. Bras, M. C. Stuart, A. E. Rowan, M. C. Feiters, and J. B. Engberts** (2003). Transfection mediated by gemini surfactants: engineered escape from the endosomal compartment. *J Am Chem Soc* **125**, 1551-1558.

206. **M. Johnsson, and J. B. F. N. Engberts** (2004). Novel sugar-based gemini surfactants: Aggregation properties in aqueous solution. *Journal of Physical Organic Chemistry* **17**, 934-944.

207. **M. Johnsson, A. Wagenaar, M. C. A. Stuart, and J. B. F. N. Engberts** (2003). Sugar-Based Gemini Surfactants with pH-Dependent Aggregation Behavior: Vesicle-to-Micelle Transition, Critical Micelle Concentration, and Vesicle Surface Charge Reversal. *Langmuir* **19**, 4609-4618.

208. **L. Wasungu, M. Scarzello, G. Dam, G. Molema, A. Wagenaar, J. B. F. N. Engberts, and D. Hoekstra** (2006). Transfection mediated by pH-sensitive sugar-based gemini surfactants; potential for in vivo gene therapy applications. *Journal of Molecular Medicine (Heidelberg, Germany)* **84**, 774-784.

209. **L. Wasungu, and D. Hoekstra** (2006). Cationic lipids, lipoplexes and intracellular delivery of genes. *Journal of Controlled Release* **116**, 255-264.

210. **M. Castro, D. Griffiths, A. Patel, N. Pattrick, C. Kitson, and M. Ladlow** (2004). Effect of chain length on transfection properties of spermine-based gemini surfactants. *Organic & Biomolecular Chemistry* **2**, 2814-2820.

211. **K. H. Jennings, I. C. B. Marshall, M. J. Wilkinson, A. Kremer, A. J. Kirby, and P. Camilleri** (2002). Aggregation Properties of a Novel Class of Cationic Gemini Surfactants Correlate with Their Efficiency as Gene Transfection Agents. *Langmuir* **18**, 2426-2429.

212. **E. Dauty, J.-S. Remy, T. Blessing, and J.-P. Behr** (2001). Dimerizable Cationic Detergents with a Low cmc Condense Plasmid DNA into Nanometric Particles and Transfect Cells in Culture. *Journal of the American Chemical Society* **123**, 9227-9234.

213. **G. Zuber, L. Zammut-Italiano, E. Dauty, and J.-P. Behr** (2003). Targeted gene delivery to cancer cells: Directed assembly of nanometric DNA particles

coated with folic acid. *Angewandte Chemie, International Edition* **42**, 2666-2669.

214. **E. Dauty, J. P. Behr, and J. S. Remy** (2002). Development of plasmid and oligonucleotide nanometric particles. *Gene Therapy* **9**, 743-748.

215. **B. Wetzer, G. Byk, M. Frederic, M. Airiau, F. Blanche, B. Pitard, and D. Scherman** (2001). Reducible cationic lipids for gene transfer. *Biochem J* **356**, 747-756.

216. **G. Byk, B. Wetzer, M. Frederic, C. Dubertret, B. Pitard, G. Jaslin, and D. Scherman** (2000). Reduction-Sensitive Lipopolyamines as a Novel Nonviral Gene Delivery System for Modulated Release of DNA with Improved Transgene Expression. *Journal of Medicinal Chemistry* **43**, 4377-4387.

217. **J. Huang, X. Xie, and X. Mei** (2008). Application of lipid-based nanoparticle carrier in nucleic acid drug delivery system. *Guoji Yaoxue Yanjiu Zazhi* **35**, 145-147, 150.

218. **S. D. Wettig, and R. E. Verrall** (2001). Thermodynamic Studies of Aqueous m-s-m Gemini Surfactant Systems. *Journal of Colloid and Interface Science* **235**, 310-316.

219. **S. D. Wettig, C. Wang, R. E. Verrall, and M. Foldvari** (2007). Thermodynamic and aggregation properties of aza- and imino-substituted gemini surfactants designed for gene delivery. *Physical Chemistry Chemical Physics* **9**, 871-877.

220. **J. Sandri, and J. Viala** (1992). Convenient conversion of cis-homoallylic alcohols into corresponding bromides with dibromotriphenylphosphorane (Ph3PBr2). *Synthetic Communications* **22**, 2945-2948.

221. **S. D. Wettig, and R. E. Verrall** (2001). Studies of the Interaction of Cationic Gemini Surfactants with Polymers and Triblock Copolymers in Aqueous Solution. *Journal of Colloid and Interface Science* **244**, 377-385.

222. **K. M. Jenkins** (2000) MSc Thesis: Thermodynamic studies of bis(quanternary ammonium) and (N-alkyl-) ionic surfactants, University of Saskatchewan, Saskatoon.

223. **X. Li, S. D. Wettig, C. Wang, M. Foldvari, and R. E. Verrall** (2005). Synthesis and solution properties of gemini surfactants containing oleyl chains. *Physical Chemistry Chemical Physics* **7**, 3172-3178.

224. **W. D. Harkins, and H. F. Jordan** (1930). A method for the determination of surface tension from the maximum pull on a ring. *Journal of the American Chemical Society* **52**, 1751-1772.

225. **T. Maniatis, E. F. Fritsch, and J. Sambroook** (1986). Molecular Cloning: A Laboratory Manual, Cold Spring Harbor Lab. Press, Plainview, NY, USA).

226. **K. V. Wood** (1990). Firefly luciferase: A new tool for molecular biologists. *Promega Notes* **28**, 1-3.

227. **M. Antonietti** (1994). The colloidal domain: where physics, chemistry, biology and technology meet, **Vol 45**).

228. **R. Zana** (2002). Alkanediyl-a,w-bis(dimethylalkylammonium bromide) surfactants: II. Krafft temperature and melting temperature. *Journal of Colloid and Interface Science* **252**, 259-261.

229. **A. Pinazo, M. Diz, C. Solans, M. A. Pes, P. Erra, and M. R. Infante** (1993). Synthesis and properties of cationic surfactants containing a disulfide bond. *Journal of the American Oil Chemists' Society* **70**, 37-42.

230. **A. Espert, R. v. Klitzing, P. Poulin, A. Colin, R. Zana, and D. Langevin** (1998). Behavior of Soap Films Stabilized by a Cationic Dimeric Surfactant. *Langmuir* **14**, 4251-4260.

231. **A. Pinazo, M. R. Infante, C. H. Chang, and E. I. Franses** (1994). Surface tension properties of aqueous solutions of disulfur betaine derivatives. *Colloids and Surfaces, A: Physicochemical and Engineering Aspects* **87**, 117-123.

232. **T. Takemura, N. Shiina, M. Izumi, K. Nakamura, M. Miyazaki, K. Torigoe, and K. Esumi** (1999). Aqueous Properties of Cationic Biphenyl Type Surfactants. *Langmuir* **15**, 646-648.

233. **M. Dreja, W. Pyckhout-Hintzen, H. Mays, and B. Tieke** (1999). Cationic Gemini Surfactants with Oligo(oxyethylene) Spacer Groups and Their Use in the Polymerization of Styrene in Ternary Microemulsion. *Langmuir* **15**, 391-399.

234. **E. Alami, G. Beinert, P. Marie, and R. Zana** (1993). Alkanediyl-Alpha,Omega-Bis(Dimethylalkylammonium Bromide) Surfactants .3. Behavior at the Air-Water-Interface. *Langmuir* **9**, 1465-1467.

235. **M. J. Rosen** (1989). Surfactants and Interfacial Phenomena, Wiley).

236. **S. D. Wettig** (2000) PhD Thesis: Studes of the interaction of gemini surfactants with polymers and triblock copolymers, University of Saskatoon, Saskatoon.

237. **P. Carpena, J. Aguiar, P. Bernaola-Galvan, and C. C. Ruiz** (2002). Problems Associated with the Treatment of Conductivity-Concentration Data in Surfactant Solutions: Simulations and Experiments. *Langmuir* **18**, 6054-6058.

238. **J. Aguiar, J. A. Molina-Bolivar, J. M. Peula-Garcia, and C. Carnero Ruiz** (2002). Thermodynamics and micellar properties of

tetradecyltrimethylammonium bromide in formamide-water mixtures. *Journal of Colloid and Interface Science* **255**, 382-390.

239. **J. Haensler, and F. C. Szoka, Jr.** (1993). Synthesis and characterization of a trigalactosylated bisacridine compound to target DNA to hepatocytes. *Bioconjugate Chemistry* **4**, 85-93.

240. **M. Johnsson, A. Wagenaar, and J. B. F. N. Engberts** (2003). Sugar-Based Gemini Surfactant with a Vesicle-to-Micelle Transition at Acidic pH and a Reversible Vesicle Flocculation near Neutral pH. *Journal of the American Chemical Society* **125**, 757-760.

241. **M. Bergsma, M. L. Fielden, and J. B. F. N. Engberts** (2001). pH-Dependent Aggregation Behavior of a Sugar-Amine Gemini Surfactant in Water: Vesicles, Micelles, and Monolayers of Hexane-1,6-bis(hexadecyl-1'-deoxyglucitylamine). *Journal of Colloid and Interface Science* **243**, 491-495.

242. **L. Wasungu, M. C. A. Stuart, M. Scarzello, J. B. F. N. Engberts, and D. Hoekstra** (2006). Lipoplexes formed from sugar-based gemini surfactants undergo a lamellar-to-micellar phase transition at acidic pH. Evidence for a non-inverted membrane-destabilizing hexagonal phase of lipoplexes. *Biochimica et Biophysica Acta, Biomembranes* **1758**, 1677-1684.

243. **A. Pinazo, L. Perez, M. R. Infante, and R. Pons** (2004). Unconventional vesicle-to-ribbon transition behavior of diacyl glycerol amino acid based surfactants in extremely diluted systems induced by pH-concentration effects. *Physical Chemistry Chemical Physics* **6**, 1475-1481.

244. **I. Badea** (2006) PhD thesis, *Gemini cationic surfactant-based delivery systems for non-invasive cutaneous gene therapy*, University of Saskatchewan, Saskatoon, SK.

245. **I. Badea, S. Wettig, R. Verrall, and M. Foldvari** (2007). Topical non-invasive gene delivery using gemini nanoparticles in interferon-g-deficient mice. *European Journal of Pharmaceutics and Biopharmaceutics* **65**, 414-422.

246. **J. Gustafsson, G. Arvidson, G. Karlsson, and M. Almgren** (1995). Complexes between cationic liposomes and DNA visualized by cryo-TEM. *Biochim Biophys Acta* **1235**, 305-312.

247. **Y. Xu, S. W. Hui, P. Frederik, and F. C. Szoka, Jr.** (1999). Physicochemical characterization and purification of cationic lipoplexes. *Biophys J* **77**, 341-353.

248. **B. Sternberg, F. L. Sorgi, and L. Huang** (1994). New structures in complex formation between DNA and cationic liposomes visualized by freeze-fracture electron microscopy. *FEBS Letters* **356**, 361-366.

249. **Y. S. Mel'nikova, S. M. Mel'nikov, and J.-E. Lofroth** (1999). Physicochemical aspects of the interaction between DNA and oppositely charged mixed liposomes. *Biophysical Chemistry* **81**, 125-141.

250. **P. C. Ross, and S. W. Hui** (1999). Lipoplex size is a major determinant of in vitro lipofection efficiency. *Gene Ther* **6**, 651-659.

251. **J. C. Birchall, I. W. Kellaway, and S. N. Mills** (1999). Physico-chemical characterisation and transfection efficiency of lipid-based gene delivery complexes. *Int J Pharm* **183**, 195-207.

252. **C. Kawaura, A. Noguchi, T. Furuno, and M. Nakanishi** (1998). Atomic force microscopy for studying gene transfection mediated by cationic liposomes with a cationic cholesterol derivative. *FEBS Lett* **421**, 69-72.

253. **M. Ouyang, J. S. Remy, and F. C. Szoka, Jr.** (2000). Controlled template-assisted assembly of plasmid DNA into nanometric particles with high DNA concentration. *Bioconjug Chem* **11**, 104-112.

254. **C. R. Dass** (2002). Biochemical and biophysical characteristics of lipoplexes pertinent to solid tumor gene therapy. *International Journal of Pharmaceutics* **241**, 1-25.

255. **I. Koltover, T. Salditt, J. O. Radler, and C. R. Safinya** (1998). An inverted hexagonal phase of cationic liposome-DNA complexes related to DNA release and delivery. *Science* **281**, 78-81.

256. **S. Chesnoy, and L. Huang** (2000). Structure and function of lipid-DNA complexes for gene delivery. *Annu Rev Biophys Biomol Struct* **29**, 27-47.

257. **O. Boussif, F. Lezoualc'h, M. A. Zanta, M. D. Mergny, D. Scherman, B. Demeneix, and J. P. Behr** (1995). A versatile vector for gene and oligonucleotide transfer into cells in culture and in vivo: polyethylenimine. *Proc Natl Acad Sci U S A* **92**, 7297-7301.

258. **R. Zana, and H. Levy** (1997). Alkanediyl-a,w-bis(dimethylalkylammonium bromide) surfactants (dimeric surfactants). Part 6. CMC of the ethanediyl-1,2-bis(dimethylalkylammonium bromide) series. *Colloids and Surfaces, A: Physicochemical and Engineering Aspects* **127**, 229-232.

259. **L. Karlsson, M. C. P. van Eijk, and O. Soderman** (2002). Compaction of DNA by gemini surfactants: Effects of surfactant architecture. *Journal of Colloid and Interface Science* **252**, 290-296.

260. **W. Saenger** (1984). Principles of Nucleic Acid Structure (New York, Springer-Verlag).

261. **J. E. Morgan, J. W. Blankenship, and H. R. Matthews** (1987). Polyamines and acetylpolyamines increase the stability and alter the conformation of nucleosome core particles. *Biochemistry* **26**, 3643-3649.

262. **J. Ruiz-Chica, M. A. Medina, F. Sanchez-Jimenez, and F. J. Ramirez** (2001). Fourier transform Raman study of the structural specificities on the interaction between DNA and biogenic polyamines. *Biophysical Journal* **80**, 443-454.

263. **V. Vijayanathan, T. Thomas, A. Shirahata, and T. J. Thomas** (2001). DNA Condensation by Polyamines: A Laser Light Scattering Study of Structural Effects. *Biochemistry* **40**, 13644-13651.

264. **A. A. Ouameur, and H.-A. Tajmir-Riahi** (2004). Structural Analysis of DNA Interactions with Biogenic Polyamines and Cobalt(III)hexamine Studied by Fourier Transform Infrared and Capillary Electrophoresis. *Journal of Biological Chemistry* **279**, 42041-42054.

265. **S. De, V. K. Aswal, P. S. Goyal, and S. Bhattacharya** (1996). Role of Spacer Chain Length in Dimeric Micellar Organization. Small Angle Neutron Scattering and Fluorescence Studies. *Journal of Physical Chemistry* **100**, 11664-11671.

266. **T. Yoshimura, K. Ishihara, and K. Esumi** (2005). Sugar-Based Gemini Surfactants with Peptide Bonds-Synthesis, Adsorption, Micellization, and Biodegradability. *Langmuir* **21**, 10409-10415.

267. **B. Pitard** (2002). Supramolecular Assemblies of DNA Delivery Systems. *Somatic Cell and Molecular Genetics* **27**, 5-15.

268. **S. Zhou, D. Liang, C. Burger, F. Yeh, and B. Chu** (2004). Nanostructures of complexes formed by calf thymus DNA interacting with cationic surfactants. *Biomacromolecules* **5**, 1256-1261.

269. **H. S. Rosenzweig, V. A. Rakhmanova, T. J. McIntosh, and R. C. MacDonald** (2000). O-Alkyl dioleoylphosphatidylcholinium Compounds: The Effect of Varying Alkyl Chain Length on Their Physical Properties and in Vitro DNA Transfection Activity. *Bioconjugate Chemistry* **11**, 306-313.

270. **A. J. Lin, N. L. Slack, A. Ahmad, C. X. George, C. E. Samuel, and C. R. Safinya** (2003). Three-dimensional imaging of lipid gene-carriers: membrane charge density controls universal transfection behavior in lamellar cationic liposome-DNA complexes. *Biophys J* **84**, 3307-3316.

271. **B. Angelov, M. Ollivon, and A. Angelova** (1999). X-ray Diffraction Study of the Effect of the Detergent Octyl Glucoside on the Structure of Lamellar and Nonlamellar Lipid/Water Phases of Use for Membrane Protein Reconstitution. *Langmuir* **15**, 8225-8234.

272. **M. Foldvari, I. Badea, S. Wettig, R. Verrall, and M. Bagonluri** (2006). Structural characterization of novel gemini non-viral DNA delivery systems for cutaneous gene therapy. *Journal of Experimental Nanoscience* **1**, 165-176.

273. **M. Foldvari, S. Wettig, I. Badea, R. Verrall, and M. Bagonluri** (2006). Dicationic gemini surfactant gene delivery complexes contain cubic-lamellar mixed polymorphic phase. *NSTI Nanotech 2006, NSTI Nanotechnology Conference and Trade Show, Boston, MA, United States, May 7-11, 2006* **2**, 400-403.

274. **L. Stewart, M. Manvell, E. Hillery, C. J. Etheridge, R. G. Cooper, H. Stark, M. van Heel, M. Preuss, E. W. F. W. Alton, and A. D. Miller** (2001). Physico-chemical analysis of cationic liposome-DNA complexes (lipoplexes) with respect to in vitro and in vivo gene delivery efficiency. *Journal of the Chemical Society, Perkin Transactions 2*, 624-632.

275. **K. D. Stewart, and T. A. Gray** (1992). Survey of the DNA binding properties of natural and synthetic polyamino compounds. *Journal of Physical Organic Chemistry* **5**, 461-466.

276. **S. Padmanabhan, V. M. Brushaber, C. F. Anderson, and M. T. Record, Jr.** (1991). Relative affinities of divalent polyamines and of their N-methylated analogs for helical DNA determined by sodium-23 NMR. *Biochemistry* **30**, 7550-7559.

277. **A. J. Geall, M. A. W. Eaton, T. Baker, C. Catterall, and I. S. Blagbrough** (1999). The regiochemical distribution of positive charges along cholesterol polyamine carbamates plays significant roles in modulating DNA binding affinity and lipofection. *FEBS Letters* **459**, 337-342.

278. **R. P. Balasubramaniam, M. J. Bennett, A. M. Aberle, J. G. Malone, M. H. Nantz, and R. W. Malone** (1996). Structural and functional analysis of cationic transfection lipids: the hydrophobic domain. *Gene Therapy* **3**, 163-172.

279. **V. Floch, S. Loisel, E. Guenin, A. C. Herve, J. C. Clement, J. J. Yaouanc, H. des Abbayes, and C. Ferec** (2000). Cation Substitution in Cationic Phosphonolipids: A New Concept To Improve Transfection Activity and Decrease Cellular Toxicity. *Journal of Medicinal Chemistry* **43**, 4617-4628.

280. **J. A. Heyes, D. Niculescu-Duvaz, R. G. Cooper, and C. J. Springer** (2002). Synthesis of Novel Cationic Lipids: Effect of Structural Modification on the Efficiency of Gene Transfer. *Journal of Medicinal Chemistry* **45**, 99-114.

281. **Z. Hyvonen, M. Ruponen, S. Ronkko, P. Suhonen, and A. Urtti** (2002). Extracellular and intracellular factors influencing gene transfection mediated by 1,4-dihydropyridine amphiphiles. *European Journal of Pharmaceutical Sciences* **15**, 449-460.

282. **P. Delepine, C. Guillaume, V. Floch, S. Loisel, J. J. Yaouanc, J. C. Clement, H. Des Abbayes, and C. Ferec** (2000). Cationic phosphonolipids as nonviral vectors: in vitro and in vivo applications. *Journal of Pharmaceutical Sciences* **89**, 629-638.

283. **T. Ren, Y. K. Song, G. Zhang, and D. Liu** (2000). Structural basis of DOTMA for its high intravenous transfection activity in mouse. *Gene Therapy* **7**, 764-768.

284. **A. Roosjen, J. Smisterova, C. Driessen, J. T. Anders, A. Wagenaar, D. Hoekstra, R. Hulst, and J. B. F. N. Engberts** (2002). Synthesis and characteristics of biodegradable pyridinium amphiphiles used for in vitro DNA delivery. *European Journal of Organic Chemistry*, 1271-1277.

285. **S. Loisel, V. Floch, C. Le Gall, and C. Ferec** (2001). Factors influencing the efficiency of lipoplexes mediated gene transfer in lung after intravenous administration. *Journal of Liposome Research* **11**, 127-138.

286. **A. Asokan, and M. J. Cho** (2004). Cytosolic delivery of macromolecules. 3. synthesis and characterization of acid-sensitive bis-detergents. *Bioconjugate Chemistry* **15**, 1166-1173.

287. **M. R. Almofti, H. Harashima, Y. Shinohara, A. Almofti, Y. Baba, and H. Kiwada** (2003). Cationic liposome-mediated gene delivery: biophysical study and mechanism of internalization. *Arch Biochem Biophys* **410**, 246-253.

288. **A. M. Aberle, F. Tablin, J. Zhu, N. J. Walker, D. C. Gruenert, and M. H. Nantz** (1998). A Novel Tetraester Construct That Reduces Cationic Lipid-Associated Cytotoxicity. Implications for the Onset of Cytotoxicity. *Biochemistry* **37**, 6533-6540.

289. **P. Camilleri, A. Kremer, A. J. Edwards, K. H. Jennings, O. Jenkins, I. Marshall, C. McGregor, W. Neville, S. Q. Rice, R. J. Smith, M. J. Wilkinson, and A. J. Kirby** (2000). A novel class of cationic gemini surfactants showing efficient in vitro gene transfection properties. [Erratum to document cited in CA133:359590]. *Chemical Communications (Cambridge)*, 1553.

7. APPENICES

Appendix A: Compound confirmation data for the gemini surfactants

Table A-I: CH&N elemental analysis results for the gemini surfactants

Surfactant	Calculated			Found – *Averages*		
	%C	%H	%N	%C	%H	%N
12-spacer-12						
12-3-13[a]	59.2	10.9	4.5	58.3	10.9	4.4
12-5N-12[b]	59.0	11.0	6.3	58.9	11.3	5.9
12-8N-12[b]	59.3	11.1	7.7	58.6	11.3	7.1
12-7N-12[b]	60.1	11.1	6.0	60.1	11.3	6.0
12-7NH-12[b]	59.6	11.0	6.1	60.1	11.2	5.9
m-3-m						
12-3-12[a]	– Same sample as the 12-3-12 sample above					
16-3-16[c]	63.2	11.4	3.8	63.0	11.5	4.0
18-3-18	64.80	11.63	3.51	63.71	11.56	3.55
18:1-3-18:1[d]	65.13	11.18	3.53	64.84	11.00	3.65
m-7-m						
12-7-12	61.39	11.19	4.09	59.81	11.30	3.99
16-7-16	64.80	11.63	3.51	64.80	11.80	3.37
18-7-18	66.17	11.81	3.28	65.30	11.88	3.25

Table A-I (con't): CH&N elemental analysis results for the gemini surfactants

Surfactant	Calculated			Found – *Averages*		
	%C	%H	%N	%C	%H	%N
m-7NH-m						
12-7NH-12	59.55	11.02	6.13	60.23	11.39	5.89
16-7NH-16	63.21	11.49	5.27	63.39	11.37	5.18
18-7NH-18	64.69	11.68	4.92	62.32	11.47	4.96
18:1-7NH-18:1	64.99	11.26	4.94	64.84	11.48	4.86

Data for the superscript-bearing surfactants used in this research have been previously published:
[a]From ref. [218; 236]
[b]From ref. [219]
[c]From ref. [222]
[d]From ref. [223]
Data for all other surfactants were obtained from analytical work carried out in this research.

Table A-II: ^{1}H NMR data for the gemini surfactants

Surfactant	Group	δ (ppm)	# of protons
12-spacer-12			
12-3-12[a]	– Data have been previously published		
12-5N-12[b]	– Data have been previously published		
12-8N-12[b]	– Data have been previously published		
12-7N-12[b]	– Data have been previously published		
12-7NH-12	N^+-C**H**$_2$-CH_2-CH_2-NH-	4.14-4.08	4
	N^+-C**H**$_2$-CH_2-$(CH_2)_9$-CH_3 , } N^+-CH_2-CH_2-C**H**$_2$-NH-	3.46-3.40	8
	N^+-C**H**$_3$	3.30	12
	N^+-CH_2-C**H**$_2$-CH_2-NH-	2.64	4
	-N**H**-	2.18	1
	N^+-CH_2-C**H**$_2$-$(CH_2)_9$-CH_3	1.78	4
	N^+-CH_2-CH_2-(C**H**$_2$)$_9$-CH_3	1.38-1.26	36
	N^+-CH_2-CH_2-$(CH_2)_9$-C**H**$_3$	0.89-0.84	6
m-3-m			
16-3-16[c]	– Data have been previously published		
18-3-18	N^+-C**H**$_2$-CH_2-C**H**$_2$-N^+	4.00-3.96	4
	N^+-C**H**$_2$-CH_2-$(CH_2)_{15}$-CH_3	3.48-3.44	4
	N^+-C**H**$_3$	3.30	12
	N^+-CH_2-C**H**$_2$-CH_2-N^+	2.82	2
	N^+-CH_2-C**H**$_2$-$(CH_2)_{15}$-CH_3	1.82	4
	N^+-CH_2-CH_2-(C**H**$_2$)$_{15}$-CH_3	1.40-1.26	60
	N^+-CH_2-CH_2-$(CH_2)_{15}$-C**H**$_3$	0.89-0.84	6
18:1-3-18:1[d]	– Data have been previously published		

Table A-II (con't): ^{1}H NMR data for the gemini surfactants

Surfactant	Group	δ (ppm)	# of protons
m-7-m			
12-7-12	N^+-C**H**$_2$-CH_2-$(CH_2)_3$-CH_2-C**H**$_2$-N^+	3.84-3.74	4
	N^+-C**H**$_2$-CH_2-$(CH_2)_9$-CH_3	3.48-3.44	4
	N^+-C**H**$_3$	3.33	12
	N^+-CH_2-C**H**$_2$-$(CH_2)_3$-C**H**$_2$-CH_2-N^+	1.85	4
	N^+-CH_2-C**H**$_2$-$(CH_2)_9$-CH_3	1.72	4
	N^+-CH_2-CH_2-$(CH_2)_3$-CH_2-CH_2-N^+	1.56-1.50	6
	N^+-CH_2-CH_2-$(CH_2)_9$-CH_3	1.38-1.20	36
	N^+-CH_2-CH_2-$(CH_2)_9$-C**H**$_3$	0.89-0.85	6
16-7-16	N^+-C**H**$_2$-CH_2-$(CH_2)_3$-CH_2-C**H**$_2$-N^+	3.92-3.86	4
	N^+-C**H**$_2$-CH_2-$(CH_2)_{13}$-CH_3	3.44-3.38	4
	N^+-C**H**$_3$	3.32	12
	N^+-CH_2-C**H**$_2$-$(CH_2)_3$-C**H**$_2$-CH_2-N^+	1.88	4
	N^+-CH_2-C**H**$_2$-$(CH_2)_{13}$-CH_3	1.72	4
	N^+-CH_2-CH_2-$(CH_2)_3$-CH_2-CH_2-N^+	1.58	6
	N^+-CH_2-CH_2-$(CH_2)_{13}$-CH_3	1.38-1.26	52
	N^+-CH_2-CH_2-$(CH_2)_{13}$-C**H**$_3$	0.89-0.85	6
18-7-18	N^+-C**H**$_2$-CH_2-$(CH_2)_3$-CH_2-C**H**$_2$-N^+	3.88-3.82	4
	N^+-C**H**$_2$-CH_2-$(CH_2)_{15}$-CH_3	3.50-3.42	4
	N^+-C**H**$_3$	3.35	12
	N^+-CH_2-C**H**$_2$-$(CH_2)_3$-C**H**$_2$-CH_2-N^+	1.86	4
	N^+-CH_2-C**H**$_2$-$(CH_2)_{15}$-CH_3	1.72	4
	N^+-CH_2-CH_2-$(CH_2)_3$-CH_2-CH_2-N^+	1.58-1.52	6
	N^+-CH_2-CH_2-$(CH_2)_{15}$-CH_3	1.36-1.20	60
	N^+-CH_2-CH_2-$(CH_2)_{15}$-C**H**$_3$	0.89-0.85	6
m-7NH-m			
16-7NH-16	N^+-C**H**$_2$-CH_2-CH_2-NH-	4.08-4.12	4
	N^+-C**H**$_2$-CH_2-$(CH_2)_{13}$-CH_3	3.36-3.45	4
	N^+-C**H**$_3$	3.32	12
	N^+-CH_2-CH_2-C**H**$_2$-NH-	2.98	4
	-N**H**-	2. 90	1
	N^+-CH_2-C**H**$_2$-CH_2-NH-	2.19	4
	N^+-CH_2-C**H**$_2$-$(CH_2)_{13}$-CH_3	1.74	4
	N^+-CH_2-CH_2-$(CH_2)_{13}$-CH_3	1.35-1.25	52
	N^+-CH_2-CH_2-$(CH_2)_{13}$-C**H**$_3$	0.88	6

Table A-II (con't): ^{1}H NMR data for the gemini surfactants

Surfactant	Group	δ (ppm)	# of protons
18-7NH-18	N^{+}-C**H**$_2$-CH_2-CH_2-NH-	4.18-4.10	4
	N^{+}-C**H**$_3$	3.40	12
	N^{+}-C**H**$_2$-CH_2-$(CH_2)_{15}$-CH_3	3.30	4
	N^{+}-CH_2-CH_2-C**H**$_2$-NH-	2.92-2.80	4
	N^{+}-CH_2-C**H**$_2$-CH_2-NH-	2.58-2.48	4
	-N**H**-	2.04	1
	N^{+}-CH_2-C**H**$_2$-$(CH_2)_{15}$-CH_3	1.76	4
	N^{+}-CH_2-CH_2-(C**H**$_2$)$_{15}$-CH_3	1.38-1.26	60
	N^{+}-CH_2-CH_2-$(CH_2)_{15}$-C**H**$_3$	0.89-0.86	6
18:1-7NH-18:1	-CH_2-C**H**=C**H**-CH_2-	5.40-5.30	4
	N^{+}-C**H**$_2$-CH_2-CH_2-NH-	4.15-4.10	4
	N^{+}-C**H**$_3$	3.50-3.45	12
	N^{+}-C**H**$_2$-CH_2-$(CH_2)_5$-CH_2-CH=CH-	3.25-3.20	4
	N^{+}-CH_2-CH_2-C**H**$_2$-NH-	2.70-2.60	4
	N^{+}-CH_2-C**H**$_2$-CH_2-NH- ,} -C**H**$_2$-CH=CH-C**H**$_2$-	2.10-1.90	12
	-N**H**-	1.90	1
	N^{+}-CH_2-C**H**$_2$-$(CH_2)_5$-CH_2-CH=CH-	1.74-1.82	4
	-(C**H**$_2$)$_5$-CH_2-CH=CH-CH_2-(C**H**$_2$)$_6$-	1.40-1.20	40
	-CH=CH-CH_2-$(CH_2)_6$-C**H**$_3$	0.91-0.82	6

Data for the superscript-bearing surfactants used in this research have been previously published:
[a]From ref. [218; 236]
[b]From ref. [219]
[c]From ref. [222]
[d]From ref. [223]
Data for all other surfactants were obtained from analytical work carried out in this research.

Table A-III: Electrospray ionization mass spectroscopic (ESI-MS) data for the gemini surfactants

Surfactant (symbol)	Gemini surfactant ion (without $2Br^-$ ions)	Results of analysis	
		m/z	Relative intensity (%)
12-spacer-12			
12-3-12	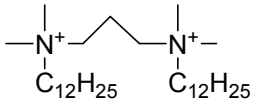 Mass = 468.88 g mol^{-1}	124.09	0.64
		234.27	100.00
		241.27	0.84
		248.29	0.18
		250.27	0.39
		254.29	0.30
12-5N-12	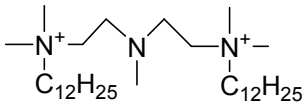 Mass = 511.95 g mol^{-1}	107.07	0.07
		135.16	0.09
		219.56	0.05
		255.79	100.00
		262.31	1.07
		280.27	0.05
12-8N-12	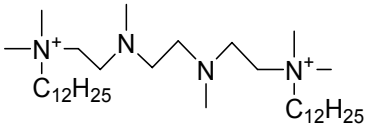 Mass = 569.05 g mol^{-1}	234.27	1.19
		241.27	0.06
		255.79	0.19
		262.30	0.07
		284.31	100.00
		291.31	0.88
		299.31	0.28
		344.37	0.32
12-7N-12	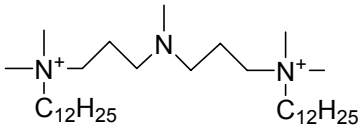 Mass = 540.00 g mol^{-1}	185.72	0.24
		236.27	0.82
		255.80	0.06
		262.79	0.17
		269.80	100.00
		276.79	0.13

Table A-III: Electrospray ionization mass spectroscopic (ESI-MS) data for the gemini surfactants, (cont'd)

Surfactant (symbol)	Gemini surfactant ion (without $2Br^-$ ions)	Results of analysis m/z	Relative intensity (%)
12-spacer-12			
12-7NH-12	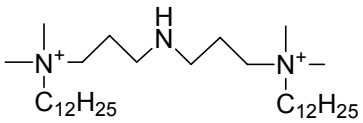 Mass = 525.98 g mol^{-1}	178.73 202.67 262.81 284.85 346.91	0.07 0.26 100.00 0.07 0.03
m-3-m			
16-3-16	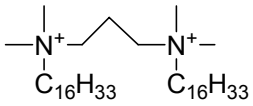 Mass = 581.10 g mol^{-1}	123.10 217.11 262.80 290.33 346.89 433.21 455.18	0.76 2.83 0.34 100.00 0.20 0.94 0.57
18-3-18	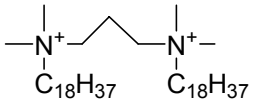 Mass = 637.20 g mol^{-1}	217.11 245.19 318.36 433.21 455.18	1.80 0.03 100.00 0.55 0.46
18:1-3-18:1	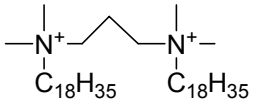 Mass = 633.17 g mol^{-1}	262.80 269.81 316.34 325.88 346.39	3.25 0.91 100.00 2.04 5.82
m-7-m			
12-7-12	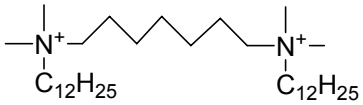 Mass = 524.99 g mol^{-1}	124.08 214.09 262.30 269.80 276.32	0.07 0.06 100.00 0.33 0.05

Table A-III: Electrospray ionization mass Spectroscopic (ESI-MS) data for the gemini surfactants, (cont'd)

Surfactant (symbol)	Gemini surfactant ion (without $2Br^-$ ions)	Results of analysis m/z	Relative intensity (%)
m-7-m			
16-7-16	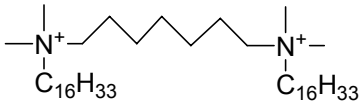 Mass = 637.20 g mol^{-1}	124.09 262.81 318.37 325.36 346.41	0.92 1.26 100.00 1.42 2.66
18-7-18	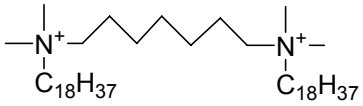 Mass = 693.31 g mol^{-1}	262.80 325.87 332.38 346.40 362.39	2.13 2.49 0.64 100.00 0.07
m-7NH-m			
16-7NH-16	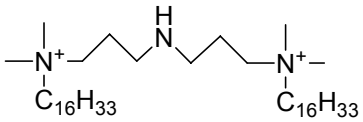 Mass = 638.19 g mol^{-1}	181.15 214.08 231.18 245.16 318.86 415.28 431.49	1.33 1.76 1.24 1.10 100.00 0.31 0.46
18-7NH-18	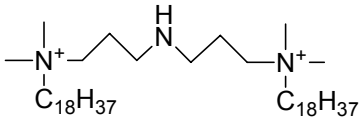 Mass = 694.30 g mol^{-1}	220.75 231.60 316.35 325.87 346.89 473.04	3.11 4.38 1.48 2.56 100.00 1.70
18:1-7NH-18:1	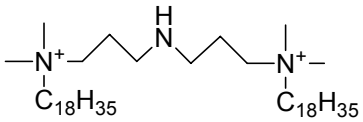 Mass = 690.30 g mol^{-1}	164.14 219.75 227.17 344.88 471.01	0.08 0.50 0.57 100.00 0.09

Appendix B: Gemini surfactant conductivity data

Table B-I: Conductance vs. temperature data; TKrafft determination

•16-7-16		•16-7NH-16	
Temperature (^{o}C)	Conductance (μS)	Temperature (^{o}C)	Conductance (μS)
14	539.62	17	960.34
15	555.61	18	996.84
17	586.86	19	1029.15
19	620.86	21	1090.13
20	638.92	23	1155.55
22	674.88	25	1256.65
24	718.76	27	1292.41
26	848.72	29	1361.42
28	893.76	31	1436.15
30*	937.68	34	1550.15
32*	980.12	37	1701.26
35	1069.15	38*	1783.29
37	1149.64	40	1830.95
40	1194.15	42	1879.94
45	1223.43	45	1981.14
50	1249.66	47	2007.33
		50	2050.44

The astericks indicate temperature(s) surrounding the start and complete clarification the saturated gemini surfactant–water system.

Table B-I (con't): Conductance vs. temperature data; T_{Krafft} determination

•18-7-18

Temperature (^oC)	Conductance (μS)
10	6.33
15	7.17
18	7.82
20	8.24
22	8.73
24	9.35
27	10.88
29	13.42
32	32.54
35	108.16
37	280.91
38	340.94
39*	351.08
40	359.53
44	388.73
45	395.47
48	420.27
50	440.02

•18-7NH-18

Temperature (^oC)	Conductance (μS)
11	26.32
13	28.05
15	29.86
18	32.92
20	35.33
22	37.85
24	41.44
26	46.11
28	53.96
29	62.48
30	66.66
31	82.79
32	97.88
33	114.10
34	132.66
35	161.88
36	193.54
37	223.48
38	251.78
39*	267.66
40	285.56
42	324.08
43	339.68
44	353.10
46	370.03
47	382.43

The astericks indicate temperature(s) surrounding the start and complete clarification the saturated gemini surfactant–water system.

Table B-I (con't): Conductance vs. temperature data; T_{Krafft} determination

•18-3-18

Temperature (^oC)	Conductance (μS)
10	18.63
15	21.02
17	21.88
20	23.99
22	25.06
24	26.19
26	27.56
28	28.88
30	30.18
33	31.48
36	33.06
38	33.89
40	56.16
41	78.58
42	96.11
44*	204.42
47*	222.37
48	225.03
49	233.81
50	251.28
52	269.22
54	278.93
55	286.41
57	287.31

•18:1-3-18:1

Temperature (^oC)	Conductance (μS)
10	277.4753
12	297.2669
14	325.4621
16	362.1394
18	423.7918
19	490.7063
20	523.5353
21	650.2173
22	768.7313
23	896.1202
24	1041.887
25	1271.375
26	1520.027
27	1755.17
29*	1977.433
30	2102.152
31	2242.735
33	2545.264
34	2667.784
35	2773.182
37	2906.147
38	3003.534

The astericks indicate temperature(s) surrounding the start and complete clarification the saturated gemini surfactant–water system.

Table B-I (con't): Conductance vs. temperature data; T_{Krafft} determination

•18:1-7NH-18:1

Temperature (^{o}C)	Conductance (μS)
10	188.79
12	201.71
15	243.66
17	405.34
18	511.84
19	624.15
21	735.13
23	916.55
25	1082.65
27	1140.41
29*	1306.42
32*	1477.15
34	1602.15
37	1760.26
38	1783.29
40	1830.95
42	1921.94
44	1989.14
46	2017.33
47	2052.44

The astericks indicate temperature(s) surrounding the start and complete clarification the saturated gemini surfactant–water system.

Table B-II: Specific conductance (κ) vs. concentrtion data; CMC determination

•12-7-12

Conc. (mM)	κ ($\mu S\ cm^{-1}$)
0	2.62
0.0397	13.90
0.0789	25.14
0.1176	36.97
0.1558	48.48
0.1935	59.78
0.2308	70.85
0.2675	81.36
0.3038	91.33
0.3396	101.80
0.3750	111.99
0.4444	131.68
0.5122	149.67
0.5783	167.46
0.6429	184.14
0.7059	200.61
0.8571	236.76
1.0000	259.93
1.1351	277.12
1.2632	291.58
1.3846	304.63
1.5000	316.20
1.6098	327.39
1.7143	337.54
1.8140	347.06
1.9091	355.97
2.0000	364.62
2.0870	372.97
2.1702	380.65
2.2500	388.05
2.4000	404.51
2.5385	417.59
2.6165	424.92

•16-7-16

Conc. (mM)	κ ($\mu S\ cm^{-1}$)
0	3.18
0.0040	3.97
0.0079	4.85
0.0118	5.84
0.0156	6.87
0.0194	7.82
0.0231	8.89
0.0268	9.73
0.0304	10.53
0.0340	11.26
0.0375	11.93
0.0410	12.56
0.0444	13.13
0.0479	13.68
0.0512	14.21
0.0545	14.67
0.0578	15.14
0.0611	15.58
0.0643	15.99
0.0675	16.39
0.0706	16.78
0.0737	17.16
0.0767	17.52
0.0798	17.89

Table B-II (con't): Specific conductance (κ) vs. concentrtion data; CMC determination

•16-7NH-16

Conc. (mM)	κ (μS cm^{-1})
0	3.93
0.0040	5.35
0.0079	6.81
0.0118	8.31
0.0156	9.71
0.0194	11.29
0.0231	12.74
0.0268	14.18
0.0304	15.57
0.0340	16.88
0.0375	18.19
0.0410	19.38
0.0444	20.71
0.0479	21.77
0.0512	22.75
0.0545	23.68
0.0578	24.55
0.0611	25.34
0.0643	26.11
0.0675	26.88
0.0706	27.66
0.0737	28.39
0.0767	29.01
0.0798	29.69
0.0828	30.35
0.0857	30.98

•18-3-18

Conc. (mM)	κ (μS cm^{-1})
0	5.58
0.0022	13.06
0.0065	14.90
0.0108	16.65
0.0150	18.04
0.0192	19.19
0.0233	20.20
0.0274	21.41
0.0314	22.43
0.0354	23.22
0.0393	24.00
0.0413	24.24
0.0451	24.73
0.0489	25.37
0.0526	25.64
0.0563	26.16
0.0600	26.49
0.0636	26.75
0.0672	27.21
0.0707	27.39
0.0742	27.87
0.0776	28.00

Table B-II (con't): Specific conductance (κ) vs. concentrtion data; CMC determination

•18-7-18

Conc. (mM)	κ ($\mu S\ cm^{-1}$)
0	4.23
0.0020	4.61
0.0040	5.99
0.0059	7.04
0.0079	8.20
0.0098	9.34
0.0118	10.55
0.0137	11.82
0.0156	12.85
0.0175	13.79
0.0194	14.92
0.0212	16.01
0.0231	16.86
0.0268	18.55
0.0304	20.07
0.0340	21.27
0.0375	22.51
0.0444	24.61
0.0512	26.51
0.0578	28.36
0.0643	30.20
0.0706	31.74

•18-7NH-18

Conc. (mM)	κ ($\mu S\ cm^{-1}$)
0	10.87
0.0033	11.94
0.0066	12.88
0.0099	13.98
0.0132	14.71
0.0164	15.69
0.0196	16.29
0.0228	16.91
0.0260	17.52
0.0291	18.19
0.0323	18.72
0.0354	19.37
0.0385	19.94
0.0415	20.51
0.0446	21.11
0.0476	21.78
0.0506	22.37
0.0536	22.93
0.0566	23.46
0.0596	23.95
0.0625	24.47
0.0683	25.26
0.0741	26.08
0.0798	26.98
0.0854	27.77
0.0909	28.71
0.0964	29.58
0.1018	30.40
0.1071	31.24
0.1124	32.13
0.1176	32.89

•18:1-7NH-18:1

Conc. (mM)	κ ($\mu S\ cm^{-1}$)
0	2.01
0.0033	18.10
0.0066	33.33
0.0099	48.54
0.0132	63.09
0.0164	77.12
0.0196	90.83
0.0228	103.94
0.0260	116.85
0.0291	127.27
0.0323	138.86
0.0385	162.55
0.0446	183.67
0.0506	203.59
0.0566	222.46
0.0625	240.41
0.0683	258.03
0.0741	274.73
0.0798	291.46
0.0854	307.12
0.0909	322.10
0.0964	336.85
0.1018	351.47
0.1071	365.82
0.1124	380.01

Appendix C: Surface tension data for the gemini surfactants

Table C: Log C vs. surface tension (γ) data; CMC determination

•12-7-12

log C (C: mol L^{-1})	γ ($mN\ m^{-1}$)
-3.88	57.31
-3.71	54.92
-3.59	53.17
-3.49	50.96
-3.41	49.64
-3.35	49.01
-3.30	47.65
-3.25	46.19
-3.20	45.36
-3.17	43.85
-3.13	43.28
-3.10	42.97
-3.07	42.66
-3.04	42.61
-3.02	42.81
-2.99	42.81
-2.97	42.92
-2.95	42.81
-2.86	42.81

•16-7-16

log C (C: mol L^{-1})	γ ($mN\ m^{-1}$)
-5.40	65.49
-5.23	60.61
-5.10	59.87
-5.01	55.98
-4.93	54.07
-4.86	51.85
-4.81	49.91
-4.71	48.91
-4.64	48.33
-4.57	47.81
-4.43	46.66

•16-7NH-16

log C (C: mol L^{-1})	γ ($mN\ m^{-1}$)
-5.60	64.31
-5.48	63.18
-5.31	59.49
-5.18	56.78
-5.01	53.07
-4.89	50.43
-4.79	48.18
-4.72	47.60
-4.65	48.18
-4.60	47.91
-4.51	47.65

•18-3-18

log C (C: mol L^{-1})	γ ($mN\ m^{-1}$)
-5.18	60.19
-5.08	57.47
-5.00	55.50
-4.94	53.12
-4.88	50.85
-4.79	46.61
-4.71	42.45
-4.59	39.26
-4.49	38.18
-4.30	37.41
-4.20	36.55
-4.13	34.06

Table C (con't): Log C vs. surface tension (γ) data; CMC determination

•18-7-18

log C (C: mol L^{-1})	γ ($mN\ m^{-1}$)
-5.70	70.72
-5.40	65.98
-5.23	59.12
-5.10	57.95
-5.01	54.55
-4.93	52.38
-4.86	51.75
-4.81	51.43
-4.76	51.17
-4.71	49.96
-4.64	49.70
-4.52	48.33
-4.43	47.50

•18-7NH-18

log C (C: mol L^{-1})	γ ($mN\ m^{-1}$)
-5.78	67.32
-5.48	60.72
-5.30	57.89
-5.18	55.40
-5.08	52.86
-5.00	51.27
-4.94	49.22
-4.88	46.82
-4.79	46.61
-4.71	45.98
-4.64	45.30
-4.59	45.25
-4.54	44.94
-4.49	44.58
-4.41	44.16
-4.35	43.49
-4.30	42.92

•18:1-7NH-18:1

log C (C: mol L^{-1})	γ ($mN\ m^{-1}$)
-4.88	65.71
-4.71	63.08
-4.59	57.68
-4.49	56.35
-4.41	54.23
-4.35	53.01
-4.30	52.59
-4.25	52.64
-4.20	52.54
-4.17	52.28
-4.13	51.91
-4.07	52.06
-4.02	51.80
-3.97	51.64

Appendix D: COS-7 cell transfection and cytotoxicity results (supplemental data)

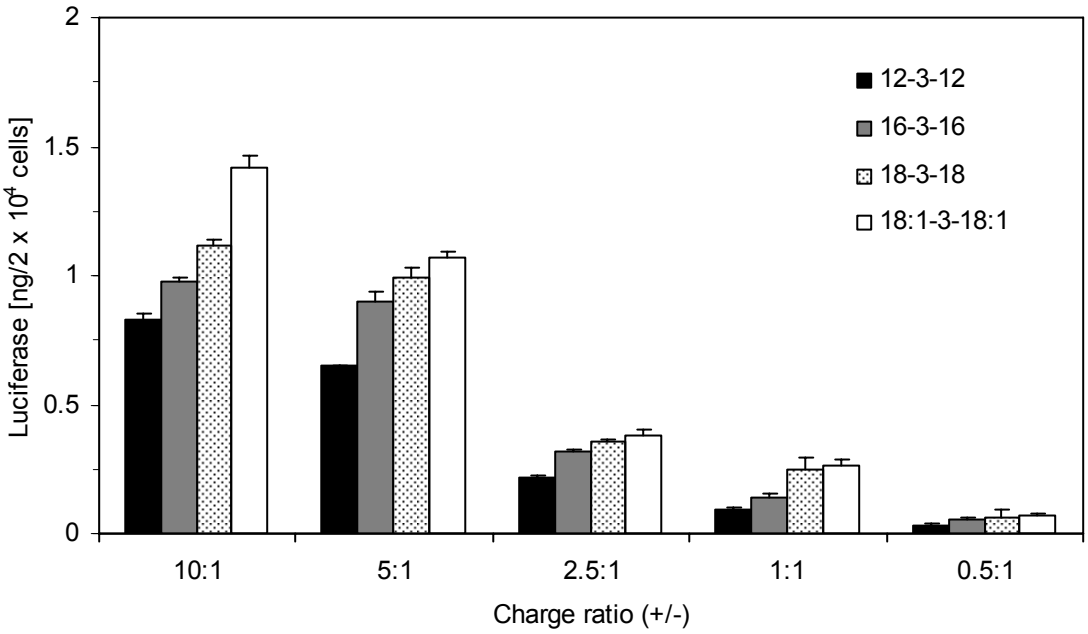

Figure D-I. Luciferase reporter gene expression in COS-7 cells measured as a function of the gemini surfactant:DNA charge ratio (i.e., the +/− charge ratio).
The PGL complexes prepared with variable $\rho_{+/-}$ values including 10:1, 5:1, 2.5:1, 1:1 and 0.5:1, featured the m-3-m surfactants. The resulting protein produced within the cells was quantified at 24 h-post transfection. n = 4, error bars = SD.

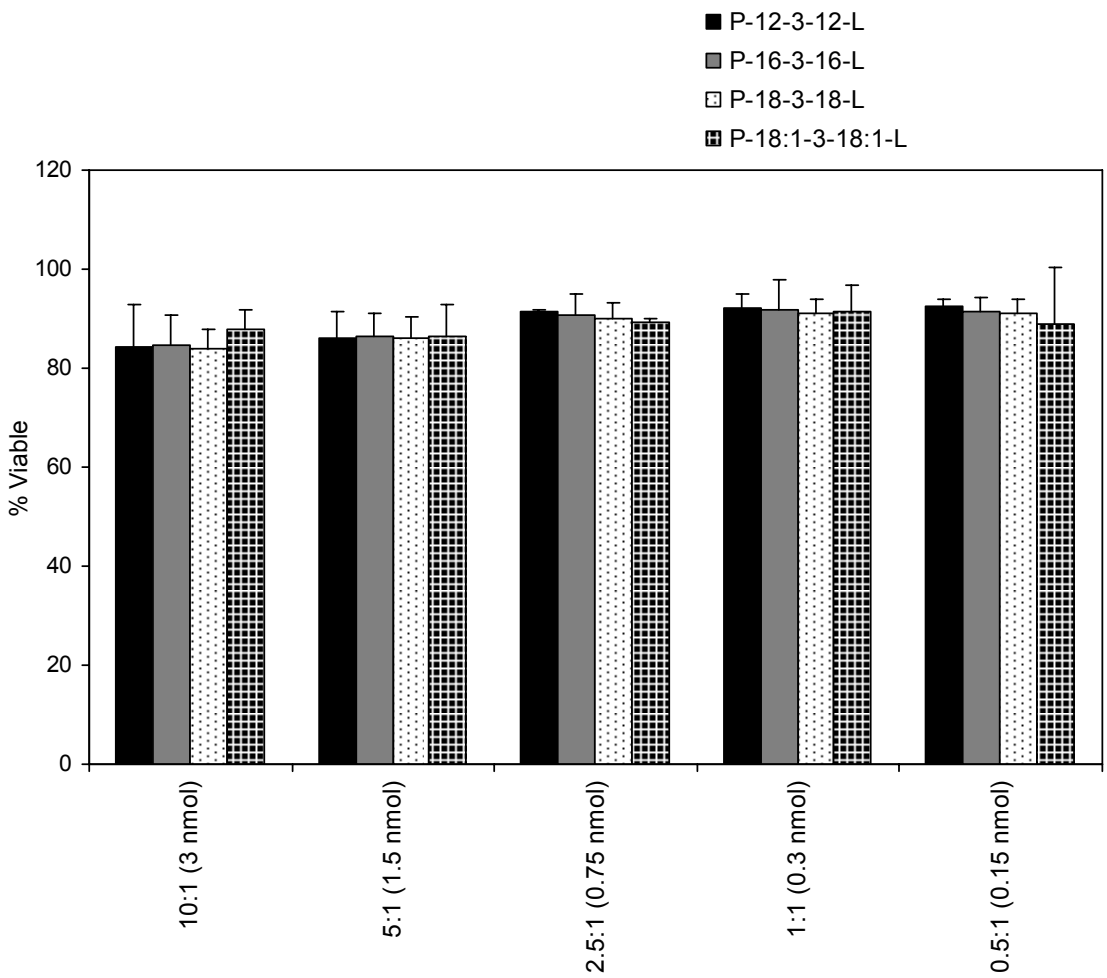

Figure D-2. Dose-dependent toxicities for gemini surfactants in COS-7 cells. Cells were transfected with PGL complexes prepared using varying concentration of m-3-m surfactants (i.e., complexes had values of $\rho_{+/-}$ ranging from 10:1 to 0.5:1. The numbers in parentheses next to each $\rho_{+/-}$ value represent the amount of surfactant used for preparing complexes based on a uniform plasmid dose of 0.2 μg). Cell viabilities were quantified after 24 h of transfection. The figure inset shows the level of cytotoxicity or motility in transfected cells (% Mortality = 100 - % cell viability). n = 4, errors bars = SD.